Biogeochemical cycling in iron-rich Lake Matano, Indonesia: An early ocean analogue

Sean Andrew Crowe, Earth and Planetary Sciences, McGill University, Montreal

June, 2008

A thesis submitted to McGill University in partial fulfillment of the requirements of the degree of Doctor of Philosophy

I dedicate this thesis to my parents, Dennis and Terry Crowe.

“Lakes are test tubes of oceans”

The father of aquatic chemistry— Werner Stumm

Contributions of Authors

This thesis is the result of the author's Ph.D. research projects in the Department of Earth and Planetary Sciences at McGill University. The thesis comprises nine chapters, four of which are scientific manuscripts, two are general introductions and conclusions, and the remaining three are bridging chapters that connect the research manuscripts. Chapter 2 was published in the journal *Limnology and Oceanography*, Chapter 4 is accepted for publication in the *Proceedings of the National Academy of Sciences*, Chapter 6 is submitted to *Geochimica et Cosmochimca Acta*, and Chapter 8 to *Environmental Science and Technology*. The research in this thesis was proposed by the author and initiated after discussions with the advisory committee (Professors Alfonso Mucci, Bjørn Sundby, and David A. Fowle), Professor G. Douglas Haffner (University of Windsor) and Professor Donald E. Canfield (Chapter 4) (University of Southern Denmark), all of whom are co-authors on all publications and manuscripts to which they contributed. Research expeditions and field work were planned by the author. Data collection in the field was largely conducted by the author with the assistance of David Fowle, Alfonso Mucci and other members of the Malili lakes research team. Members of the Malili lakes research team who contributed are included as co-authors on manuscripts (Peter Hehanussa-LIPI, Sulung Nomosatryo-LIPI, Andrew O'Neill-University of Windsor, Arne Sturm-University of Kansas, Cédric Magen-McGill University, CarriAyne Jones-University of Southern Denmark, Karla Leslie-University of Kansas). Most of the laboratory analyses were conducted by the author with help from a number of technicians and research scientists to whom the author is grateful (Constance Guignard, J-C. Barrette, Joel Gagnon, and William Minarik). These people are acknowledged in the acknowledgements sections of the individual manuscripts. Specific exceptions to this are: 1) the ^{14}C-CH_4 analyses (Chapter 6) which were conducted by Professor William S. Reeburgh (University of California-Irvine), his student Mary Pack (University of California-Irvine), and collaborator Dr. John Kessler (Princeton University) all three of whom are co-authors on Chapter 6; 2) Cr isotope analyses (Chapter 8) which were conducted by Professor Andre Ellis (University of Texas at El Paso) who is co-author on Chapter 8. The author was responsible for the interpretation of the ^{14}C-CH_4 and Cr isotope data with respect to biogeochemical cycling within Lake Matano. Numerical

modeling presented in Chapters 2, 4 and 6 was partly conducted by Professor Sergei Katsev (University of Minesota-Duluth) and the author was largely only involved in the conceptual formulations of these numerical models. Professor Katsev is co-author on Chapters 2, 4 and 6. The author is responsible for the full content of the thesis.

Abstract- Lake Matano of Indonesia, the 8th deepest lake on Earth, is an Fe-rich (ferruginous) end-member aquatic ecosystem and is the best known modern analogue for the ecology of Earth's earliest oceans. A culmination of geological, climatic and biological processes has resulted in an Fe-centric aquatic ecosystem in which anaerobic microbial communities are largely sustained by cycling Fe and CH_4. Fe-rich soils of the catchment basin supply an abundance of Fe (hydr)oxides to Lake Matano's sediments. Limited vertical mixing in Lake Matano has generated a persistent, 100 m deep pycnocline which is sustained by minimal seasonal temperature fluctuations and steep basin morphology. This pycnocline separates an oxic surface layer from Fe(II) and CH_4-rich bottom waters.

Ferruginous conditions in Lake Matano limit dissolved P concentrations in the oxic surface layer where they are apt to restrict primary production. *Chlorobiaceae,* which populate the deep ferruginous chemocline comprise an important component of Lake Matano's phototrophic community. Given the absence of sulfide, the metabolisms of these novel, deep-water, anoxygenic phototrophs are likely driven by Fe(II) oxidation. Methanogenesis dominates organic matter degradation despite Lake Matano's thermodynamic propensity for Fe reduction. Biogenic methane accumulates in the anoxic bottom water and supports the activity of aerobic and anaerobic methanotrophs. Cr concentrations in Lake Matano are relatively high and reflect the geology of the catchment basin. Removal of Cr from the surface waters is driven by the reduction of Cr(VI) by Fe(II) supplied from the anoxic bottom water. The ensuing downward Cr flux maintains dissolved Cr(VI) concentrations in the surface waters below international guidelines.

Lake Matano's physical structure, abundance of Fe and dearth of sulfate mirror the stratified ferruginous conditions thought to prevail in Earth's early oceans. The finding that anoxygenic phototrophs proliferate under ferruginous conditions supports models of early ocean ecology in which anoxygenic phototrophs dominate primary production. An active methane cycle in Lake Matano reveals that methanogenesis and methanotrophy could have been important components of the earth's early marine C cycle.

Résumé- Le lac Matano en Indonésie, le 8ème lac le plus profond sur terre, est un écosystème aquatique extrèmement riche en Fe (ferrugineux) et est le meilleur analogue moderne de l'écologie des océans primitifs terrestres. La combinaison de processus géologiques, climatiques et biologiques a résulté en un écosytème aquatique centré sur le Fe dans lequel les communautés microbiennes anaérobiques se développent largement autour des cycles du Fe et du CH_4. Les sols riches en Fe du bassin de drainage fournissent en abondance des (hydro)xides de Fe aux sédiments du lac Matano. Un mélange vertical limité dans le lac Matano a généré une pycnocline persistante à 100 m de profondeur qui est maintenue par des fluctuations de température saisonnières minimales et une morphologie de bassin pentue. Cette pycnocline sépare une couche oxique de surface des eaux de fond riches en Fe(II) et CH_4.

Les conditions ferrugineuses du lac Matano limitent les concentrations en P dissous dans la couche oxique de surface où elles peuvent restreindre la production primaire. Les Chlorobiacées, qui peuplent la profonde et ferrugineuse chimiocline, sont une importante composante de la communauté phototrophe du lac Matano. Étant donnée l'absence de sulfures, la métabolisme de ces nouveaux phototrophes anoxygéniques d'eaux profondes sont vraisemblablement contrôlés par l'oxidation de Fe(II). La méthanogénèse domine la dégradation de la matière organique malgré la propension thermodynamique du lac Matano pour la réduction du Fe. Le méthane biogénique s'accumule dans les eaux de fond anoxiques et supporte l'activité de méthanotrophes aérobiques et anaérobiques. Les concentrations en Cr dans le lac Matano sont relativement élevées et réflètent la géologie du bassin de drainage. La perte de Cr des eaux de surface se fait par la réduction du Cr(VI) par le Fe(II), apporté par l'eau de fond anoxique. Le flux descendant de Cr qui s'ensuit maintient les concentrations en Cr(VI) dissous en-dessous des valeurs internationales recommandées.

La structure physique du lac Matano, l'abondance de Fe et l'absence de sulfates réflètent les conditions stratifiées ferrugineuses pensées prévaloir selon les océans primitifs terrestres. La découverte que les anoxygéniques phototrophes prolifèrent dans des conditions ferrugineuses appuie les modèles d'écologie des océans primitifs dans lesquels les phototrophes anoxygéniques dominent la production primaire. Un cycle de

méthane actif dans le lac Matano démontre que méthanogénèse et méthanotrophie ont pu être d'importantes composantes des cycles du carbone de la terre primitive.

Acknowledgements

This thesis is the result of more than 4 years of research which benefited from the help of many people to whom I am grateful. First, I thank my thesis advisors, Professors David Fowle, Bjørn Sundby and Alfonso Mucci for their mentorship, support, patience and encouragement. When I was a M.Sc. student at the University of Windsor, David introduced me to and captivated me with the exciting fields of geomicrobiology and biogeochemistry. Through David I have travelled the world, and viewed it through the eyes of someone rapt with how microorganisms underpin the geochemical cycles that support life on our planet. I thank David for providing me with the autonomy to pursue many avenues of research with numerous collaborators. When I thought there was something to learn from an experiment, field trip, or collaboration, David was always behind me not only intellectually but also financially. Perhaps most importantly, I thank David for conceiving our study of the Malili Lakes. More than four years ago, and without having been there himself, David sparked my interest in the system when he suggested that the lateritic composition of the soils in the catchment basin might render the Malili Lakes potential analogues for both early Earth and Martian ecosystems. I thank David for giving me the opportunity to join the Malili Lakes research team which ultimately allowed me to produce this thesis.

After having completed an undergraduate analytical chemistry laboratory on voltammetry and reviewing an early paper by George Luther et al. I became enamored with analytical electrochemistry and knew I wanted to learn more about this powerful technique as a graduate student. Little did I realize then in 2001 that I would have the opportunity to work with Bjørn Sundby, one of two principal investigators on this seminal work. I am grateful to Bjørn for teaching me the science and art of constructing and using voltammetric microelectrodes, a skill I intend to use for the rest of my career and to teach to as many as are willing to learn. I am also grateful to Bjørn for sharing his insight. During the first meeting Dave, Bjørn and I had (over beer in Windsor, Ontario) to plan a research program at the Malili Lakes and establish the beginning of my thesis, Bjørn took one look at a noisy, yet instrumental, data set of dissolved Fe in Lake Matano and said ‘that lake is stratified… this is interesting, we should focus on Fe’. Bjørn’s seemingly infinite wisdom always opened my mind to the big picture. Bjørn’s simple, yet

invaluable principles such as the KISS (Keep It Simple Stupid) rule ensured that all our field expeditions and laboratory experiments produced meaningful and interpretable data. I also, appreciate the time Bjørn took to try to convey to me the art of clear communication in writing.

I am grateful to Al for his critical eye and for sharing his very deep understanding of the fundamentals of aquatic chemistry and biogeochemistry with me. Al's skill as a teacher and his enthusiasm for the subject helped me begin to understand the vast knowledge base contained in the bible; Stumm and Morgan's 'Aquatic Chemistry'. I think it might be difficult for the authors to teach it better themselves. In the field and laboratory, Al's example always led me to strive for the highest level of scientific rigor. I am also greatful to Al for introducing me to the finer aspects of oceanographic research… scotch whisky consumption. Most importantly, I am grateful to Al, Bjørn and David for their friendship.

Although not an official member of my advisory committee, I also thank Professor Douglas Haffner for his mentorship. In a memorable lunch meeting with Doug and David at 'Rock Bottom' Doug introduced me to Lake Matano, and invited me to join his research program there. Doug's early work on the Malili Lakes provided the foundation from which I built this thesis.

I appreciate the financial and logistical support provided by INCO Canada (now Vale INCO) for this research. Importantly, I thank William Napier for his role as my industry supervisor and Mike Dutton for continuing in this role after Bill's departure. The staff of PT INCO Indonesia especially Deky Tetradiono, Lili Lubis Nuria, Matt Orr, Ibu Cinta and Pak Sunarso are thanked for their friendship and tireless support during my time in Indonesia. Additionaly, I acknowledge the support of Dahalan Tase, Dula and Ali who drove our boats and provided security. Sinyo Rio is thanked for helping with logistics and sampling. Researchers from the Indoneisan Limnological Institute are thanked for their support especially Peter Hehanussa, Dr. Gadis Sri Haryani, Sulung Nomosatryo and Awalina Satya.

I am also grateful to Professor Donald Canfield for helping to establish Lake Matano as an early ocean analogue. I thank Don for sharing with me his great understanding of the conditions that likely prevailed in the earth's earliest oceans.

Without Don's involvement it would have difficult to to fully realize all of the aspects in which Lake Matano parallels ferruginous ocean conditions. I am also grateful to Don for the logistical support he provided during my final field season at Lake Matano, and when unable to come himself, for sending CarriAyne Jones in his stead.

I acknowledge the companionship of CarriAyne Jones throughout the last year of my research and writing. Not only was CarriAyne's involvement in the collection and interpretation of data for Chapter 4 critical to its development, she also provided insightful comments on Chapter 6. I also appreciate CarriAyne's help with writing Chapters 4 and 6 and for her grammatical editing throughout.

I am grateful to Cédric Magen, Arne Sturm, Karla Leslie and Andrew O'Neill for their friendship, comradery and collegiality. Without Arne, Cédric, Karla and Andrew it would have been difficult to endure the many late nights and early mornings in the office and laboratory. Andrew, Arne and Cédric were also invaluable to the success of our field trips in Indonesia. I also thank all of the Post Docs with whom I collaborated on various aspects of this thesis especially Drs Sergei Katsev and Andrew O'Neill. I have learned a great deal from a number of other Post Docs and Ph.D. students in Windsor and Montreal including Chris Weisener, Gwen Chaillou, Adrian Villegas-Jimenez, Sang-Tae Kim, Denis Roy and David Porta-Tena. Similarly, Professor Jennifer Roberts is thanked for the use of her lab and for many helpful suggestions and discussions throughout my thesis. I thank the other graduate students with whom I shared many good experiences and who helped me at various points during my thesis including Ezra Kulczycki, Paul Kenward, Ryan Walter, Christine DesJardins, Andrew Bramburger and Amy Snook. I am grateful to Elisabeth Sabo who spent many long nights in the laboratory with me and contributed significantly to the intellectual development of this thesis. Lis was instrumental to the success of our first two field seasons at Lake Matano which resulted in the writing of Chapter 1 and the formulation of many of the hypothesis which resulted in Chapters 4 and 6.

Finally, I thank my family, especially my parents Dennis and Terry Crowe, and my daughter Tenneal Crowe for their patience and understanding of my absence during the last 4 years. I am exceptionally grateful to my father for his example as a role model and for his guidance during the many decisions that led me to pursue this degree. I am

equally grateful to my mother for her unconditional support and for the encouragement she provided when I needed it, especially before my comprehensive examinations.

Table of Contents

Contributions of Authors 4
Abstract 6
Résumé 7
Acknowledgements 9
Chapter 1 15
1.1 Fe in the Earth 15
1.2 Abundance and speciation of Fe in aquatic environments 15
1.3 Fe-redox transformations and microbial energy derivation 17
1.4 The ecology and evolution of iron driven metabolisms 20
1.5 An end-member system: The Malili Lakes 22
1.6 Thesis objectives 23
1.7 Thesis outline 23
1.8 References 24
Chapter 2. The biogeochemistry of tropical lakes: A case study from Lake Matano, Indonesia 32
2.1 Abstract 32
2.2 Introduction 33
2.3 Regional setting 34
2.4 Methods 36
2.5 Results and discussion 38
2.6 References 55
2.7 Supplementary Information (Numerical description of reaction-transport model) 72
Chapter 3. Link between Chapters 2 and 4 77
3.1 Linking Lake Matano to the earth's early oceans 77
3.2 Primary production and pathways of C fixation 77
3.3 References 77
Chapter 4. Anoxygenic phototrophs thrive in an Archean Ocean analogue 79
4.1 Abstract 79
4.2 Introduction 80
4.3 Physical, chemical and microbial features of Lake Matano 82
4.4 Lake Matano as an ancient ocean analog 84
4.5 Conclusions and Extensions 86
4.6 Materials and Methods 87
4.7 References 94
4.8 Supplementary Information (Voltammetric Speciation Analyses) 99
4.9 Supplementary References 100
Chapter 5. Link between Chapters 4 and 6 107
5.1 Dissolved gases? 107
5.2 C cycling 107
5.3 References 107
Chapter 6. The methane cycle in tropical Lake Matano: Methanogenesis, methane accumulation, and anaerobic methane oxidation 108
6.1 Abstract 108
6.2 Introduction 110

6.3 Methods 112
6.4 Results 114
6.5 Discussion 119
6.6 References 132
6.7 Supplementary Information (Competition between methanotrophs and Fe(II) for O_2) 137
6.8 Supplementary Information (Modeling isotope fluxes) 139
Chapter 7. Link between Chapters 6 and 8 149
7.1 Limiting Primary Production? 149
7.2 References 149
Chapter 8. Cr cycling in Wallace's Dreamponds 150
8.1 Abstract 150
8.2 Introduction 150
8.2 Methodology 152
8.3 Results and Discussion 154
8.4 References 166
Chapter 9. Conclusions 172

Chapter 1. Introduction. The Aquatic Geochemistry and Geomicrobiology of Fe

1.1 Fe in the Earth

Comprising 4.3% by mass, iron is the 4th largest constituent of the earth's crust (Canfield et al. 2005) but the most abundant metal on Earth. Within the earth's crust Fe exists largely in the trivalent, ferric (Fe(III)) and divalent, ferrous (Fe(II)) oxidation states with a ratio of Fe(II):Fe(III) of nearly 1.5 (Faure 1997). The abundance of Fe in both oxidation states imparts significant redox buffering capacity at the earth's surface. It is not surprising therefore that both Fe(III) and Fe(II) are important and ubiquitous constituents of aquatic environments where they exist in a plethora of solid and dissolved forms with a wide range of chemical and physical properties (Davison 1993; De Vitre et al. 1994; Stumm and Morgan 1996). The positioning of Fe(II)/Fe(III) redox couples at potentials between that of organic matter and molecular oxygen (O_2), poises Fe to mediate electron transfer between these two photosynthetic energy reservoirs (Canfield et al. 2005; Stumm and Morgan 1996). Thus, Fe plays a critical role in biogeochemical cycling.

.

1.2 Abundance and speciation of Fe in aquatic environments

Two factors dictate the importance of Fe to biogeochemical cycling in a given environment: its relative abundance and speciation (Canfield et al. 2005). For example, it has been shown that the significance of microbial Fe-reduction to organic C oxidation in marine and freshwater sediments is directly proportional to the abundance of poorly crystalline Fe (hydr)oxides (Thamdrup 2000). The Fe content of marine sediments typically varies by less than one order of magnitude and a survey of more than 200 sediments, from continental shelves to the deep sea, yielded Fe concentrations ranging from 0.5 % to 6 % (dry weight) (Raiswell and Canfield 1998). The differences in Fe content were largely attributed to pre-depositional factors including the relative supply of Fe-free and Fe-bearing minerals derived from continental weathering. The Fe content of lacustrine sediments is more variable and reflects regional heterogeneities in the geology of catchment basins and local weathering rates.

The speciation of Fe in aquatic environments is highly dependent on both pH and pe (Stumm and Morgan 1996). At circumneutral and alkaline pH values, ferric Fe is highly insoluble. For example, seawater at pH 8 in equilibrium with poorly crystalline Fe (hydr)oxides (e.g. ferrihydrite) contains on the order of 10^{-8} mol l^{-1} dissolved Fe(III) (Thamdrup 2000). In freshwaters at neutral pH, the dominant dissolved inorganic Fe species is $Fe(OH)_3^0$ (~10^{-11} mol l^{-1}) whereas the concentration of the simple hydrated aquo Fe^{3+} ion is negligible (< 10^{-17} mol l^{-1}) (De Vitre et al. 1994). The solubility of ferric Fe (Fe(III)) in both fresh and seawater can be markedly enhanced by complexation with dissolved organic ligands (Boukhalfa and Crumbliss 2002; Liu and Millero 2002; Nagai et al. 2007). Strong natural ligands are produced by cyanobacteria as a strategy to gain access to Fe(III), an essential nutrient for the biosynthesis of proteins like cyctochromes which facilitate intracellular electron transport (Hutchins et al. 1999; Reid and Butler 1991; Wilhelm et al. 1996; Wilhelm and Trick 1994). Dissolved Fe(III) organic complexes have also been detected in sediment pore waters, although the origin, identity, and potential biological role of the ligands remain unknown (Luther et al. 1996). Given its low solubility, most Fe(III) in aquatic environments occurs as particulate or colloidal material. Solid Fe(III) is found with a broad range of non-crystalline to highly ordered chemical structures. In the presence of high, dissolved Si concentrations, solid Fe(III) can persist as amorphous gels. In contrast, when dried, poorly crystalline ferric (hydr)oxides readily convert to highly crystalline hydroxides and oxides like goethite (α-FeOOH) or hematite (Fe_2O_3) (Davison 1993). In silicate rocks, the ultimate source of Fe in aquatic environments, Fe(III) largely occurs as hematite and the mixed valence oxide magnetite (Fe_3O_4), but it can also be found in silicate minerals including Fe(III) bearing clays. A comprehensive survey of marine sediments revealed that an average of 25 % of total sedimentary Fe was in the form of oxides (Raiswell and Canfield 1998). This is comparable to the 35 % present as oxides in particulates sampled from rivers of the United States (Canfield 1997). To our knowledge, similar surveys have not been conducted for a comprehensive suite of lake sediments but the distribution of Fe could be expected to be similar to that in marine sediments, with more variability.

Ferrous Fe (Fe(II)) is much more soluble than ferric Fe under circumneutral and alkaline conditions and it is not uncommon for Fe(II) to reach concentrations on the order

of 10^{-4} mol l^{-1} in anoxic pore waters and in the bottom of stratified water bodies (Davison 1993; De Vitre et al. 1994; Millero et al. 1995). Nevertheless, Fe(II) concentrations in circumneutral anoxic waters are often limited in the presence of sulfide by the solubility of FeS (KSp = $10^{-2.95}$, (Davison 1991)) species. In addition to sulfides, Fe(II) may also form carbonates (siderite, $FeCO_3$), phosphates (vivianite, $Fe_3(PO_4)_2 \bullet 8H_2O$) or mixed valence oxides (magnetite, Fe_3O_4) in anoxic aquatic environments (De Vitre et al. 1994).

Dissolution and precipitation often accompany Fe reduction or oxidation reactions due to the dramatic difference between the solubilities of ferrous and ferric Fe under conditions encountered in most aquatic environments. As phase changes frequently accompany Fe redox reactions, physical transport of the products is often induced leading to a spatial separation of the oxidation and reduction halves of the Fe-cycle. The gradients produced by the transport of Fe generate disequilibrium conditions conducive to the proliferation of stratified microbial communities partially or wholly supported by Fe redox transformations.

1.3 Fe-redox transformations and microbial energy derivation

Many Fe redox reactions can proceed abiologically but a number are facilitated by microorganisms, many of which support their metabolic activities with energy gained from Fe oxidation or reduction (see below) (Canfield et al. 2005). Perhaps the two most important abiotic Fe redox transformations in aquatic environments are the oxidation of Fe(II) by O_2 and reduction of Fe(III) by sulfide. Fe(III) oxidation by O_2 is very rapid under circumneutral and alkaline pH conditions (Millero et al. 1987). The rapid oxidation of Fe(II) by O_2 and subsequent hydrolysis of Fe^{3+} yields highly reactive, poorly crystalline Fe (hydr)oxides with exceptionally small particle sizes (De Vitre et al. 1988; Taillefert et al. 2000; Taillefert and Gaillard 2002). In turn, the surfaces of the Fe (hydr)oxides further enhance oxidation rates through a heterogeneous autocatalytic reaction (Millero et al. 1987). In freshwaters, authigenic Fe (hydr)oxide particles remain finely divided and settle slowly, whereas the high ionic strength of seawater favors coagulation and flocculation. Sedimentation of fine particulate Fe (hydr)oxides can also be accelerated by the presence of dissolved or particulate organic compounds such as extracellular polymeric substances and cellular debris which bind to Fe (hydr)oxide

surfaces and induce aggregation. Abiotic Fe(II) oxidation by Mn (hydr)oxides is also possible, but the quantitative significance of this pathway is unclear.

The most important abiotic reductant of Fe(III) in aquatic environments is sulfide (HS^-). Sulfide is produced by microbial dissimilatory sulfate reduction (DSR) (Canfield et al. 2005), an anaerobic respiratory microbial metabolism which couples the oxidation of organic compounds to the reduction of dissolved sulfate. Locally, sulfide can also originate from geothermal sources where it emanates through hydrothermal vents (Canfield et al. 2005). Reactions of HS^- with Fe (hydr)oxide minerals are complicated and highly dependent on the relative abundances of Fe and HS^-, the Fe(II) speciation, pH and the concentration of Fe binding ligands (Luther et al. 1992; Rickard and Luther 2007; Taillefert et al. 2002; Yao and Millero 1996). Typically, the reaction involves the adsorption of HS^- to Fe (hydr)oxide surfaces followed by the reductive dissolution of Fe(III) and production of dissolved Fe(II), sulfate, elemental S, and FeS surface precipitates, colloids and larger particles (Luther et al. 2003; Luther et al. 1992; Yao and Millero 1996). Fe(III) may also be reduced abiotically by organic compounds but the quantitative significance of this pathway in the environment is thought to be minimal (De Vitre et al. 1994; Lovley et al. 1991).

Microorganisms play a substantial role in mediating Fe redox cycling (Emerson and Weiss 2004; Lovley et al. 2004; Weber et al. 2006a). This is most evident in the case of Fe(III) reduction. Almost all Fe(III) reduction under non-sulfidic conditions occurs through a respiratory metabolism termed dissimilatory iron reduction (DIR), for which energy is typically gained through the oxidation of organic carbon with Fe(III) as the sole electron acceptor (Lovley et al. 2004; Lovley et al. 1991; Thamdrup 2000). H_2 is also used as an electron donor by DIR microorganisms and most of these are also capable of using alternative electron acceptors such as Mn(VI) (Canfield et al. 2005; Lovley et al. 2004; Thamdrup 2000). Substantial DIR can occur in many sulfate reducing environments and DIR can account for more than 50% of total organic carbon degradation in Fe-rich marine sediments (Canfield et al. 1993a; Canfield et al. 1993b). As noted above, the extent of Fe reduction and its importance to organic C degradation reflects the abundance of poorly crystalline Fe (hydr)oxides such as ferrihydrite. Crystalline Fe (hydr)oxides like goethite, hematite (Roden and Zachara 1996), magnetite

(Kostka and Nealson 1995) as well as Fe(III) bearing silicates (Jaisi et al. 2007; Kostka et al. 1999; Kostka et al. 1996) also support DIR (see Glasauer et al. 2003 for an alternate opinion), but the more crystalline Fe substrates typically yield slower rates of reduction in laboratory experiments. Rates of solid Fe(III) reduction are mostly controlled by the availability of reactive surface sites whose abundance decreases with progressive Fe reduction as a result of Fe(II) adsorption (Roden 2003; Roden 2004; Roden and Zachara 1996). Growth from DIR is also supported by dissolved Fe(III) organic complexes (Lovley et al. 2004) and the rates of DIR are inversely proportional to the stability of the complex (Haas and Dichristina 2002). On the other hand, a significant reservoir of dissolved Fe(III) has yet to be identified in aquatic environments and environmental DIR microorganisms appear to be sustained largely on solid Fe (hydr)oxides. Yet, the transfer of electrons generated within the cell to a sink in solid phase extracellular Fe (hydr)oxides is a substantial impediment to DIR microorganisms (Canfield et al. 2005; Lovley et al. 2004; Nevin and Lovley 2002a; Thamdrup 2000). A number of strategies have been proposed for DIR microorganisms to achieve extracellular electron transport including: 1) direct contact of outer membrane cytochromes with Fe (hydr)oxide surfaces (Lies et al. 2005; Lower et al. 2001; Mehta et al. 2005; Nevin and Lovley 2000); 2) use of exogenous (Lovley et al. 1996) or cell derived (Hernandez et al. 2004; Marsili et al. 2008; Newman and Kolter 2000) soluble redox active molecules like quinones to shuttle electrons from within the cell to Fe (hydr)oxides; 3) production of soluble Fe ligands to complex and dissolve Fe (hydr)oxides (Crowe et al. 2007; Nevin and Lovley 2002b); and 4) construction of electrically conductive extracellular appendages or 'nanowires' that allow electron flow from within cells to Fe (hydr)oxides (Gorby et al. 2006; Reguera et al. 2005). Laboratory evidence exists to support all of these mechanisms yet their respective importance in the environment remains unknown.

Fe(II) oxidation can also be mediated by microorganisms (Emerson and Weiss 2004). Some iron oxidizing microorganisms (FOM) can grow autotrophically with Fe(II) as the sole electron donor and O_2 as the sole electron acceptor (Emerson and Moyer 1997). In many aquatic environments, these organisms are often responsible for substantial Fe(II) oxidation despite the rapid rates of abiotic oxidation with O_2 at near neutral and alkaline pHs (Emerson and Weiss 2004). To effectively compete with abiotic

Fe(II) oxidation, aerobic FOM dwell in microoxic zones with low oxygen concentrations, conditions under which the rates of abiotic Fe(II) oxidation are diminished (Emerson and Weiss 2004). FOM are widespread and have been identified in both marine and freshwater environments (Emerson and Weiss 2004). FOM are not restricted to the use of O_2 as an electron acceptor and can also grow with NO_3^-, perchlorate, and chlorate as terminal electron sinks (Bruce et al. 1999; Straub et al. 1996; Weber et al. 2001; Weber et al. 2006b; Weber et al. 2006c). These alternative electron acceptors facilitate a completely anaerobic Fe-cycle, whereby Fe can be reduced and oxidized repeatedly in the absence of O_2. The widespread availability of NO_3^- in aquatic environments makes the recently discovered nitrate-dependent Fe(II) oxidation of special environmental significance. In nitrate-dependent Fe(II) oxidation, FOM couple Fe(II) oxidation with the reduction of NO_3^- to N_2 (i.e. denitrification). Hence, FOM can potentially interact with the N cycle and their activity may reduce the availability of N, an essential nutrient for all organisms. Anaerobic Fe oxidation can also be achieved phototrophically (Heising et al. 1999; Heising and Schink 1998; Straub et al. 1999; Widdel et al. 1993). Phototrophic Fe(II) oxidizers use the oxidation of Fe(II) to resupply electrons lost from the photosystem during C fixation . To date, Fe-oxidizing phototrophs have only been identified in ephemeral environments like groundwater seeps and springs and some shallow marine sediments. Their distribution, activity and importance to Fe cycling have yet to be determined and the ecological significance of FOM is remains unclear.

In summary, redox transformations of Fe support substantial microbial life in aquatic environments. Although many of the qualitative aspects of the Fe-cycle have been known since the seminal studies by Mortimer (Mortimer 1941; Mortimer 1942), many of the intricacies remain elusive, partly because of the involvement of microorganisms and the inherent complexity of microbial metabolism and ecology (Newman and Banfield 2002).

1.4 The ecology and evolution of iron driven metabolisms

As Fe is ubiquitous in aquatic environments so are DIR microorganisms and FOM (Canfield et al. 2005). DIR microorganisms are found in almost all anaerobic marine and freshwater sediments as well as anoxic basins and soils (Lovley et al. 2004) and the

distribution of FOM may be nearly as broad (Emerson and Weiss 2004; Straub et al. 2004; Weber et al. 2006c). DIR microorganisms isolated to date have been found to grow at extremes in temperature, acidity and basicity (Lovley et al. 2004). Indeed, DIR Archea most closely related to *Pyrodictium occultum* can lay claim to the upper limit of tolerance to temperature and are capable of growing at greater than 121º C (Kashefi and Lovley 2003). The broad distribution of DIR microorganisms in the environment is mirrored by their phylogenic diversity and distribution amongst many lineages in both the Archeal and Bacterial prokaryotic domains (Lovley et al. 2004). This exceptional phyllogenetic diversity has led to the hypothesis that the metabolic capacity for Fe reduction evolved early in the earth's history and may have been the first respiratory metabolism. Indeed, the capacity to respire iron is more universal among deeply branching lineages than respiration using any other terminal electron acceptor (Lovley et al. 2004). This is consistent with what is known about the availability of electron acceptors in the earliest oceans (abundant Fe(III), scarce O_2, NO_3^-, and SO_4^{2-}) (Canfield et al. 2006) and is also supported by phyllogenetic analyses which reveal that the extant microorganisms most closely related to the last common ancestor (LCA) respire through DIR (Vargas et al. 1998). Arguably, a critical step in the development of DIR would have been the acquisition of an enzyme system enabling the access of extracellular Fe(III) electron acceptors. Such an enzyme system may be a unifying attribute among the diverse lineages of DIR microorganisms. Nonetheless, as noted above, the specific enzyme systems allowing DIR microorganisms to access solid Fe(III), and the genes that encode for them remain elusive.

A requirement of both the early evolution of DIR microorganisms and their presence in modern environments is the availability of Fe(III). There is abundant geological evidence, in the form of banded iron formations which are common Fe-rich, marine, sedimentary rocks that formed more than 1.8 Ga ago, that the early oceans contained appreciable amounts of Fe(III) (Canfield et al. 2006). The origin of this Fe(III) is a subject of debate but the available evidence points towards Fe(II) oxidation by iron oxidizing microorganisms (FOM) (Kappler et al. 2005; Konhauser et al. 2007; Konhauser et al. 2002). The early evolution of FOM is also indicated by their phylogenetic diversity. This argument, however, is not as well supported as for DIR microorganisms, as the

FOM do not appear to be as widely distributed (Weber et al. 2006a) or as closely related to the last common ancestor (LCA). Of particular importance however, is the potential role of phototrophic FOM in the early oceans which could have produced Fe(III) prior to the evolution of cyanobacteria and the oxygenation of the atmosphere (Canfield et al. 2006). In fact, molecular microbiological evidence reveals that the anoxygenic photosystems utilized by phototrophic FOM evolved prior to the oxygenic photosystems of cyanobacteria (Xiong et al. 2000). One hypothesis is that marine productivity in the early ferruginous oceans was dominated by phototrophic FOM (Canfield et al. 2006). Organic matter and Fe(III) produced by Fe oxidizing phototrophs could have driven early ocean Fe and C cycles (Canfield et al. 2006). The relative importance of iron based metabolisms to C cycling would have diminished with the advent of oxygenic photosynthesis and the development of S-rich oceans in the Proterozoic. Vestiges of the ancient anaerobic Fe-cycle and its Fe-centric microbial ecosystems may now be preserved in small niches where anaerobic Fe-cycling is invariably complicated by interactions with O_2 and species of N and S. Unraveling the development of iron based metabolisms and their ecological controls stands to benefit from the availability of model Fe-rich end-member environments from which analogies can be drawn to the early ferruginous oceans. By extension, much could be learned about the early evolution of life and the bioshpere from the ecology of such modern analogues.

1.5 An end-member system: The Malili Lakes

The Malili Lakes of Indonesia comprise a set of limnological conditions that offer a unique opportunity to study an Fe-rich, end-member aquatic environment (Crowe et al. 2004; Haffner et al. 2001). The lakes, which are located on Sulawesi Island, are a morphologically diverse group that includes Lake Matano, Lake Mahalona, Lake Towuti, Lake Lawontoa and Lake Masapi. Lake Matano, the headwater lake of the system, has been the most extensively investigated to date (Crowe et al. 2004; Haffner et al. 2001). Lake Matano is a graben hosted tectonic lake, and, at >550 m deep, is one of the 10 deepest lakes in the world. It has been suggested, based on geological and biological information, that Lake Matano is between one and four million years old (Doug Haffner personal communication). Due to the relatively steep regional topography (the highest

point is 1400-1700 m asl, the lake surface is at 382 m asl), the lake's catchment basin is relatively small (~436 km^2). It is dominated by nickeliferrous lateritic soils (up to 60 % Fe oxides) that developed on ultramafic rocks of ophiolitic origin (Golightly 1981). The Fe-rich nature of the catchment soils suggests that Lake Matano receives a large flux of allogenic Fe (hydr)oxides.

Limnological analyses of Lake Matano have been conducted as part of an ongoing environmental monitoring program initiated by PT INCO International and the Great Lakes Institute for Environmental Research (GLIER) since the 1990's (Crowe et al. 2004; Haffner et al. 2001). Results of these investigations suggest that Lake Matano stratifies periodically allowing for the accumulation of Fe(II) in the hypolimnion. Analyses of Lake Matano's sediments revealed that they comprise up to 20 wt. % Fe (hydr)oxides (Crowe et al. 2004), nearly 4 times the abundance found in Fe-rich marine sediments. The composition of Lake Matano's sediments dictates an important role for Fe in biogeochemical cycling. Given its estimated age, ferruginous Lake Matano may have harbored the evolution of its own Fe-centric microbial ecosystem and, thus, further studies may yield valuable insights into the functioning of the Earth's early oceans and the early evolution of life on Earth.

1.6 Thesis objectives

Broadly, the objectives of this thesis are to enhance our understanding of the biogeochemistry of Lake Matano and by extension other Fe-rich aquatic environments. A primary goal is to understand the physical dynamics of Lake Matano and to test the hypothesis that it stratifies periodically. With this understanding, my second objective is to determine how the physical dynamics control the cycling of Fe, nutrients and trace elements within Lake Matano's water column. Finally, this information on biogeochemical cycling can be used to test the hypotheses that Fe abundance influences microbial ecology and that Lake Matano is a suitable analogue for the Archean Ocean.

1.7 Thesis outline

In the Chapters that follow, I explore the biogeochemistry of Fe and its impact on the ecology of an Fe-rich (ferruginous) lacustrine environment, Lake Matano. In Chapter

2, I describe the limnology of ferruginous Lake Matano, Indonesia with an emphasis on the distribution of trace elements and nutrients as well as the physical dynamics. Chapter 4 describes the photosynthetic communities and primary productivity of Lake Matano. It also documents a novel Fe(II) oxidizing phototrophic community and draws analogies between Lake Matano and the ferruginous Archean and Proterozoic oceans. The methane cycle in Lake Matano is described in Chapter 6, in which I test the hypotheses that ferruginous conditions impede methanogenesis and preclude anaerobic methane oxidation. The importance of the methane cycle in ferruginous environments is analyzed in the context of its role in C cycling. Finally, in Chapter 8, I describe Cr cycling in Lake Matano and highlight the importance of Fe-cycling in maintaining Cr concentrations below international guidelines. The Cr isotope system is used to constrain rates of Cr reduction

1.8 References

Boukhalfa, H. and Crumbliss, A. L., 2002. Chemical aspects of siderophore mediated iron transport. *BioMetals* **15**, 325-339.

Bruce, R. A., Achenbach, L. A., and Coates, J. D., 1999. Reduction of (per)chlorate by a novel organism isolated from paper mill waste. *Environ. Microbiol.* **1**, 319-329.

Canfield, D. E., 1997. The geochemistry of river particulates from the continental USA: Major elements. *Geochim. Cosmochim. Acta* **61**, 3349-3365.

Canfield, D. E., Jorgensen, B. B., Fossing, H., Glud, R., Gundersen, J., Ramsing, N. B., Thamdrup, B., Hansen, J. W., Nielsen, L. P., and Hall, P. O. J., 1993a. Pathways of organic-carbon oxidation in 3 continental-margin sediments. *Mar. Geol.* **113**, 27-40.

Canfield, D. E., Kristensen, E., and Thamdrup, B., 2005. *Aquatic Geomicrobiology*. Elsevier, San Diego.

Canfield, D. E., Rosing, M. T., and Bjerrum, C., 2006. Early anaerobic metabolisms. *Philosophical Transactions of the Royal Society B-Biological Sciences* **361**, 1819-1834.

Canfield, D. E., Thamdrup, B., and Hansen, J. W., 1993b. The anaerobic degradation of organic-matter in Danish coastal sediments - Iron reduction, manganese reduction, and sulfate reduction. *Geochim. Cosmochim. Acta* **57**, 3867-3883.

Crowe, S. A., Pannalal, S. J., Fowle, D. A., Cioppa, M. T., Symons, D. T. A., Haffner, G. D., Fryer, B. J., McNeely, R., Sundby, B., and Hehanussa, P. E., 2004. Biogeochemical cycling in Fe-rich sediments from Lake Matano, Indonesia *13th International symposium on water-rock interaction*, Saratoga Springs, USA.

Crowe, S. A., Roberts, J. A., Weisener, C. G., and Fowle, D. A., 2007. Alteration of iron-rich lacustrine sediments by dissimilatory iron-reducing bacteria. *Geobiology* **5**, 63-73.

Davison, W., 1991. The Solubility of iron sulfides in synthetic and natural-waters at ambient-temperature. *Aquatic Sciences* **53**, 309-329.

Davison, W., 1993. Iron and manganese in lakes. *Earth-Sci Rev* **34**, 119-163.

De Vitre, R. R., Buffle, J., Perret, D., and Baudat, R., 1988. A study of iron and manganese transformations at the O_2/S(II) transition layer in a eutrophic lake (Lake Bret, Switzerland) - a multimethod approach. *Geochim. Cosmochim. Acta* **52**, 1601-1613.

De Vitre, R. R., Sulzberger, B., and Buffle, J., 1994. Transformations of Iron at Redox Boundaries. In: Buffle, J. and Devitre, R. R. Eds.), *Chemical and Biological Regulation of Aquatic Systems*. CRC press, Boca Raton.

Emerson, D. and Moyer, C., 1997. Isolation and characterization of novel iron-oxidizing bacteria that grow at circumneutral pH. *Appl. Environ. Microbiol.* **63**, 4784-4792.

Emerson, D. and Weiss, J. V., 2004. Bacterial iron oxidation in circumneutral freshwater habitats: Findings from the field and the laboratory. *Geomicrobiol. J.* **21**, 405-414.

Faure, G., 1997. *Principles and Applications of Geochemistry*. Prentice Hall, Upper Saddle River, New Jersey, USA.

Glasauer, S., Weidler, P. G., Langley, S., and Beveridge, T. J., 2003. Controls on Fe reduction and mineral formation by a subsurface bacterium. *Geochim. Cosmochim. Acta* **67**, 1277-1288.

Golightly, J. P., 1981. Nickeliferous Laterite Deposits. *Economic Geology* **75th Anniversary Volume**, 710-735.

Gorby, Y. A., Yanina, S., McLean, J. S., Rosso, K. M., Moyles, D., Dohnalkova, A., Beveridge, T. J., Chang, I. S., Kim, B. H., Kim, K. S., Culley, D. E., Reed, S. B., Romine, M. F., Saffarini, D. A., Hill, E. A., Shi, L., Elias, D. A., Kennedy, D. W., Pinchuk, G., Watanabe, K., Ishii, S., Logan, B., Nealson, K. H., and Fredrickson, J. K., 2006. Electrically conductive bacterial nanowires produced by Shewanella oneidensis strain MR-1 and other microorganisms. *Proceedings of the National Academy of Sciences of the United States of America* **103**, 11358-11363.

Haas, J. R. and Dichristina, T. J., 2002. Effects of Fe(III) chemical speciation on dissimilatory Fe(III) reduction by Shewanella putrefaciens. *Environ. Sci. Technol.* **36**, 373-380.

Haffner, G. D., Hehanussa, P. E., and Hartoto, D., 2001. The biology and physical processes of large lakes of Indonesia. In: Munawar, M. and Hecky, R. E. Eds.), *The Great Lakes of the World: Food web, health and integrity*. Backhuys Publishers, Leiden.

Heising, S., Richter, L., Ludwig, W., and Schink, B., 1999. *Chlorobium ferrooxidans* sp nov., a phototrophic green sulfur bacterium that oxidizes ferrous iron in coculture with a "*Geospirillum*" sp strain. *Arch. Microbiol.* **172**, 116-124.

Heising, S. and Schink, B., 1998. Phototrophic oxidation of ferrous iron by a *Rhodomicrobium vannielii* strain. *Microbiol. UK* **144**, 2263-2269.

Hernandez, M. E., Kappler, A., and Newman, D. K., 2004. Phenazines and other redox-active antibiotics promote microbial mineral reduction. *Appl. Environ. Microbiol.* **70**, 921-928.

Hutchins, D. A., Witter, A. E., Butler, A., and Luther, G. W., 1999. Competition among marine phytoplankton for different chelated iron species. *Nature* **400**, 858-861.

Jaisi, D. P., Dong, H. L., and Liu, C. X., 2007. Influence of biogenic Fe(II) on the extent of microbial reduction of Fe(III) in clay minerals nontronite, illite, and chlorite. *Geochim. Cosmochim. Acta* **71**, 1145-1158.

Kappler, A., Pasquero, C., Konhauser, K. O., and Newman, D. K., 2005. Deposition of banded iron formations by anoxygenic phototrophic Fe(II)-oxidizing bacteria. *Geology* **33**, 865-868.

Kashefi, K. and Lovley, D. R., 2003. Extending the upper temperature limit for life. *Science* **301**, 934-934.

Konhauser, K. O., Amskold, L., Lalonde, S. V., Posth, N. R., Kappler, A., and Anbar, A., 2007. Decoupling photochemical Fe(II) oxidation from shallow-water BIF deposition. *Earth. Planet. Sci. Lett.* **258**, 87-100.

Konhauser, K. O., Hamade, T., Raiswell, R., Morris, R. C., Ferris, F. G., Southam, G., and Canfield, D. E., 2002. Could bacteria have formed the Precambrian banded iron formations? *Geology* **30**, 1079-1082.

Kostka, J. E., Haefele, E., Viehweger, R., and Stucki, J. W., 1999. Respiration and dissolution of iron(III) containing clay minerals by bacteria. *Environ. Sci. Technol.* **33**, 3127-3133.

Kostka, J. E. and Nealson, K. H., 1995. Dissolution and reduction of magnetite by bacteria. *Environ. Sci. Technol.* **29**, 2535-2540.

Kostka, J. E., Stucki, J. W., Nealson, K. H., and Wu, J., 1996. Reduction of structural Fe(III) in smectite by a pure culture of Shewanella putrefaciens strain MR-1. *Clays Clay Miner.* **44**, 522-529.

Lies, D. P., Hernandez, M. E., Kappler, A., Mielke, R. E., Gralnick, J. A., and Newman, D. K., 2005. Shewanella oneidensis MR-1 uses overlapping pathways for iron reduction at a distance and by direct contact under conditions relevant for biofilms. *Appl. Environ. Microbiol.* **71**, 4414-4426.

Liu, X. W. and Millero, F. J., 2002. The solubility of iron in seawater. *Mar. Chem.* **77**, 43-54.

Lovley, D. R., Coates, J. D., BluntHarris, E. L., Phillips, E. J. P., and Woodward, J. C., 1996. Humic substances as electron acceptors for microbial respiration. *Nature* **382**, 445-448.

Lovley, D. R., Holmes, D. E., and Nevin, K. P., 2004. Dissimilatory Fe(III) and Mn(IV) reduction. *Advances in Microbial Physiology, Vol. 49* **49**, 219-286.

Lovley, D. R., Phillips, E. J. P., and Lonergan, D. J., 1991. Enzymatic Versus Nonenzymatic Mechanisms for Fe(III) Reduction in Aquatic Sediments. *Environ. Sci. Technol.* **25**, 1062-1067.

Lower, S. K., Hochella, M. F., and Beveridge, T. J., 2001. Bacterial recognition of mineral surfaces: Nanoscale interactions between Shewanella and alpha-FeOOH. *Science* **292**, 1360-1363.

Luther, G. W., Glazer, B., Ma, S. F., Trouwborst, R., Shultz, B. R., Druschel, G., and Kraiya, C., 2003. Iron and sulfur chemistry in a stratified lake: Evidence for iron-rich sulfide complexes. *Aquat. Geochem.* **9**, 87-110.

Luther, G. W., Kostka, J. E., Church, T. M., Sulzberger, B., and Stumm, W., 1992. Seasonal iron cycling in the salt-marsh sedimentary environment - the importance of ligand complexes with Fe(II) and Fe(III) in the dissolution of Fe(III) minerals and pyrite, respectively. *Mar. Chem.* **40**, 81-103.

Luther, G. W., Shellenbarger, P. A., and Brendel, P. J., 1996. Dissolved organic Fe(III) and Fe(II) complexes in salt marsh porewaters. *Geochim. Cosmochim. Acta* **60**, 951-960.

Marsili, E., Baron, D. B., Shikhare, I. D., Coursolle, D., Gralnick, J. A., and Bond, D. R., 2008. Shewanella secretes flavins that mediate extracellular electron transfer. *Proceedings of the National Academy of Sciences of the United States of America* **105**, 3968-3973.

Mehta, T., Coppi, M. V., Childers, S. E., and Lovley, D. R., 2005. Outer membrane c-type cytochromes required for Fe(III) and Mn(IV) oxide reduction in Geobacter sulfurreducens. *Appl. Environ. Microbiol.* **71**, 8634-8641.

Millero, F. J., Sotolongo, S., and Izaguirre, M., 1987. The oxidation-kinetics of Fe(II) in Seawater. *Geochim. Cosmochim. Acta* **51**, 793-801.

Millero, F. J., Yao, W. S., and Aicher, J., 1995. The Speciation of Fe(II) and Fe(III) in natural-waters. *Mar. Chem.* **50**, 21-39.

Mortimer, C. H., 1941. The exchange of dissolved substances between mud and water in lakes. *J. Ecol.* **29**, 280-329.

Mortimer, C. H., 1942. The exchange of dissolved substances between mud and water in lakes. *J. Ecol.* **30**, 147-201.

Nagai, T., Imai, A., Matsushige, K., Yokoi, K., and Fukushima, T., 2007. Dissolved iron and its speciation in a shallow eutrophic lake and its inflowing rivers. *Water Res.* **41**, 775-784.

Nevin, K. P. and Lovley, D. R., 2000. Lack of production of electron-shuttling compounds or solubilization of Fe(III) during reduction of insoluble Fe(III) oxide by Geobacter metallireducens. *Appl. Environ. Microbiol.* **66**, 2248-2251.

Nevin, K. P. and Lovley, D. R., 2002a. Mechanisms for Fe(III) oxide reduction in sedimentary environments. *Geomicrobiol. J.* **19**, 141-159.

Nevin, K. P. and Lovley, D. R., 2002b. Mechanisms for accessing insoluble Fe(III) oxide during dissimilatory Fe(III) reduction by Geothrix fermentans. *Appl. Environ. Microbiol.* **68**, 2294-2299.

Newman, D. K. and Banfield, J. F., 2002. Geomicrobiology: How molecular-scale interactions underpin biogeochemical systems. *Science* **296**, 1071-1077.

Newman, D. K. and Kolter, R., 2000. A role for excreted quinones in extracellular electron transfer. *Nature* **405**, 94-97.

Raiswell, R. and Canfield, D. E., 1998. Sources of iron for pyrite formation in marine sediments. *American Journal of Science* **298**, 219-245.

Reguera, G., McCarthy, K. D., Mehta, T., Nicoll, J. S., Tuominen, M. T., and Lovley, D. R., 2005. Extracellular electron transfer via microbial nanowires. *Nature* **435**, 1098-1101.

Reid, R. T. and Butler, A., 1991. Investigation of the mechanism of iron acquisition by the marine bacterium Alteromonas-Luteoviolaceus - Characterization of siderophore production. *Limnol. Oceanogr.* **36**, 1783-1792.

Rickard, D. and Luther, G. W., 2007. Chemistry of iron sulfides. *Chem. Rev.* **107**, 514-562.

Roden, E. E., 2003. Fe(III) oxide reactivity toward biological versus chemical reduction. *Environ. Sci. Technol.* **37**, 1319-1324.

Roden, E. E., 2004. Analysis of long-term bacterial vs. chemical Fe(III) oxide reduction kinetics. *Geochim. Cosmochim. Acta* **68**, 3205-3216.

Roden, E. E. and Zachara, J. M., 1996. Microbial reduction of crystalline iron(III) oxides: Influence of oxide surface area and potential for cell growth. *Environ. Sci. Technol.* **30**, 1618-1628.

Straub, K. L., Benz, M., Schink, B., and Widdel, F., 1996. Anaerobic, nitrate-dependent microbial oxidation of ferrous iron. *Appl. Environ. Microbiol.* **62**, 1458-1460.

Straub, K. L., Rainey, F. A., and Widdel, F., 1999. *Rhodovulum iodosum* sp. nov, and *Rhodovulum robiginosum* sp. nov., two new marine phototrophic ferrous-iron-oxidizing purple bacteria. *Intl. J. Syst. Bacteriol.* **49**, 729-735.

Straub, K. L., Schonhuber, W. A., Buchholz-Cleven, B. E. E., and Schink, B., 2004. Diversity of ferrous iron-oxidizing, nitrate-reducing bacteria and their involvement in oxygen-independent iron cycling. *Geomicrobiol. J.* **21**, 371-378.

Stumm, W. and Morgan, J. J., 1996. *Aquatic Chemistry: Chemical Equillibria and Rates in Natual Waters*. John Wiley & Sons, New York.

Taillefert, M., Bono, A. B., and Luther, G. W., 2000. Reactivity of freshly formed Fe(III) in synthetic solutions and (pore)waters: Voltammetric evidence of an aging process. *Environ. Sci. Technol.* **34**, 2169-2177.

Taillefert, M. and Gaillard, J. F., 2002. Reactive transport modeling of trace elements in the water column of a stratified lake: iron cycling and metal scavenging. *J Hydrol* **256**, 16-34.

Taillefert, M., Hover, V. C., Rozan, T. F., Theberge, S. M., and Luther, G. W., 2002. The influence of sulfides on soluble organic-Fe(III) in anoxic sediment porewaters. *Estuaries* **25**, 1088-1096.

Thamdrup, B., 2000. Bacterial manganese and iron reduction in aquatic sediments. *Advances in Microbial Ecology, Vol 16* **16**, 41-84.

Vargas, M., Kashefi, K., Blunt-Harris, E. L., and Lovley, D. R., 1998. Microbiological evidence for Fe(III) reduction on early Earth. *Nature* **395**, 65-67.

Weber, K. A., Achenbach, L. A., and Coates, J. D., 2006a. Microorganisms pumping iron: anaerobic microbial iron oxidation and reduction. *Nature Reviews Microbiology* **4**, 752-764.

Weber, K. A., Picardal, F. W., and Roden, E. E., 2001. Microbially catalyzed nitrate-dependent oxidation of biogenic solid-phase Fe(II) compounds. *Environ. Sci. Technol.* **35**, 1644-1650.

Weber, K. A., Pollock, J., Cole, K. A., O'Connor, S. M., Achenbach, L. A., and Coates, J. D., 2006b. Anaerobic nitrate-dependent iron(II) bio-oxidation by a novel lithoautotrophic betaproteobacterium, strain 2002. *Appl. Environ. Microbiol.* **72**, 686-694.

Weber, K. A., Urrutia, M. M., Churchill, P. F., Kukkadapu, R. K., and Roden, E. E., 2006c. Anaerobic redox cycling of iron by freshwater sediment microorganisms. *Environ. Microbiol.* **8**, 100-113.

Widdel, F., Schnell, S., Heising, S., Ehrenreich, A., Assmus, B., and Schink, B., 1993. Ferrous iron oxidation by anoxygenic phototrophic bacteria. *Nature* **362**, 834-836.

Wilhelm, S. W., Maxwell, D. P., and Trick, C. G., 1996. Growth, iron requirements, and siderophore production in iron-limited Synechococcus PCC 7002. *Limnol. Oceanogr.* **41**, 89-97.

Wilhelm, S. W. and Trick, C. G., 1994. Iron-Limited Growth of Cyanobacteria - Multiple Siderophore Production Is a Common Response. *Limnol. Oceanogr.* **39**, 1979-1984.

Xiong, J., Fischer, W. M., Inoue, K., Nakahara, M., and Bauer, C. E., 2000. Molecular evidence for the early evolution of photosynthesis. *Science* **289**, 1724-1730.

Yao, W. S. and Millero, F. J., 1996. Oxidation of hydrogen sulfide by hydrous Fe(III) oxides in seawater. *Mar. Chem.* **52**, 1-16.

Chapter 2. The biogeochemistry of tropical lakes: A case study from Lake Matano, Indonesia

Sean A. Crowe[1,2,6], Andrew H. O'Neill[2], Sergei Katsev[1,3], Peter Hehanussa[4], G. Douglas Haffner[2], Bjørn Sundby[1,5], Alfonso Mucci[1,6], and David A. Fowle[2,7]

1 Earth and Planetary Sciences, McGill University, Montreal, Quebec H3A 2A7, Canada
2 Great Lakes Institute for Environmental Research, University of Windsor, Windsor, Ontario N9B 3P4, Canada
3 Large Lakes Observatory and Department of Physics, University of Minnesota Duluth, Duluth, MN 55812
4 Center for Limnology Research and Development, LIPI, Cibinong, West Java, Indonesia 16911
5 ISMER, Université du Québec à Rimouski, Rimouski, Quebec G5L 3A1, Canada
6 GEOTOP-McGill-UQAM, Montreal, Quebec H3C 3P8, Canada
7 Department of Geology, University of Kansas, Lawrence, Kansas, 66047

Disclaimer: This Chapter is an integral version of a paper published in *Limnology and Oceanography* and therefore contains some information that I now know to be incorrect. This includes the DOC concentrations that are reported on page 41. DOC concentrations measured in 2007 range from 130 μmol l^{-1} in the surface water to as low as 16 μmol l^{-1} at 150 m depth. Therefore, allocthonous DOC is unlikely to drive anaerobic metabolims in Lake Matano, as reported in this Chapter. I now know from measurements of carbon fixation rates (Chapter 4) that primary production supplies sufficient organic matter to account for the observed accumulation of anaerobic metabolic products. Also in this Chapter, the bottom waters of Lake Matano are reffered to as the "hypolimnion". The term hypolimnion typically refers to the lower portion of a water column that stratifies seasonally. The bottom water in Lake Matano may be better defined as a "monimolimnion" which refers to the bottom water of a permanently stratified meromictic lake. Note that Lake Matano is not the same as typical meromictic lakes as it does not have the strong gradient in dissolved salts that maintains density stratification. It therefore does not strictly fit the definition of a meromictic lake and the term "monimolimnion" may not perfectly apply to the bottom waters of Lake Matano.

2.1 Abstract

We examined the chemical composition of the water column of Lake Matano, Sulawesi Island, Indonesia, to document how the high abundances of Fe (hydr)oxides in tropical soils and minimal seasonal temperature variability affect biogeochemical cycling in lakes. Lake Matano exhibits weak thermal stratification; however, a persistent

pycnocline separates an oxic epilimnion from anoxic meta- and hypolimnions. The concentration of soluble P in the epilimnetic waters is very low and can be attributed to scavenging by Fe (hydr)oxides. Chromium concentrations in the epilimnion are high (up to 180 nmol L^{-1}), but below USEPA guidelines for aquatic ecosystems. The concentration of chromium decreases sharply across the oxic-anoxic boundary revealing that the hypolimnion is a sink for Cr. Flux calculations using a one-dimensional transport-reaction model for the water column fail to satisfy mass balance requirements and indicate that sediment transport and diagenesis play an important role in the exchange of Fe, Mn, P, and Cr between the epilimnion and hypolimnion. Exchange of water between the epilimnion and hypolimnion is slow and on a time-scale similar to temperate meromictic lakes. This limits recycling of P and N to the epilimnion and removal of Cr to the hypolimnion, both of which likely restrict primary production in the epilimnion. Due to the slow exchange, steep concentration gradients in Fe and Mn species develop in the metalimnion. These concentration gradients are conducive to the proliferation of chemoautotrophic and anoxygenic phototrophic microbial communities, which may contribute a significant fraction to the total primary production in the lake.

2.2 Introduction

Tropical lakes differ from their temperate counterparts in several important aspects. The higher annual irradiance, the lack of large seasonal variations in irradiance, and the smaller Coriolis effects at low latitudes combine to create weakly stratified lakes with relatively warm and uniform temperatures and low physical stability (Lewis 1987). The effects of latitude on the ecology of lakes are well documented (Lewis 1987; Reynolds et al. 2000) but the influence of latitude on the biogeochemistry of lakes has received much less attention. Nevertheless, two features can be expected to distinguish biogeochemical cycling in tropical from temperate lakes: the absence of the temperature-driven convective overturn that annually oxygenates the entire water column in temperate lakes, and significantly higher fluxes of allochthonous Fe and Mn (hydr)oxides resulting from intense chemical weathering in the catchments of tropical lakes.

Under low energy conditions, lakes are generally physically stratified: a surface layer (epilimnion) overlies a denser deep layer (hypolimnion) (Hutchinson 1957).

Physically stratified lakes often exhibit chemical stratification. For example, when oxygen in the hypolimnion cannot be replenished as fast as it is consumed, microbial respiration switches to anaerobic pathways and redox stratification develops (i.e., the water column becomes stratified in terms of the distribution and speciation of redox-sensitive elements) (Hutchinson 1957; Wetzel 1983; Buffle and Stumm 1994). Anaerobic respiration typically proceeds first through NO_3^- reduction, followed by Mn(III/IV) and Fe(III) reduction, SO_4^{2-} reduction, and finally fermentation or methanogenesis (Stumm and Morgan 1996). The sequential use of oxidants (electron acceptors) generates gradients of electron acceptors, electron donors, and metabolites. These concentration gradients drive diffusive fluxes between layers and maintain chemical disequilibrium (Stumm and Morgan 1996). The oxidants Mn(III/IV) and Fe(III) typically exist as solid and colloidal (hydr)oxides with surfaces exhibiting both strong chemical affinities for many trace elements and large specific surface areas (Stumm and Morgan 1996). These Mn and Fe (hydr)oxides are susceptible to reductive dissolution (Stumm and Morgan 1996) and therefore, the redox cycling of Fe and Mn can control the fate, distribution, and bioavailability of many trace elements (Buffle and Stumm 1994; Hamilton-Taylor and Davison 1995). Thus, Fe and Mn (hydr)oxides are not only important as terminal electron acceptors for anaerobic respiration but are also intimately linked to the biogeochemical cycling of many other minor and trace elements.

In this study we examine how the abundance of metal (hydr)oxides in catchment soils, the relative dearth of other electron acceptors, and the absence of marked seasonal temperature fluctuations influence biogeochemical cycling in tropical lakes as revealed by the chemistry of the water column in Lake Matano, Indonesia.

2.3 Regional setting

Lake Matano is part of the Malili Lakes system of Indonesia. The Malili Lakes are situated on Sulawesi Island and constitute a morphologically diverse group that includes Lake Matano, Lake Mahalona, Lake Towuti, Lake Lawontoa, and Lake Masapi. To date, Lake Matano is the most extensively characterized (Lehmusluoto et al. 1999; Haffner et al. 2001; Crowe et al. 2004). Lake Matano is tectonic in origin and is hosted by a cryptodepression with a graben structure. More than 590 m deep, Lake Matano is

among the 10 deepest lakes in the world. The lake is 28 km long, 8 km wide, and has a relatively small surface area (164 km^2). It has been suggested, based on geological and biological information, that Lake Matano is between one and four million years old (Brooks 1950). Due to the relatively steep regional topography (the highest point is 1400-1700 m a.s.l., the lake surface is at 382 m a.s.l.), the total catchment area of Lake Matano is relatively small (~436 km^2). The surficial geology of the catchment basin is dominated by nickeliferrous lateritic soils (which contain up to 60% iron oxides) that have developed on ultramafic rocks of ophiolitic origin (Golightly 1981). As a result, the sediments of the Malili lakes are Fe-rich and can contain more than 20 weight percent Fe (hydr)oxides (Crowe et al. 2004). In addition to the ultramafic rocks, limestones and cherts outcrop along the southern shore of Lake Matano. The regional climate is humid-tropical and lacks marked seasonal temperature fluctuations or year-to-year variability (Hope 2001). The region around Lake Matano receives an average rainfall of 2737 mm per year and has an average temperature of 24ºC with a range of 22-31ºC (Hope 2001). The Malili Lakes are the principal freshwater resource in the region and also host a unique and diverse aquatic ecosystem (Von Rintelen and Glaubrecht 2003; Roy et al. 2004; Herder et al. 2006). Ancient lakes, such as Lake Matano, have relatively stable physical characteristics and are therefore conducive to the development of high degrees of species endemism. The Malili Lakes have been cited as "a superb natural laboratory" for studying evolutionary processes and have been likened to the aquatic equivalent of the Galapagos Islands (F. Herder pers. comm.). In addition, Myers et al. (2000) have identified Sulawesi as a 'hotspot' for biological conservation based on the two-fold criterion of exceptionally high concentrations of endemic species and rapid habitat loss. Though Lake Matano is characterized by very high degrees of endemism, the species richness and endemicity are not matched by high levels of productivity (Sabo 2006). The standing crops of phytoplankton in Lake Matano are very low (0.013 mg L^{-1}), even compared to ultra-oligotrophic lakes such as Great Bear Lake (0.06 – 0.09 mg L^{-1}) in the Canadian Arctic (Sabo 2006). It has been proposed that the low levels of primary production in Lake Matano, and the Malili Lakes in general, result from a combination of both nutrient limitation and metal toxicity (Sabo 2006).

Iron and manganese are abundant in the soils of the Malili Lakes catchment area and thus Fe and Mn redox cycling may be especially important in regulating the chemical composition of Lake Matano (Crowe et al. 2004). Previous studies reported that the deep waters of Lake Matano are characterized by low oxygen concentrations (Haffner et al. 2001; Lehmusluoto et al. 1999), but the presence of a suboxic to anoxic hypolimnion remained speculative. The absence of strong seasonal temperature fluctuations on Sulawesi Island precludes seasonal convective overturn as a mechanism to transport oxygen into the deep waters of Lake Matano. The main seasonality on Sulawesi Island, and in the tropics in general, is in the amount of precipitation delivered during the wet (October-June) and dry (July-September) seasons. Intense precipitation during the wet season, coupled with the steep topography around Lake Matano suggest that runoff may contribute to mixing (Haffner et al. 2001) and may generate lateral intrusions of oxygen-rich water into deeper waters in a situation partly analogous to the Bosporus plume in the Black Sea (Konovalov et al. 2003). Given the great depth of Lake Matano, its mountainous setting, and its moderate surface area (short fetch), it is unlikely that local winds could generate sufficient energy to mix the water in the deep basins of Lake Matano.

2.4 Methods

Sampling and storage. Sampling was conducted at a central deep-water location (2°28'00" S and 121°17'00"N, Figure 2.1) in August-September 2004 (end of the dry season), and June-July 2005 (end of the wet season) aboard the R/V Watu Lonto. Water samples were collected using 5-L Go-Flow (Niskin) bottles attached in series to a stainless steel airline cable and a hand winch. Bottles were placed at depth to an accuracy of ± 5 m using a commercial sonar device to monitor the position of the bottles within the water column. Once at the surface, the Niskin bottles were sub-sampled according to USEPA guidelines (USEPA 1983). Unfiltered water samples were transferred directly to a voltammetric cell for electrochemical analyses or to acid-washed high-density polyethylene (HDPE) bottles (14% v/v HNO_3 for 24 h followed by quadruplicate rinsing in Milli-Q (MQ) water and drying in class 1000 laminar flow hood) via acid-washed Tygon tubing. Other water samples were filtered after drawing the water into an acid-

washed 60 mL syringe through the Tygon tubing. Waters were filtered through 0.45 (Whatman) and/or 0.02 (Millipore) μm polypropylene syringe filters directly into HDPE bottles. There was no significant difference between concentrations (Fe(II), Mn, Cr, Ni, Co, P) in the 0.02 or 0.45 μm filtrates. In the rest of the text the term "dissolved" refers to material passing through a 0.02 μm filter. All samples were transported to the field station and acidified to 1% equivalent volume with trace-metal grade HNO_3 (purified by sub-boiling distillation) within 8 hours of sampling. Unfiltered samples were not digested, but acidification to 1% (pH <2) with HNO_3 should dissolve most of the inorganic particulate material with the exception of crystalline silicates and some clay minerals. Concentrations determined by analyses of acidified, unfiltered samples are hereafter referred to as 'total' concentrations despite the fact that some refractory material may not have been digested. All samples were refrigerated and maintained at 4°C until analysis.

Methods of analysis. Water temperature, conductivity, and pH profiles were collected in-situ using a submersible CTD (RBR). Measurements of dissolved oxygen were also conducted in-situ to a depth of 100 m using a Clark-type electrode, calibrated to 100% saturation in air, fixed to a multi-parameter probe (Hydrolab). Oxygen measurements at deeper depths were made by linear sweep voltammetry (see below) on whole water samples collected using the Niskin bottles. Eh (2004 only) was measured on whole water samples with a VWR SympHony SP301 meter using an Orion 96-78 combination electrode (Ag-AgCl reference) calibrated with Zobell's solution and corrected to the standard hydrogen electrode (SHE). The colorimetric methods described below were conducted on-site using a HACH DR2010 spectrophotometer. Fe(II) was determined using a modified version of the ferrozine method (Viollier et al. 2000). Alkalinity (2005 only) was determined using the colorimetric method described by Sarazin et al. (1999). In 2004, nitrogen species (i.e., NO_3^-, NO_2^-, and NH_4^+) were determined using HACH Accuvac® ampuls (Nitra/Nitriver 5LR) and the HACH ammonium-nitrogen salicylate kit. In 2005, nitrogen species were determined by Ion Chromatography (DIONEX), on samples preserved by acidification (to 1% equivalent volume H_2SO_4), using an IonPAC ASHC-11 column with conductivity detection (Dionex CD-25).

An Analytical Instrument Systems (AIS) DLK-60 with cell stand was used for all electrochemical analyses. Voltammetric measurements were conducted with a three-electrode configuration using a Au-Hg amalgam micro-electrode (50 μm radius), a saturated Ag-AgCl, and a platinum wire as the working, reference and counter electrodes respectively (Brendel and Luther 1995). The voltammetric techniques used in this work are described by Luther et al. (2003). Briefly, dissolved O_2 was measured by linear sweep (LS) voltammetry, and Fe(II), Mn(II), S(-II) species, and organo-Fe(III) were measured by square-wave voltammetry. The detection limits are 5, 15, 5, and < 0.2 μmol L^{-1} for O_2, Fe(II), Mn(II), and HS^- respectively (Luther et al. 1998). As discussed by Taillefert et al. (2000), it is not possible to calibrate quantitatively for organo-Fe(III). The macro-elements (Ca, Mg, Si, and Mn, Fe, and P in the bottom waters) were determined by Inductively Coupled Plasma-Optical Emission Spectrometry (ICP-OES; Thermo Jarrell Ash). Trace metals and P were determined by Inductively Coupled Plasma-Mass Spectrometry (ICP-MS) using either a ThermoElemental X7 (2004 samples) or an Elan 6100 *plus* (2005 samples). Mass bias corrections were made using a three element internal standard (Be, In, Tl or Bi). Instrumental detection limits were calculated as 3 times the standard deviation of 8 measurements of MQ water containing the internal standards in an acid matrix (P = 0.05, Fe = 0.02, Mn = 0.003, Cr = 0.03, Co = 0.00015, Ni = 0.008 all in μmol L^{-1}). Estimates of the precision and accuracy of the measurements were made by repeated analyses of the riverine water standard reference material SLRS-4 and both epilimnetic and hypolimnetic waters (precision: P < 5%, Fe < 1%, Mn < 3%, Cr < 1%, Co < 2%, Ni < 1% RSD, accuracy: better than 5% all elements).

Speciation calculations and stability diagrams were obtained using the JChess geochemical modeling software (Van Der Lee 1993) and the MINTEQA2 thermodynamic database (Allison et al. 1991).

2.5 Results and discussion

In this section, we describe the physical characteristics of the lake that pertain to mixing and oxygen transport in the water column; evaluate trace element redox speciation in the lake water using measured pE and pH profiles in combination with

thermodynamic equilibrium calculations; and use reaction-transport modeling to provide a quantitative description of the rates of biogeochemical cycling. Emphasis is placed on the fate and distribution of macronutrients and heavy metals so that future studies can more readily identify the factors that regulate the biological composition and productivity of this and other tropical lakes as well as their capacity to buffer increasing anthropogenic stresses. A representative compilation of the data presented in the figures is available in tables 2.3 and 2.4 at the end of the Chapter.

Physical characteristics. Lake Matano water density was calculated from profiles of temperature and conductivity (Imboden and Wüest 1995) collected at the end of the 2004 dry season and the end of the 2005 wet season. Stratification in both temperature and total dissolved solids resulted in a well-developed pycnocline at ~100 m depth and a metalimnion that extended from 100 m to ~220 m depth during both seasons (Figure 2.2). Most of the density gradient was generated by the temperature gradient, but the difference between the total dissolved solids concentration (TDS, estimated from conductivity; Langmuir 1997) in the epilimnion and hypolimnion accounted for approximately 20%. Although the thermal stratification was relatively weak compared to seasonally stratified temperate lakes, the TDS gradient imparted additional stability to the stratification: the epilimnetic waters would need to cool to less than 25°C (0.5°C degrees below the hypolimnion temperature) to achieve homogenous density throughout the water column. The similarity of the density profiles between the wet and dry seasons and between 2004 and 2005, as well as the accumulation of TDS in the hypolimnion suggest that the lake has not been vertically mixed recently. Nevertheless, it is difficult to estimate how long it has been since complete vertical mixing occurred.

The higher concentration of dissolved solids in the hypolimnion was due to higher concentrations of HCO_3^-, which were largely balanced by equivalent increases in Ca^{2+}, Mg^{2+}, and Fe^{2+} concentrations. The higher concentration of HCO_3^- most likely originated from the accumulation of heterotrophic respiration products, but higher concentrations of dissolved Mg^{2+} and Ca^{2+} probably arose from their release during the reductive dissolution of Fe (hydr)oxide carrying phases (Sholkovitz 1985). These observations are

consistent with biogenic meromixis, a feature common to deep equatorial lakes (Wetzel 1983).

Redox stratification. Vertical profiles of oxygen (Figure 2.3a) show that in both 2004 and 2005, oxygen was only measurable to a depth of 100 m. Oxygen was below the detection limit of linear sweep voltammetry (5 μmol L^{-1}) in deeper samples (110 m, 120 m, 140 m, 160 m, 180 m, 500 m). The discrepancy in the oxygen concentration profiles in the epilimnion between the two samplings was due to differences in the mixing regime and is consistent with the presence of a seasonal pycnocline that developed during the wet season. This seasonal pycnocline developed due either to a decrease in evaporative cooling or lower wind stress during the rainy season.

Below 100 meters, the concentrations of dissolved Mn increased sharply to a maximum of 9.5 μmol L^{-1} at 110 meters, whereas dissolved Fe(II) concentrations increased to a maximum of 140 μmol L^{-1} at 300 meters depth (Figure 2.3b). The latter are at the upper end of the range of concentrations reported for suboxic freshwaters (Hamilton-Taylor and Davison 1995). The virtually identical profiles of dissolved Fe and Mn over consecutive years of sampling imply that redox stratification persists over annual and likely longer time-scales. This is consistent with the well-developed density stratification and slow mixing through the metalimnion. The invariance of the Fe and Mn profiles further suggests that steady-state redox conditions prevailed.

The concentrations of dissolved Mn and Fe were approximately constant at 6.4 and 140 μmol L^{-1} respectively, below 300 m depth. Saturation Indices (SI) with respect to common mineral phases for water at 300 m depth are presented in Table 2.1. The index is given by:

$$SI = \log\left[\frac{IAP}{K_{SP}}\right] \quad (1)$$

where IAP is the ion activity product and K_{sp} is the solubility product of a given mineral phase at the same temperature and pressure. According to these calculations, Lake Matano bottom waters were supersaturated with respect to magnetite, hematite, maghemite, ferrihydrite, strengite, and siderite. The precipitation of these minerals should

buffer the aqueous concentrations of Fe, Mn, PO_4^{3-}, and CO_3^{2-} therefore regulating the influence of increased or decreased input fluxes.

The dominant N, Mn, Fe, and S species can be predicted using thermodynamic equilibrium calculations that can be visualized in pE-pH predominance diagrams (Stumm and Morgan 1996). Plots of pE, calculated from field measurements of Eh versus pH (Stumm and Morgan 1996), along with stability fields for Lake Matano waters are shown in Figure 2.4. These diagrams reveal that Lake Matano waters exhibit a bimodal distribution in terms of pE and pH with lower values in the hypolimnetic waters. The equilibrium calculations predict that NO_3^- should be the dominant dissolved (non-gaseous) species in the epilimnion and that NH_4^+ should dominate in the hypolimnion. Very low concentrations of N precluded the quantitative determination of N species in the epilimnetic waters but > 10 μmol L^{-1} NH_4^+ was detected in the hypolimnion (data not shown). With respect to Mn, the epilimnetic waters plot in the stability field of poorly soluble Mn (hydr)oxide (MnO_2), whereas under the reducing conditions encountered in the hypolimnion Mn(III/IV) (hydr)oxides should reductively dissolve to Mn(II). Indeed, the concentration of dissolved Mn increased sharply below the redoxcline (Figure 2.3). With respect to Fe, the epilimnetic waters plot largely in the stability field of poorly soluble (hydr)oxides ($Fe(OH)_3$) as is also the case for Mn. The hypolimnetic waters plot near the boundary between the oxidized species $Fe(OH)^{2+}$ and the reduced aqueous species Fe^{2+}. Accordingly, the redox potential of the hypolimnetic waters appears to be buffered by the Fe^{2+}-$Fe(OH)^{2+}$ redox couple. High concentrations of dissolved Fe(II) were observed in the hypolimnion (Figure 2.3). Both epilimnetic and hypolimnetic waters plot within the stability field of SO_4^{2-} (Figure 2.4), suggesting that sulfate reduction should not occur in the water column. Nevertheless, trace concentrations of free sulfide were detected immediately below the redoxcline (Figure 2.5). This sulfide may emanate from the underlying sediment, but sulfate reduction would only occur in sediments overlain by water containing sulfate. Therefore, only sediments within a narrow depth interval below the pycnocline could be a source of sulfide to the water column. The peak shape of the sulfide profile (Figure 2.5) can be explained by sulfide oxidation at depths less than 120 m, and the precipitation of FeS resulting from the reaction of HS^- with

upward diffusing Fe(II) at depths below 120 m. The presence of sulfide in the hypolimnion may be important in governing Ni and Co cycling (see below).

Origin and distribution of organic matter in the water column. Redox stratification is linked to the microbially mediated oxidation of organic matter. Due to the low primary productivity in Lake Matano (Lehmusluoto et al. 1999; Haffner et al. 2001; Sabo 2006), the organic matter content of the water column is very low. The autochthonous particulate organic carbon (POC) component, estimated from the biomass given in Sabo (2006) (assuming Redfield organic matter stoichiometry: C:N:P = 106:16:1; Redfield et al. 1963), is less than 1 μmol L^{-1} and is mostly remineralized within the epilimnion (Haffner et al. 2001). This implies that redox cycling in Lake Matano is likely driven by allochthonous organic matter. Dissolved organic carbon (DOC) concentrations (D. Haffner, unpubl. data) in the epilimnion are uniform and approximately 1000 μmol L^{-1} but decrease to <100 μmol L^{-1} below 100 m depth. The sharp concentration gradient across the metalimnion should drive a strong flux of DOC to the hypolimnion. Taken together these observations suggest that redox cycling in Lake Matano is fueled by allochthonous DOC and that DOC is almost completely mineralized by anaerobic respiration within a narrow depth interval between 100 and 200 m. The depth interval in which dissolved Fe(II) increased coincides with the depth interval of DOC mineralization and suggests that DOC is mineralized predominantly via Fe reduction. This situation may be unique to tropical lakes that have catchments rich in Fe (hydr)oxides and that are poor in more energetic electron acceptors.

P and trace metal distribution and speciation. The concentrations of both soluble reactive phosphate (SRP) and total P were below our detection limit (0.05 μmol L^{-1}) in the epilimnion but SRP increased concomitantly with dissolved Fe(II) in the metalimnion (Figure 2.6). The ratio of dissolved Fe to dissolved P was approximately 16:1 in the metalimnion and remained relatively constant with depth. This suggests that the geochemistry of P in Lake Matano is intimately linked to the Fe cycle and that the P concentration in the epilimnion is likely limited by sorption to particulate or colloidal Fe (hydr)oxides. Assuming a 30 Å particle size, Anschutz et al. (1998) estimated that

ferrihydrite (a poorly crystalline Fe (hydr)oxide) could sorb phosphate up to a molar Fe:P ratio of 6.7. Therefore, the ratio of dissolved Fe:P in the hypolimnion of Lake Matano (16:1) suggests that the Fe (hydr)oxides supplying ferrous Fe and P to the meta- and hypolimnions were either: 1) undersaturated in P; 2) were dissolving incongruently with P being preferentially incorporated into a secondary mineral or retained in a refractory Fe (hydr)oxide component, or 3) P was taken up in biomass. The low POC concentrations negate biological uptake and imply either undersaturation of Fe oxyhydroxide surfaces in P or secondary precipitation of minerals with low Fe:P ratios like strengite (Fe:P = 1:1) or $MnHPO_4$ (Fe:P = 0:1). Both strengite and $MnHPO_4$ are supersaturated in the hypolimnion (Table 2.1).

The concentration of dissolved Cr in the epilimnion was uniform at ~180 nmol L^{-1} and virtually identical in both 2004 and 2005 (Figure. 2.7a). Speciation calculations reveal that at equilibrium most of this Cr should be in the hexavalent state (Figure 2.7b). The Cr(VI) concentration was below USEPA guidelines (Criterion Continuous Concentration (CCC); USEPA 2006). The CCC is an estimate of the highest concentration of a substance in surface water to which an aquatic community can be exposed indefinitely without resulting in an unacceptable effect (USEPA 2006). It is thus unlikely that the presence of Cr(VI) is solely responsible for the low productivity in Lake Matano. Dissolved Cr concentrations decreased dramatically below 100 m depth to less than our detection limit of 30 nmol L^{-1}. The decrease is consistent with the reduction of Cr(VI) to the less soluble and more particle reactive Cr(III) by Fe(II) (Johnson et al. 1992). Thermodynamic equilibrium calculations predict that, in the presence of micromolar concentrations of Fe, chromite ($FeCr_2O_4$) should precipitate from the hypolimnetic waters. However, laboratory experiments with Fe-reducing bacteria have shown that the dominant product of Cr reduction by ferrous Fe is a mixed Fe, Cr (hydr)oxide ($Fe_{1-x}Cr_x(OH)_3 \cdot nH_2O$) (Hansel et al. 2003). Hansel et al. proposed the following reaction to describe the precipitation of Cr induced by the reaction with Fe(II):

$$3Fe^{2+} + CrO_4^{2-} + 8H_2O \Leftrightarrow 4Cr_{0.25}Fe_{0.75}(OH)_3 + 4H^+$$

Such an amorphous Cr-Fe (hydr)oxide may be more reactive towards re-oxidation to Cr(VI) than chromite if mixed into the zone of Mn oxidation.

The concentration of dissolved Ni was relatively high (~60 nmol L^{-1}) throughout the water column, but it peaked at 210 nmol L^{-1} near the pycnocline, likely as a result of the reductive dissolution of particulate Mn (hydr)oxides (Figures 2.3b, 2.8). Mn (hydr)oxides have a strong affinity for Ni (Manceau et al. 1992; Manceau et al. 2003; Manceau et al. 2005) and serve as carrier phases for this and many other elements (e.g., Mo). Similar to Mn and Fe, dissolved Co concentrations were also very low in the epilimnion. They increased concomitantly with Fe (R^2 = 0.77) in the metalimnion (Figures 2.3b, 2.8). The much greater abundance of Ni than Co in the catchment area soils (Golightly 1981) may explain why the concentration of Ni was higher than Co in the epilimnion. In contrast to the concentration of Co which, increased below the redoxcline, the concentration of Ni decreased by ~30%. The concentrations of Ni and Co were almost identical below 150 m depth and remained constant at ~40 nmol L^{-1} below 200 meters. This similarity within the anoxic hypolimnion suggests that dissolved Ni and Co concentrations are buffered by incorporation into a solid phase. Solid phases with the potential to incorporate Ni and Co include Fe, Mn and Ca carbonate or phosphate minerals, authigenic oxides of Fe, and sulfide minerals. Despite the apparently minor role for sulfate reduction in organic matter oxidation within the water column, small amounts of sulfate reduction could play an important role in the dynamics of trace metals. Speciation and saturation index calculations over a range of sulfide concentrations, pH = 7.00, HCO_3^- = 2 mmol L^{-1} (Figure 2.9), reveal that at dissolved Ni concentrations of 50 nmol L^{-1}, waters become saturated with respect to Ni monosulfide (NiS, millerite) at sulfide concentrations as low as 50 nmol L^{-1}. In contrast, at dissolved Co concentrations of 50 nmol L^{-1}, water remains undersaturated with respect to Co monosulfide until the sulfide concentration is nearly one order of magnitude greater (Figure 2.9). This reflects the lower solubility of NiS (K_{sp}= $10^{-8.0345}$) than CoS (K_{sp}= $10^{-7.374}$). Concentrations of dissolved sulfide in the hypolimnion of Lake Matano were within the range necessary to induce NiS precipitation but not to precipitate CoS. Although the high concentrations of Fe(II) in the hypolimnion would effectively scavenge any free sulfide, the solubility of FeS is much higher than either NiS or CoS. Therefore, the presence of dissolved Fe(II)

would not inhibit NiS or CoS precipitation until the concentration of Fe(II) is over 1 mmol L^{-1}.

One-dimensional description of Fe cycling. The uniform increase in dissolved Fe(II) concentrations within the metalimnion suggests the presence of a source and a sink for Fe(II) within this depth interval. To quantify the rates of Fe cycling in the metalimnion we analyzed the available concentration data with a one-dimensional reaction-transport model that includes: 1) sinking of particulate Fe(III) (hydr)oxides through the metalimnion; 2) reductive dissolution of Fe(III) (hydr)oxides coupled to organic matter oxidation in the metalimnion; 3) upward diffusion of Fe(II) towards the epilimnion; and 4) Fe(II) oxidation and the re-precipitation of Fe(III) (hydr)oxides at the upper boundary of the metalimnion. The numerical formulation of the reaction-transport model is provided in section 2.7.

The close fit between the modeled profile and the field data (Figure 2.10) suggests that the Fe(II) profile is indeed shaped by an interplay between diffusion-like transport and a reaction rate that decreases approximately exponentially below the pycnocline. By fitting the measured Fe(II) profile, the value obtained for the product of the rate of Fe release to solution by reductive dissolution ($R_{Fe}(0)$) and the inverse of the coefficient of vertical eddy diffusion (K_z^{-1}) is 0.056 μmol m^{-2} (*see* section 2.7).

Attempts to derive the individual values of $R_{Fe}(0)$ and K_z, however, highlight incongruencies between the field data and the one-dimensional model. For the concentrations of organic matter and particulate iron in Lake Matano, and for typical first- or second-order iron reduction kinetics (Taillefert and Gaillard 2002, Katsev et al. 2004), model-estimated values of K_z in the hypolimnion could be no less than 200 m^2 d^{-1}. Such values of K_z are unrealistic for the hypolimnion of a lake displaying a salinity gradient and a deep thermocline (Imboden and Schwarzenbach 1985).

In addition to requiring unrealistically high vertical eddy diffusivities, the one-dimensional model for dissolved Fe(II) requires that the large amount of dissolved iron diffusing upward be balanced by a high downward flux of particulate Fe(III) (Figure 2.10), which is not supported by the data. The concentration of particulate (i.e., mostly ferric) iron in the vicinity of the pycnocline is several orders of magnitude smaller than

the concentration of dissolved (i.e., mostly ferrous) iron. If both phases are transported at comparable rates (e.g., by the same process of eddy diffusion), the quantity of particulate iron observed is insufficient to sustain the high concentrations of dissolved Fe(II) in the hypolimnion. The excess downward flux of Fe(III) required to sustain the high dissolved Fe(II) concentrations in the hypolimnion could conceivably be supplied by fast particle settling, but the particle sizes required to produce high settling rates are unrealistic (see section below on fluxes). A possible explanation for the discrepancies between the model and observations is that the one-dimensional model does not take into account the potential for the sediment to act as a source or sink for dissolved and particulate Fe.

The contribution of the sediment to the exchange of Fe, Mn, P, and Cr between the epilimnion and hypolimnion can be estimated from the disparity between particulate and diffusive fluxes. In other words, discrepancies in the water column must be balanced by exchange with the sediment. To estimate fluxes in the water column requires knowledge of the intensity of vertical eddy diffusivity (K_z). In the absence of temporal variations in temperature gradients, K_z cannot be estimated using the standard temperature method (Jassby and Powell 1975). Alternatively, we use an empirical relationship between K_z and the Brunt-Väisälä or stability frequency (N^2) (Jassby and Powell 1975). The intensity of vertical eddy diffusivity in a lake (K_z) results from the balance between the water column resistance to mixing (e.g., due to stratification) and the applied forcing (wind, density flows, seiches, etc.). The stability frequency characterizes the first part of this balance. We calculated the stability frequency for Lake Matano from the vertical density variation. Despite the variety of driving forces, in environments ranging from shallow lakes to the deep ocean, the relationship between K_z and N^2 can typically be formulated as (Lerman 1979):

$$K_z = a\left(N^2\right)^b \tag{6}$$

in which the exponent, *b*, is related to the origin and nature of turbulence and *a* is a proportionality coefficient (Jassby and Powell 1975). In the absence of data from lakes of similar size, shape and latitude to Lake Matano, to constrain the values of *a* and *b*, we use a more general correlation (Lerman 1979). For values of $a = 3.5 \times 10^{-6}$ and $b = -1$, the

relationship between K_z and N^2 appears to describe (within a factor of 5) a diverse suite of water bodies. Applying these values for the coefficients *a* and *b* and the calculated value of the stability frequency to Lake Matano reveals that the transport of solutes between the epilimnion and hypolimnion at 100 m depth is characterized by a $K_z = 0.39$ m^2 d^{-1}. This value is well within the range (0.1-10 m^2 d^{-1}) of values reported for the hypolimnions of other lakes (Imboden and Schwarzenbach 1985).

Fluxes and the role of the sediment. Vertical fluxes of dissolved Fe, Mn, P and Cr towards the pycnocline were calculated using measured concentration gradients and a K_z of 0.39 m^2 d^{-1} (Table 2.2). Fluxes of particulate species settling through the pycnocline were estimated from Stokes law (Stokes 1851) using particulate concentrations obtained from the difference between the concentrations of unfiltered and filtered samples (0.02 μm), a particle density of 2.82 g cm^{-3} (Taillefert and Gaillard 2002), and a particle size of 1 μm (De Vitre et al. 1994). These are upper estimates for particulate fluxes as most of the particles are likely smaller than 1 μm and therefore would sink slower (De Vitre et al. 1994). If the one-dimensional model described in the previous section (and its analogues for dissolved Mn and P associated with Fe (hydr)oxides) were valid, the downward fluxes of particulate species should be equal to or greater than the upward fluxes of dissolved species. This is not the case, for the estimates of downward particulate fluxes of Fe, Mn, and P are more than one order of magnitude smaller than the corresponding upward diffusive fluxes (Table 2.2). One possible interpretation for this relies on a combination of turbulent vertical mixing in the epilimnion and horizontal mixing along isopycnals that would disperse particulate metals precipitated in the epilimnion towards the lake margins. Consequently, part of the downward return flux of particulate metals would take place in water shallower than 100 m and be captured by sediment overlain by oxygenated water. To make up for the deficit in the particulate flux, quantities of dissolved Fe, Mn, and P, equivalent to those captured by the oxic sediment, must be released from the sediments below the oxycline (i.e. below 100 m). Transport of surface sediment from oxic to anoxic depths, for example by resuspension and sediment focusing, is required to close the cycle. The overall scenario is depicted schematically in Figure 2.11. Such a scenario is consistent with the steep bathymetry of the lake, which would favor down-slope sediment

transport (Figure 2.12) and is also in line with previous observations of density currents at the lake margins (Haffner et al. 2001). The latter would re-suspend particles and enhance sediment focusing. Fluctuations in the position of the redox boundary with respect to an isopleth along the lake bottom can also redistribute Fe and drive fluxes of Fe(II) into the hypolimnion (Shaffer 1986; Katsev et al. 2006b). Short-term (several hours) fluctuations could result from seiching, whereas longer-term fluctuations could be sustained by changes in the lake level. Such vertical excursions of the redox boundary could result in an accumulation of particulate Fe, Mn, and P in sediments above the oxycline and create an Fe, Mn, and P enriched 'bathtub ring'. Physical modeling, based on the size and bathymetry of the lake agrees with preliminary observations that the amplitude of seiches in Lake Matano may be as large as 9 m with a periodicity of several hours.

A similar reasoning can be applied to the dynamics of Cr recycling across the pycnocline. In a one-dimensional model, the downward flux of soluble Cr(VI) in the epilimnion, above the pycnocline, should be balanced by the downward flux of particulate Cr below the pycnocline. However, the particulate Cr flux is more than one order of magnitude less than the estimated downward diffusive flux above the pycnocline, which suggests that a large fraction of the Cr reduced and precipitated at the pycnocline must settle at depths of 100 m or less.

Time scales of exchange between the epilimnion and hypolimnion. On a lake-wide scale, the value of K_z at the pycnocline can be used to estimate the time-scale on which water exchanges between the epilimnion and the hypolimnion (Imboden and Schwarzenbach 1985):

$$k = \frac{K_z}{L_z^{\max} \bullet h_{mix}} \qquad [8]$$

where k is the rate of exchange between the epi- and hypolimnion, L_z^{max} is the maximum lake depth (590 m), and h_{mix} is the depth of the epilimnion (100 m). Based on this relationship, the time scale of exchange between the epi- and hypolimnion (1/k) is on the

order of 400 years if there is no large-scale convective overturn. This time scale is similar to those of temperate meromictic lakes (Imboden and Schwarzenbach 1985).

Ecological implications. According to the directions of concentration gradients at the pycnocline, exchange of water across the pycnocline should add P (and N) to the epilimnion while removing Cr(VI). Even though the gradients are steep, the exchange rate is slow. The result is low fluxes that do not favor primary production within the epilimnion. Conversely, the slow exchange allows steep concentration gradients of redox-sensitive species to develop and persist within the metalimnion. These steep gradients are conducive to the proliferation of chemoautotrophic and anoxygenic phototrophic microbial communities. Hence, in tropical lakes where the abundance of metal (hydr)oxides maintain low P concentrations in oxic waters, and where minimal seasonality precludes convective overturn and allows stable redox boundaries to develop, chemoautotrophic carbon fixation may play a comparatively larger role in the total primary production.

The large particulate Fe flux to Lake Matano may help buffer anthropogenic stresses. Sorption of phosphate on Fe (hyrd)oxides precludes the accumulation of P in surface waters and eutrophication that commonly accompanies regional development (Boström et al. 1982). The potency of Fe (hydr)oxides as scavengers of divalent metals would also mitigate fluxes of Ni, Co, and other metals from the catchment soils and industrial effluents.

Acknowledgments. We thank the International Nickel Company (INCO) Canada and PT INCO Tbk. for their financial and logistical support of both field and laboratory work. Support for Sean A. Crowe was partly provided by a Natural Sciences and Engineering Research Council (NSERC) Industrial Partnership Scholarship sponsored by INCO Canada. We are grateful to Bill Napier, Les Huelett, and Matt Orr for logistical support; Jim Gowans for the use of his patio boat, the R/V Watu Lonto; Paul Hamilton, Lis Sabo, Ryan Walters, Andy Bramburger, and Denis Roy for help in collecting samples and informative discussions; Deky Tetradiono, Lili Lubis, Hari Ananto, and Kai Modin for their hospitality and logistical support; and Dahalan Tase, Sinyo Rio, Nurhalem, and Wahap, for help in collecting samples. Brian Fryer, Joel Gagnon, and Bill Minarik helped with the Inductively Coupled Plasma Mass Spectrometry (ICP-MS) analyses. Ilia Ostrovsky, Cédric Magen, Gwénaëlle Chaillou, and Arne Sturm are acknowledged for informative discussions. Finally, we would like to thank the three anonymous journal reviewers and Robert Hecky for their incisive comments.

Table 2.1 Saturation Indices calculated for 300m depth (2005)

Mineral	Chemical Formula	SI
Magnetite	Fe_3O_4	22.13
Hematite	Fe_2O_3	20.63
Maghemite	Fe_2O_3	10.19
Goethite	FeOOH	9.311
-	$Fe_3(OH)_8$	5.572
Ferrihydrite	$Fe(OH)_3$	3.399
Strengite	$Fe(PO_4)_2 \bullet H_2O$	2.722
-	$MnHPO_4$	1.885
Siderite	$FeCO_3$	0.3443
Rhodocrosite	$MnCO_3$	-0.068
Vivianite	$Fe_3(PO_4)_2$	-0.2992
Calcite	$CaCO_3$	-0.747
Aragonite	$CaCO_3$	-0.89
Dolomite	$CaMg(CO_3)_2$	-1.012
Hydroxyapatite	$Ca_{10}(PO_4)_6(OH)_2$	-2.752

Table 2.2 Flux calculations

	Diffusive flux ($\mu mol\ m^{-2}\ d^{-1}$)	Direction	Particulate ($\mu mol\ m^{-3}$)	Stokes flux ($\mu mol\ m^{-2}\ d^{-1}$)	Deficit (%)
Fe	460	Up	350	35	92
Mn	360	Up	34	3.4	99
P	28	Up	22	2.2	92
Cr	6.0	Down	1	0.1	98

Figure 2.1 Lake Matano bathymetry. The circle marks the position of the deep-water master sampling station. Modified from Haffner et al. (Haffner et al. 2001).

Figure 2.2 Density as a function of depth at the end of the dry season 2004 and the end of the wet season 2005.

Figure 2.3 (a) Vertical profiles of dissolved oxygen from 2004 and 2005. (b) Vertical profiles of dissolved (<0.45 μm) Fe and Mn from 2004 and 2005. Note that measurements of dissolved Fe(II) are indistinguishable from dissolved total Fe.

Figure 2.4 pE vs. pH diagrams for species of (a) nitrogen, (b) manganese, (c) iron, and (d) sulphur. Symbols are pE-pH coordinates for selected samples of Lake Matano waters. The bimodal distribution represents waters from the hypolimnion with low pE and pH values and waters from the epilimnion at relatively higher values.

Figure 2.5 Profiles of dissolved HS^- (2004 and 2005) and dissolved sulfate (2004 only).

Figure 2.6 (a) Profile of soluble reactive phosphate (SRP) from 2004 and 2005. (b) SRP as a function of dissolved (<0.45 μm) Fe for 2004 and 2005 (not distinguished). The confidence band on the linear regression represents the 95% interval.

Figure 2.7 (a) Vertical profiles of dissolved (<0.45 μm) Cr from 2004 and 2005. (b) pE vs. pH diagram for Cr species. The bimodal distribution represents waters from the hypolimnion with low pE and pH values and waters from the epilimnion at relatively higher values.

Figure 2.8 Vertical profiles of dissolved (<0.45 μm) Ni and Co from 2004 and 2005.

Figure 2.9 Saturation indices for Ni and Co monosulfides as a function of HS^- concentration. The solid line at SI = 0 corresponds to equilibrium, above the line Ni and

Co monosulfides are expected to precipitate and below the line dissolve. The shaded area delineates the sulfide concentrations present in Lake Matano.

Figure 2.10 The Fe(II) concentration profile generated by a one-dimensional reaction-transport model plotted with dissolved Fe(II) concentrations (2004 and 2005), and particulate Fe concentrations (2005). Note that particulate Fe concentrations could be up to 5% of the dissolved Fe concentrations below 100 m. The high limit for detection in the hypolimnetic waters is due to the limit in precision at high concentrations of dissolved Fe.**Note that this detection limit does not apply to the surface waters which lack Fe(II). The detection limit in the absence of Fe(II) is 0.02 μmol l^{-1}.

Figure 2.11 A conceptual model for Fe cycling in Lake Matano. (A) upward diffusion of dissolved Fe(II); (B) oxidation of Fe(II) to Fe(III) followed by hydrolysis and precipitation as $Fe(OH)_3$ particles in the metalimnion; (C) diffusion of atmospheric O_2 into the epilimnion; (D,E) partial redox recycling of Fe (II) and $Fe(OH)_3$ within the metalimnion and across the pycnocline with a net lateral transport of $Fe(OH)_3$ in the epilimnion; (F) sedimentation of $Fe(OH)_3$; (G) sediment re-suspension and focusing towards deeper parts of the lake; (H) reductive dissolution of $Fe(OH)_3$

Figure 2.12 Plot of the percent areal extent of bottom sediments at different depth intervals. Sixty-five percent is below 100 m depth and is suboxic at the sediment-water interface.

2.6 References

ALLISON, J. D., D. S. BROWN, AND K. J. NOVO-GRADAC. 1991. MINTEQA2/PRODEF2, A Geochemical Assessment Model for Environmental Systems: Version 3.0 User's Manual, p. 3-91. EPA.

ANSCHUTZ, P., S. ZHONG, B. SUNDBY, A. MUCCI, AND C. GOBEIL (1998). Burial efficiency of phosphorus and the geochemistry of iron in continental margin sediments. Limnology and Oceanography **43:** 53-64.

BRENDEL, P. J., AND G. W. LUTHER. 1995. Development of a gold amalgam voltammetric Microelectrode for the determination of dissolved Fe, Mn, O_2, and S(-II) in porewaters of marine and fresh-water sediments. Environmental Science & Technology **29:** 751-761.

BOSTRÖM, B., M. JANSSON, AND C. FORSBERG 1982. Phosphorus release from lake sediments. Archiv für Hydrobiologie–Beiheft Ergebnisse der Limnologie, **18**: 5–59.

BROOKS, J. L. 1950. Speciation in ancient lakes (concluded). The Quarterly Review of Biology **25:** 131-176.

BUFFLE, J., AND W. STUMM. 1994. General chemistry of aquatic systems, p. 1-42. *In* J. Buffle and R. R. De Vitre [eds.], Chemical and Biological Regulation of Aquatic Systems. CRC press.

CROWE, S. A., S.J. PANNALAL, D.A. FOWLE, M.T. CIOPPA, D.T.A. SYMONS, G.D. HAFFNER, B.J. FRYER, R. MCNEELY, B. SUNDBY, AND P.E. HEHANUSSA. 2004. Biogeochemical cycling in Fe-rich sediments from Lake Matano, Indonesia, p. 1185-1189, 11th International symposium on water-rock interaction. A.A. Balkema

DE VITRE, R. R., B. SULZBERGER, AND J. BUFFLE. 1994. Transformations of Iron at Redox Boundaries, p. 91-137. *In* J. Buffle and R. R. Devitre [eds.], Chemical and Biological Regulation of Aquatic Systems. CRC press.

GOLIGHTLY, J. P. 1981. Nickeliferous laterite deposits. Economic Geology 75th Anniversary Volume: 710-735.

HAFFNER, G. D., P. E. HEHANUSSA, AND D. HARTOTO. 2001. The biology and physical processes of large lakes of Indonesia, p. 183-194. *In* M. Munawar and R. E.

Hecky [eds.], The Great Lakes of the World: Food web, health and integrity. Backhuys Publishers.

HAMILTON-TAYLOR, J., AND W. DAVISON. 1995. Redox-driven cycling of trace elements in lakes, p. 217-258. *In* A. Lerman, D. Imboden and J. Gat [eds.], Physics and Chemistry of Lakes. Springer-Verlag.

HANSEL, C. M., B. W. WIELINGA, AND S. R. FENDORF. 2003. Structural and compositional evolution of Cr/Fe solids after indirect chromate reduction by dissimilatory iron-reducing bacteria. Geochimica et Cosmochimica Acta **67:** 401-412.

HERDER, F., J. NOLTE, J. Pfaender, J. SCHWARZER, R.K. HADIATY, AND U. K. SCHLIEWEN. (2006). Adaptive radiation and hybridization in Wallace's Dreamponds: evidence from sailfin silversides in the Malili Lakes of Sulawesi. Proceedings of the Royal Society B **273**: 2209-2217.

HOPE, G. 2001. Environmental change in the Late Pleistocene and later Holocene at Wanda site, Soroako, South Sulawesi, Indonesia. Palaeogeography Palaeoclimatology Palaeoecology **171:** 129-145.

HUTCHINSON, G. E. 1957. A Treatise on Limnology: Geography, Physics and Chemistry. John Wiley & Sons.

IMBODEN, D., AND R. P. SCHWARZENBACH. 1985. Spatial and temporal distribution of chemical substances in lakes: Modeling concepts, p. 1-28. *In* W. Stumm [ed.], Chemical Processes in Lakes. Jon Wiley & Sons.

IMBODEN, D. M., AND A. WÜEST. 1995. Mixing mechanisms in lakes, p. 83-138. *In* A. Lerman, D. Imboden and J. Gat [eds.], Physics and Chemistry of Lakes. Springer-Verlag.

JASSBY, A., AND T. POWELL. 1975. Vertical patterns of eddy diffusion during stratification in Castle Lake, California. Limnology and Oceanography **20:** 530-543.

JOHNSON, C. A., L. SIGG, AND U. LINDAUER. 1992. The chromium cycle in a seasonally anoxic lake. Limnology and Oceanography **37:** 315-321.

KATSEV, S., D. G. RANCOURT, AND I. L'HEUREUX. 2004. dSED: a database tool for modeling sediment early diagenesis. Computers & Geosciences **30:** 959-967.

KATSEV, S., I. TSANDEV, I. L'HEUREUX, AND D. G. RANCOURT. 2006a. Factors controlling long-term phosphorus efflux from lake sediments: Exploratory reactive-transport modeling. Chemical Geology **234**: 127-147.

KATSEV, S., B. SUNDBY, and A. MUCCI. 2006b. Modeling vertical excursions of the redox boundary in sediments: Application to deep basins of the Arctic Ocean. Limnology and Oceanography **51:** 1581-1593

KONOVALOV, S. K., G.W. LUTHER, G.E. FREIDERICH, D.B. NUZZIO, B.M. TEBO, J.W. MURRAY, T. OGGUZ, B. GLAZER, R.E. TROUWBORST, B. CLEMENT, K.J. MURRAY, AND A. ROMANOV. 2003. Lateral injection of oxygen with the Bosporus plume - fingers of oxidizing potential in the Black Sea. Limnology and Oceanography **48:** 2369-2376.

LEHMUSLUOTO, P., B. MACHBUB, N. TERANGNA, F. ACHMAD, L. BOER, S. BRAHMANA, B. SETIADJI, B. PRIADIE, K.H. TIMOTIUS, AND F. GOELTENBOTH. 1999. Limnology in Indonesia, p. 119-234. *In* R. G. Wetzel and B. Gopal [eds.], Limnology in Developing Countries, Volume 2. International Scientific Publications.

LERMAN, A. 1979. Geochemical Processes Water and Sediment Environments. John Wiley and Sons.

LEWIS, W. M. 1987. Tropical Limnology. Annual Review of Ecology and Systematics **18:** 159-184.

LUTHER, G. W., BRENDEL, P.J., LEWIS, B.L., SUNDBY, B., LEFRANÇOIS L., SILVERBERG, N., AND NUZZIO D.B.. 1998. Simultaneous measurement of O_2, Mn, Fe, I^-, and S(II) in marine pore waters with a solid-state voltammetric microelectrode. Limnology and Oceanography **43:** 325-333.

LUTHER, G.W., B. GLAZER, S. MA,, R. TROUWBORST, B.R. SHULTZ, G. DRUSCHEL, AND C. KRAIYA. 2003. Iron and sulfur chemistry in a stratified lake: Evidence for iron-rich sulfide complexes. Aquatic Geochemistry **9:** 87-110.

MANCEAU, A., A. I. GORSHKOV, AND V. A. DRITS. 1992. Structural chemistry of Mn, Fe, Co, and Ni in manganese hydrous oxides.2. Information from EXAFS spectroscopy and electron and X-Ray-diffraction. American Mineralogist **77:** 1144-1157.

MANCEAU, A., N. TAMURA, R.S. CELESTRE, A.A. MACDOWELL, N. GEOFFROY, G. SPOSITO, AND H.A. PADMORE. 2003. Molecular-scale speciation of Zn and Ni in soil ferromanganese nodules from loess soils of the Mississippi Basin. Environmental Science & Technology **37:** 75-80.

MANCEAU, A., M. SCHLEGEL, S. RIHS, AND M. A. MARCUS. 2005. Natural speciation of Mn, Ni and Zn at the micrometer scale in a clayey paddy soil using X-ray fluorescence, absorption, and diffraction. Geochimica et Cosmochimica Acta **69:** A612-A612.

MYERS, N., R. A. MITTERMEIER, C. G. MITTERMEIER, G. A. B. DA FONSECA, AND J. KENT. 2000. Biodiversity hotspots for conservation priorities. Nature **403:** 853-858.

REDFIELD, A. C., B. H. KETCHUM, AND F. A. RICHARDS. 1963. The influence of organisms on the composition of sea water. The Sea Vol. 2.

REYNOLDS, C. S., S. N. REYNOLDS, I. F. MUNAWAR, AND M. MUNAWAR. 2000. The regulation of phytoplankton population dynamics in the world's largest lakes. Aquatic Ecosystem Health and Management **3:** 1-21.

ROY, D., M. F. DOCKER, P. HEHANUSSA, D. D. HEATH, AND G. D. HAFFNER. 2004. Genetic and morphological data supporting the hypothesis of adaptive radiation in the endemic fish of Lake Matano. Journal of Evolutionary Biology **17:** 1268-1276.

SABO, E. M. 2006. Characterization of the pelagic plankton assemblage of Lake Matano and determination of factors regulating primary and secondary production dynamics. M.Sc. thesis. Univ. of Windsor.

SARAZIN, G., G. MICHARD, AND F. PREVOT. 1999. A rapid and accurate spectroscopic method for alkalinity measurements in sea water samples. Water Research **33:** 290-294.

SHAFFER, G.. 1986. Phosphate pumps and shuttles in the Black-Sea. Nature **321:** 515-517.

SHOLKOVITZ, E. R. 1985. Redox-related geochemistry in lakes: Alkali metals, alkaline-earth elements, and ^{137}Cs, p. 119-138. *In* W. Stumm [ed.], Chemical Processes in Lakes. John Wiley & Sons.

STOKES, G. C. 1851. On the effect of internal friction of fluids on the motion of pendulums. Transcripts of the Cambridge Philosophical Society **9:** 8-106.

STUMM, W., AND J. J. MORGAN. 1996. Aquatic Chemistry: Chemical Equilibria and Rates in Natural Waters, 3rd ed. John Wiley & Sons.

TAILLEFERT, M., AND J. F. GAILLARD. 2002. Reactive transport modeling of trace elements in the water column of a stratified lake: iron cycling and metal scavenging. Journal of Hydrology **256:** 16-34.

TAILLEFERT, M., T. F. ROZAN, B. T. GLAZER, J. HERSZAGE, R. E. TROUWBORST, AND G. W. LUTHER. 2000. Seasonal variations of soluble Fe(III) in sediment porewaters as revealed by voltammetric microelectrodes. Abstracts of Papers of the American Chemical Society **220:** U320-U321.

USEPA. 1983. Handbook for Sampling and Sample Preservation of Water and Wastewater, Report No. EPA 600482029. USEPA.

---. 2006. National Recommended Water Quality Criteria (4304T), p. 25. United States Environmental Protection Agency, Office of Science and Technology.

VAN DER LEE, J. 1993. CHESS, another speciation and surface complexation computer code. CIG-Ecole des Mines de Paris.

VIOLLIER, E., P. W. INGLETT, K. HUNTER, A. N. ROYCHOUDHURY, AND P. VAN CAPPELLEN. 2000. The ferrozine method revisited: Fe(II)/Fe(III) determination in natural waters. Applied Geochemistry **15:** 785-790.

VON RINTELEN, T., M., GLAUBRECHT. 2003. New discoveries in old lakes: Three new species of *Tylomelania* Sarasin & Sarasin, 1897 (Gastropoda: Cerithioidea: Pachychilidae) from the Malili Lake system on Sulawesi, Indonesia. J. Moll. Stud. **69:** 3-17.

WETZEL, R. G. 1983. Limnology, 2nd ed. CBS College Publishing.

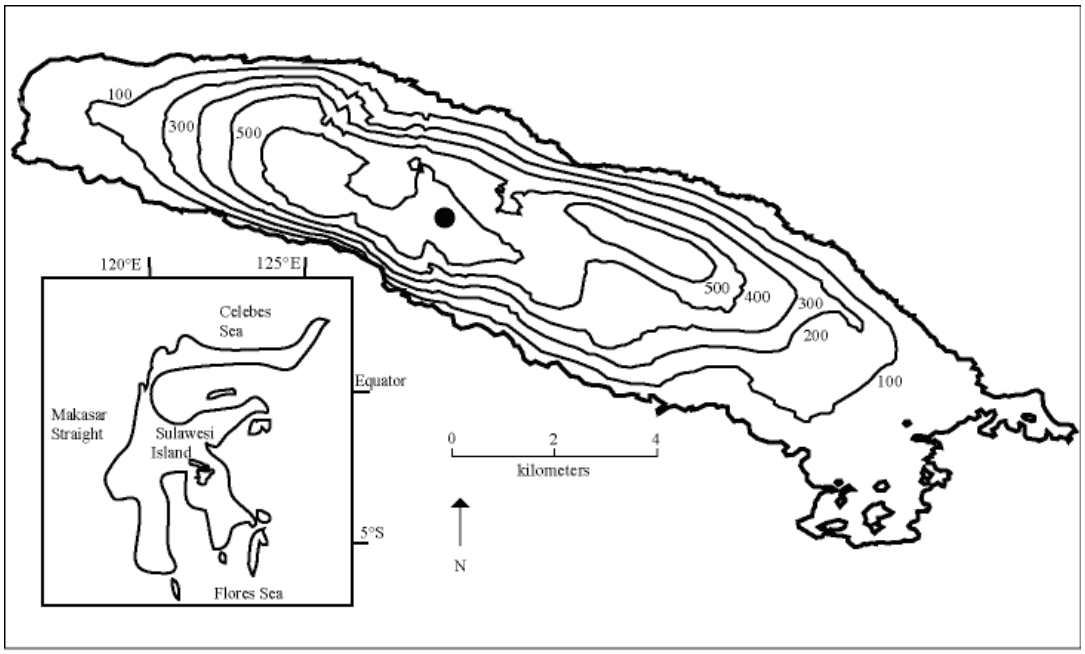
100
300
500
120°E
125°E
Celebes
Sea
Equator
Makasar
Straight
Sulawesi
Island
5°S
Flores Sea
500
400
300
200
100
0
2
4
kilometers
N

Figure 2.1

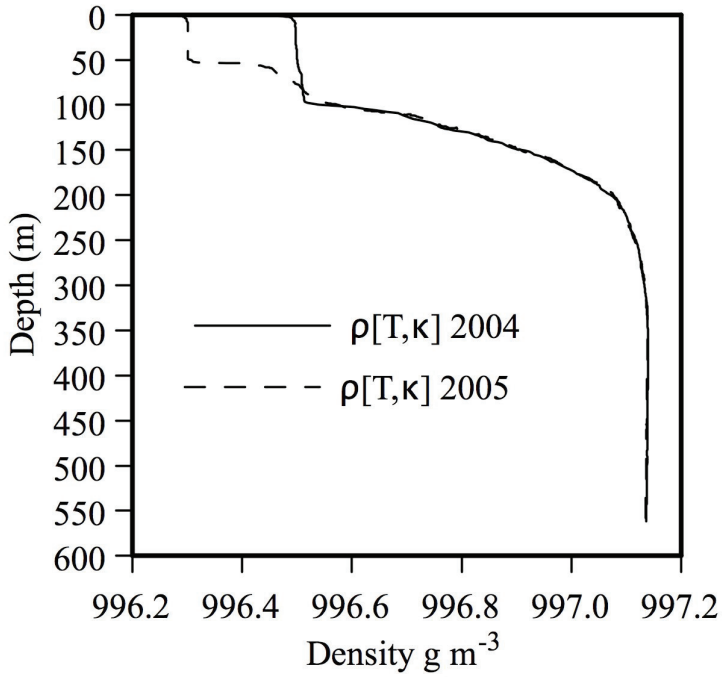
0
50
100
150
200
250
300
350
400
450
500
550
600
Depth (m)
ρ[T,κ] 2004
ρ[T,κ] 2005
996.2
996.4
996.6
996.8
997.0
997.2
Density g m-3

Figure 2.2

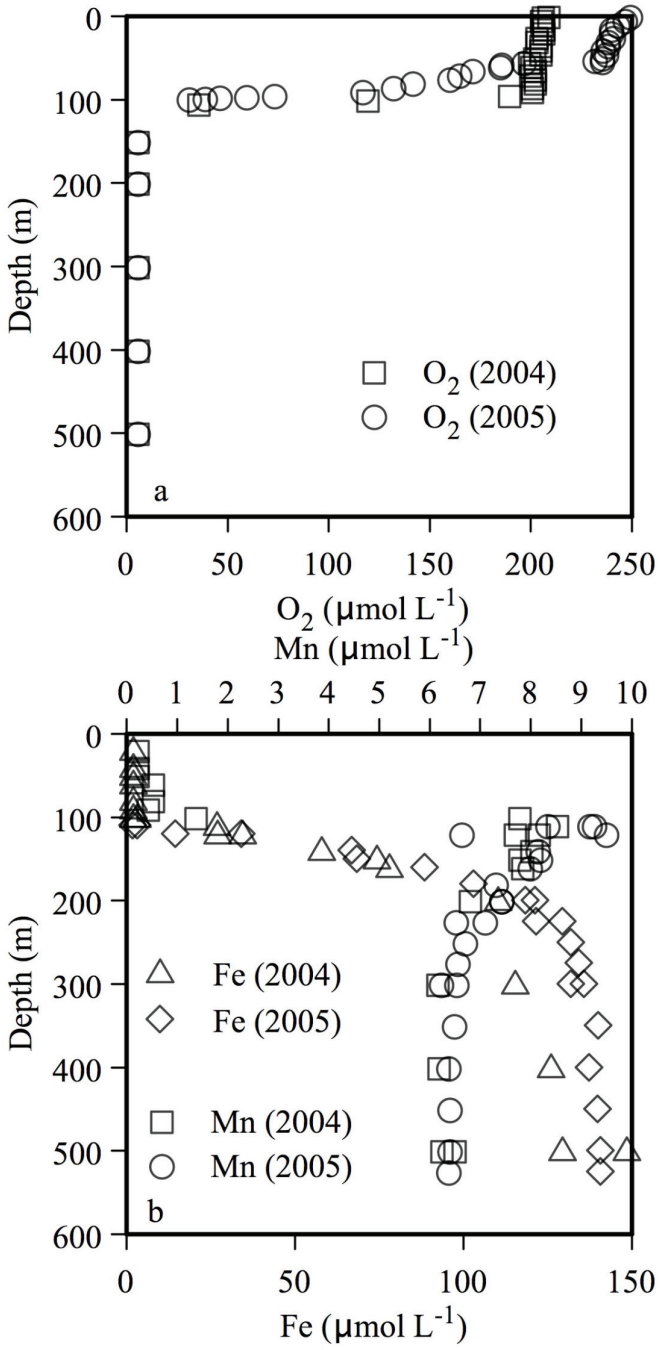
Depth (m)
0
100
200
300
400
500
600
O2 (2004)
O2 (2005)
a
0
50
100
150
200
250
O2 (μmol L-1)
Mn (μmol L-1)
0 1 2 3 4 5 6 7 8 9 10
Fe (2004)
Fe (2005)
Mn (2004)
Mn (2005)
b
0
50
100
150
Fe (μmol L-1)

Figure 2.3

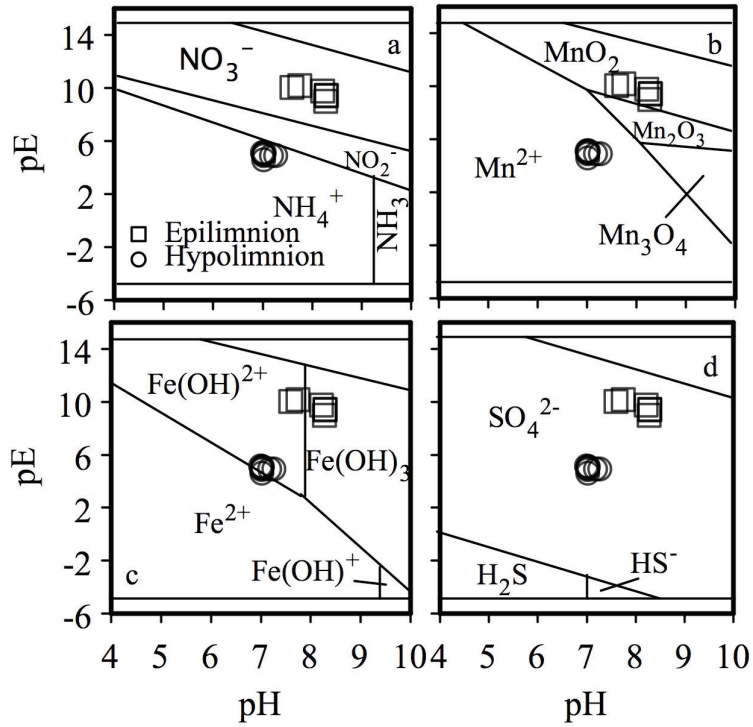
a
b
c
d
NO_3^-
NO_2^-
NH_4^+
NH_3
Epilimnion
Hypolimnion
MnO_2
Mn_2O_3
Mn^{2+}
Mn_3O_4
$Fe(OH)^{2+}$
$Fe(OH)_3$
Fe^{2+}
$Fe(OH)^+$
SO_4^{2-}
H_2S
HS^-
pE
pH
14
10
6
2
-2
-6
4 5 6 7 8 9 10

Figure 2.4

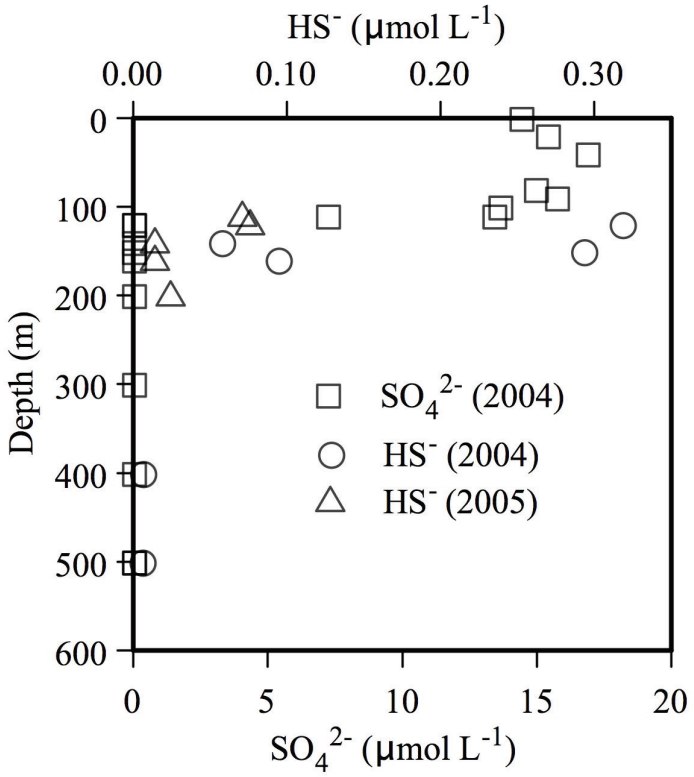
HS- (µmol L-1)
0.00
0.10
0.20
0.30
0
100
200
300
400
500
600
Depth (m)
SO4 2- (2004)
HS- (2004)
HS- (2005)
0
5
10
15
20
SO4 2- (µmol L-1)

Figure 2.5

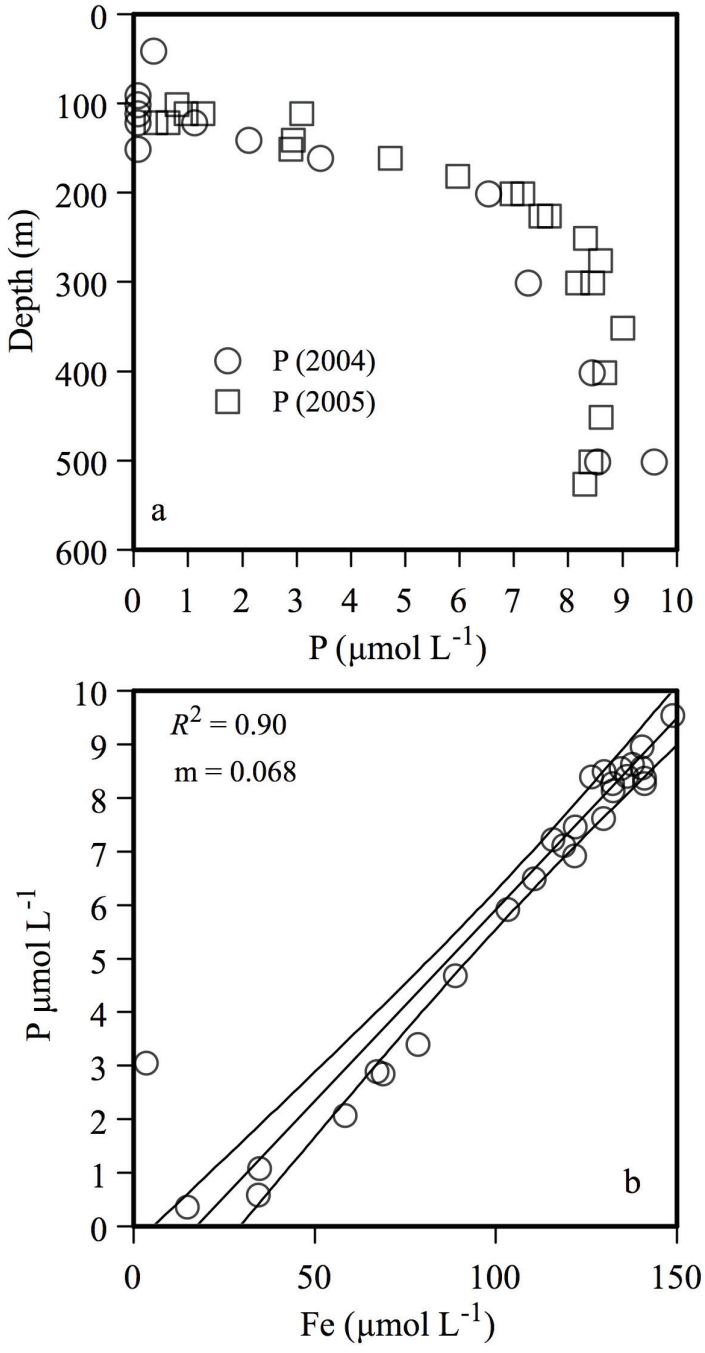
Depth (m)
P (2004)
P (2005)
a
P (µmol L-1)
R2 = 0.90
m = 0.068
P µmol L-1
b
Fe (µmol L-1)

Figure 2.6

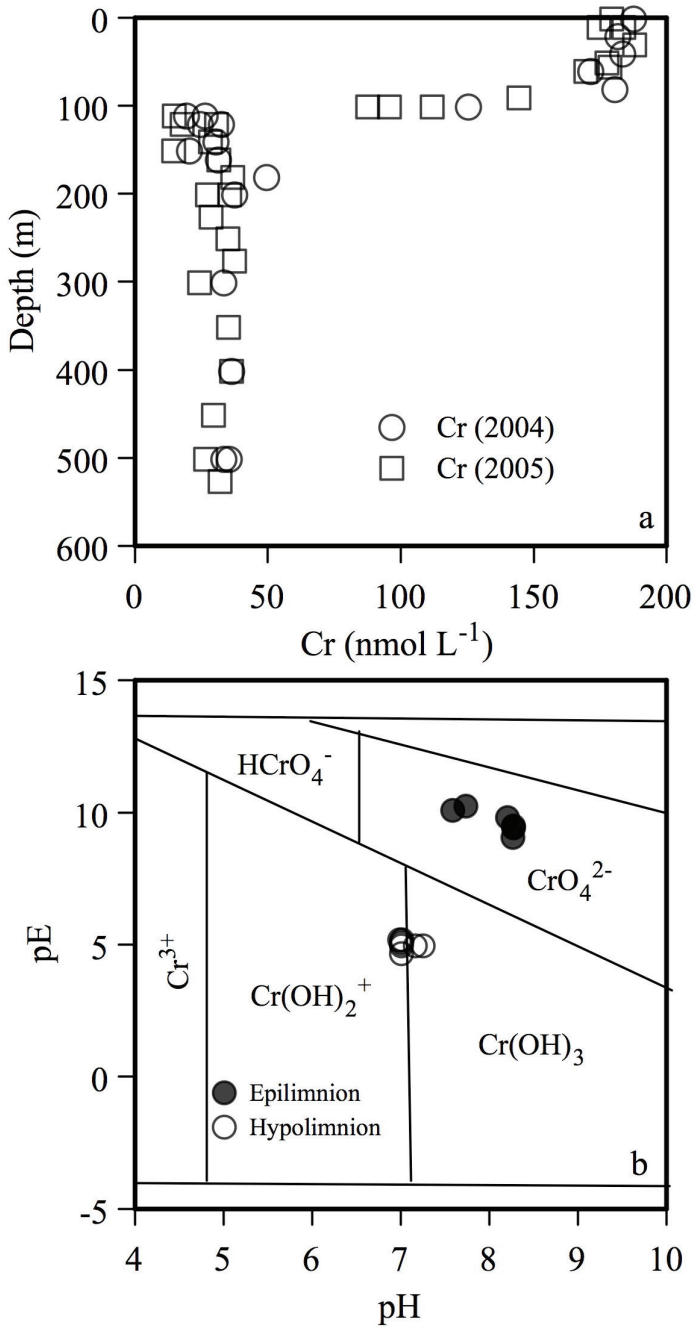
Depth (m)
0
100
200
300
400
500
600
Cr (2004)
Cr (2005)
a
0
50
100
150
200
Cr (nmol L-1)
pE
15
10
5
0
-5
HCrO4-
CrO4 2-
Cr3+
Cr(OH)2+
Cr(OH)3
Epilimnion
Hypolimnion
b
4
5
6
7
8
9
10
pH

Figure 2.7

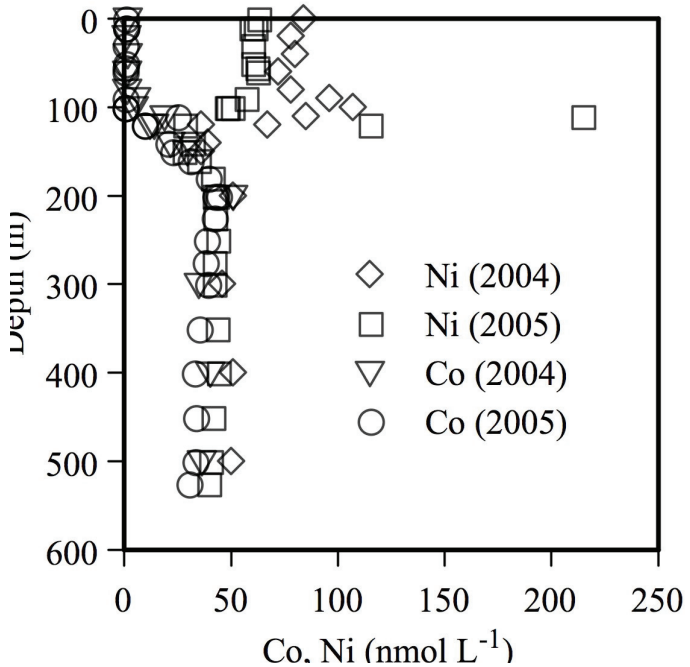
0
100
200
300
400
500
600
0
50
100
150
200
250
Ni (2004)
Ni (2005)
Co (2004)
Co (2005)
Co, Ni (nmol L-1)

Figure 2.8

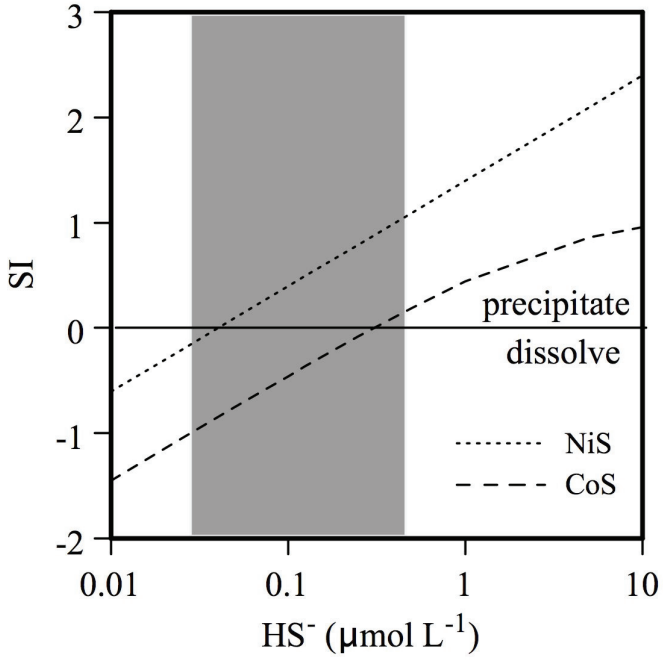

Figure 2.9

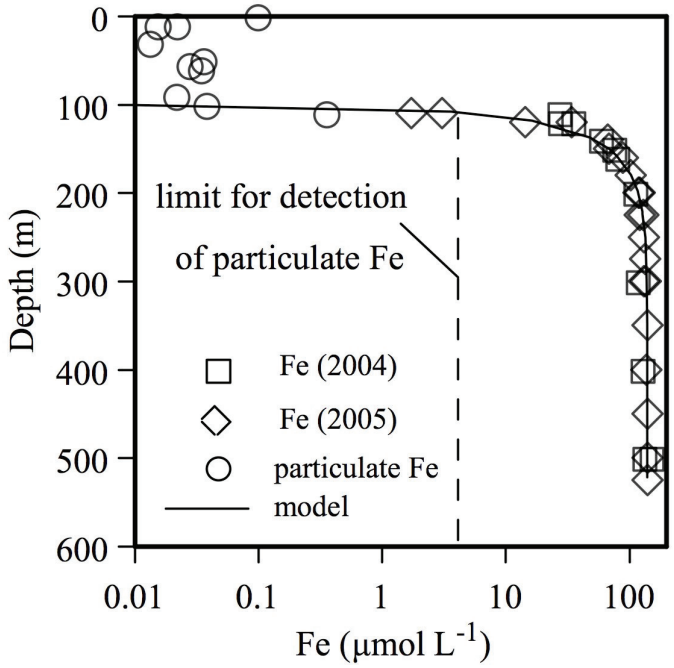
0
100
200
300
400
500
600
Depth (m)
limit for detection
of particulate Fe
Fe (2004)
Fe (2005)
particulate Fe
model
0.01
0.1
1
10
100
Fe (μmol L-1)

Figure 2.10

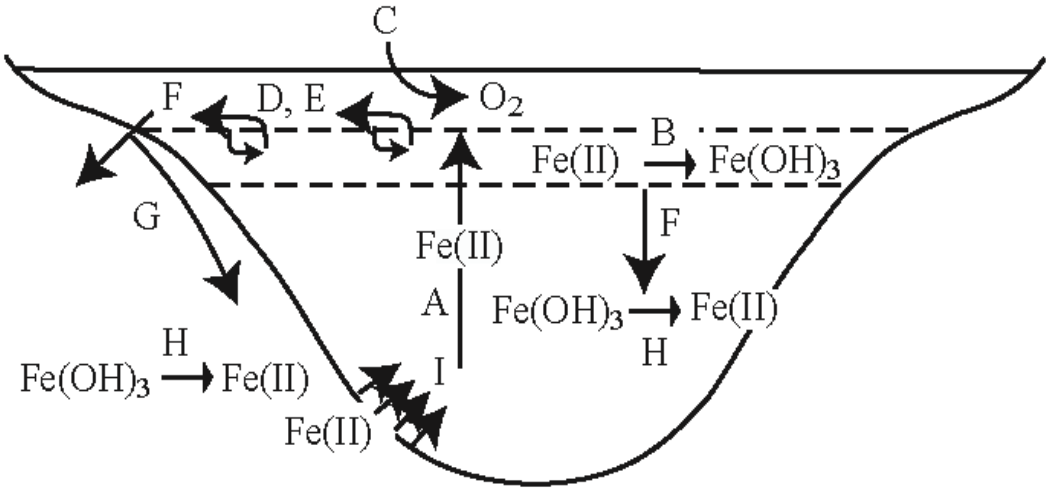

Figure 2.11

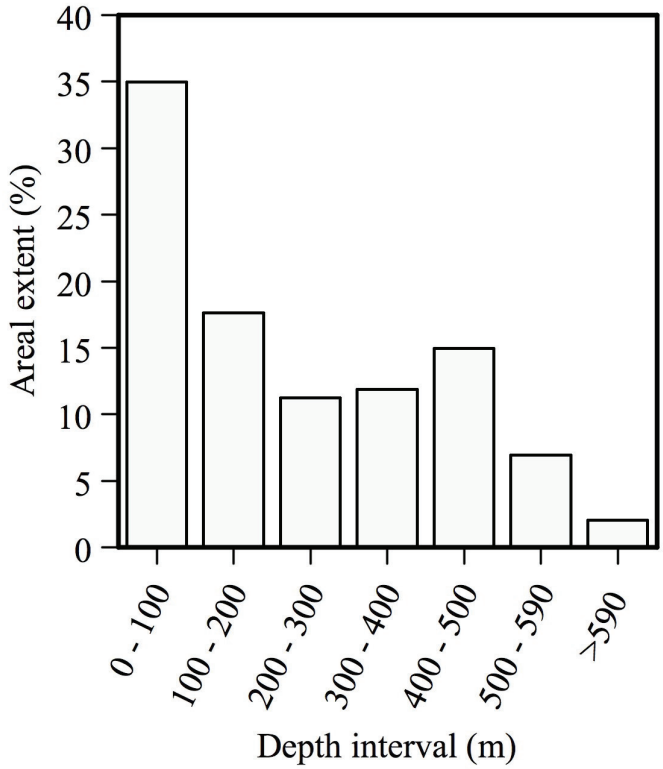
40
35
30
25
20
15
10
5
0
Areal extent (%)
0 - 100
100 - 200
200 - 300
300 - 400
400 - 500
500 - 590
>590
Depth interval (m)

Figure 2.12

2.7 Supplementary Information (Numerical description of reaction-transport model)

Assuming that eddy diffusion is the dominant mode of transport, the profile of Fe(II) can be described at steady state by (Taillefert and Gaillard 2002):

$$\frac{1}{A_z}\frac{d}{dz}\left(A_z K_z \frac{d[Fe(II)]}{dz}\right) + R_{Fe}(z) = 0 \qquad (2)$$

where A_z is the lateral surface area (m^2) at each depth z (m), K_z is the vertical eddy diffusion coefficient, [Fe(II)] is the concentration (mol L^{-1}) of dissolved Fe(II), and R_{Fe} (z) (mol L^{-1} yr^{-1}) is the rate at which Fe(II) is released to the water by Fe reduction. As the Fe(II) concentration in the epilimnion is close to zero (due to rapid oxidation kinetics) and the Fe(II) concentration in the deep water is constant, the boundary conditions for Eq. 2 are:

$$[\text{Fe(II)}]\ (z=0) = 0; \quad \left.\frac{d[Fe(II)]}{dz}\right|_{z=L} = 0 \qquad (3)$$

where z = 0 corresponds to the pycnocline (100 m depth) and z = L corresponds to the deep water (590 m). The rate $R_{Fe}(z)$ is likely proportional to both the particulate Fe(III) (hydr)oxides and the reductant (organic carbon) concentrations. In turn, the rate of their consumption is largely proportional to $R_{Fe}(z)$. Therefore, the decrease in $R_{Fe}(z)$ with depth is typically exponential (e.g., Katsev et al. 2006a):

$$R_{Fe}(z) = R_{Fe}(0)e^{(-\alpha z)} \ . \qquad (4)$$

Assuming, for simplicity, that K_z does not vary significantly below the pycnocline and neglecting the gradient in A_z because of the steep morphology of Lake Matano, we obtain the following solution to Eqs. 2-4:

$$[Fe(II)](z) = \frac{R_{Fe}(0)}{K_z \alpha^2}\left[1 - \exp(-\alpha z) - \alpha z \exp(-\alpha L)\right]. \quad (5)$$

Table 2.3. Representative physical data

Depth m	Temperature (°C)		Conductivity (µS)		Density (g m^{-3})	
	2004	2005	2004	2005	2004	2005
0	27.8	28.4	193	191	996.5	996.3
20	27.7	28.4	192	191	996.5	996.3
40	27.6	28.4	192	192	996.5	996.3
60	27.6	27.8	192	193	996.5	996.5
80	27.6	27.6	192	194	996.5	996.5
100	27.4	27.4	205	201	996.6	996.6
120	26.8	26.8	229	229	996.7	996.8
140	26.5	26.4	254	254	996.9	996.9
160	26.2	26.1	278	277	997.0	997.0
180	25.9	25.9	294	290	997.0	997.0
200	25.8	25.8	303	302	997.1	997.1
250	25.6	25.6	314	311	997.1	997.1
300	25.6	25.6	318	317	997.1	997.1
350	25.6	25.6	320	318	997.1	997.1
400	25.6	25.6	321	319	997.1	997.1
450	25.6	25.6	321	319	997.1	997.1
500	25.6	25.6	321	319	997.1	997.1
550	25.6	25.6	321	319	997.1	997.1

Table 2.4.

Depth m	pH	pE	O_2 (µmol L^{-1})		Mn (µmol L^{-1})		Fe (µmol L^{-1})		P (µmol L^{-1})		Cr (nmol L^{-1})		Ni (nmol L^{-1})		Co (nmol L^{-1})	
	2004	2004	2004	2005	2004	2005	2004	2005	2004	2005	2004	2005	2004	2005	2004	2005
Detection limit (DL)*			5		0.003		0.02		0.05		30		8		0.15	
0	7.72	10.3	249	208						DL	187	179	84	63	1.6	0.6
1				206												
5			246	205												
10			243	205								183		59		0.4
15			239	206												
20	8.19	9.86	239	206	0.2		2			DL	181		78		1.1	
25			240	203												
30			238	203								188		60		0.3
35			238	204												
40	8.25	9.09	235	204	0.2		2				183		80		1.6	
45			237	204												
50			235	201	0.2		2			DL		177		60		0.4
55			196	199								178		62		0.3
60	8.26	9.48	184	200	0.5		2				171	169	72	62	1.2	0.3
65			171	202												
70			164	199												
75			159	202												
80	8.26	9.53	141	202	0.5		2				180		78		1.3	
85			132	200												
90			116	200	0.4		2		DL	DL		144	96	57	5.5	0.3
95			73	189												
96			59													
97			46													
98			38													
99			30													
100	7.57	10.1		119	1.3		2		DL	0.8	125	95	107	48	4.4	0.3
105				35												

110	7.24	5.0	DL	DL	8.5	9.2	27	2	DL	0.9	DL	DL	85	215	19	25
120	7.15	5.0	DL	DL	7.7	9.5	34	34	DL	0.4	DL	DL	36	28	14	9
140					8.0	8.1	58	67		2.9	DL	DL	39	32	22	20
150	7.0	5.22	Dl	DL	7.8	8.2	74	68		2.9	DL	DL	36	28	29	22
160					7.8	8.0	78	88	3.4	4.7	DL	DL				
180						7.3		103		5.9	DL	DL	51	41	51	39
200	6.97	5.23	DL	DL		7.4	110	118	6.5	7.1	Dl	DL		42		44
225						6.5		122		7.5		DL		42		42
250						6.7		132		8.3		DL		43		38
275						6.5		134		8.6		DL		42		38
300	6.99	5.08	DL	DL	6.1	6.2	115	132	7.2	8.2	DL	DL	46	42	35	39
350						6.5		140		9.0		DL		43		35
400	6.99	5.16	DL	DL	6.2	6.4	126	137	8.4	8.7	DL	DL	51	44	40	33
450						6.4		140		8.6		DL		42		33
500	6.99	4.99	DL	DL	6.5	6.4	149	141	9.6	8.4	DL	DL	50	40	36	33
525	6.99	4.70				6.4		141		8.3		DL		40		30

*DL is the analytical detection limit. Concentrations reported as DL are at or below the detection limits. Detection limits are given in the third row of the table header.

Chapter 3. Link between Chapters 2 and 4

3.1 Linking Lake Matano to the earth's early oceans

In Chapter 2, I described the physics and chemistry of Lake Matano. Previously, high concentrations of Fe seem to have been the sole requisite for linking modern environments like thermal springs to the Fe-rich oceans of the Archean (Pierson et al. 1999; Trouwborst et al. 2007). Good analogues for the ecology of early ferruginous oceans have yet to be identified (Konhauser et al. 2005). Lake Matano is a stratified aquatic ecosystem unlike the thermal springs and groundwater springs previously used as analogues, and it likely represents a more appropriate early ocean analogue. In Chapter 4, I evaluate the merits of Lake Matano as an analogue to the earth's Fe-rich Archean and Proterozoic Oceans.

3.2 Primary production and pathways of C fixation

Lake Matano has low productivity which, in Chapter 2, I attribute to the combined effects of low dissolved P concentrations and relatively high concentrations of Cr(VI). Although the planktonic biomass has been used to qualitatively describe productivity (Haffner et al. 2001; Sabo 2006), to date no C-fixation measurements have been conducted in Lake Matano. In Chapter 4, I characterize the phototrophic communities in Lake Matano. I also measure rates of C fixation at two depths in Lake Matano and use chlorophyll concentrations to calculate rates of primary production.

3.3 References

Haffner, G. D., P. E. Hehanussa, and D. Hartoto. 2001. The biology and physical processes of larhe lakes of Indonesia, p. 183-194. *In* M. Munawar and R. E. Hecky [eds.], The Great Lakes of the World: Food web, health and integrity. Backhuys Publishers.

Konhauser, K. O., D. K. Newman, and A. Kappler. 2005. The potential significance of microbial Fe(III) reduction during deposition of Precambrian banded iron formations. Geobiology **3:** 167-177.

Pierson, B. K., M. N. Parenteau, and B. M. Griffin. 1999. Phototrophs in high-iron-concentration microbial mats: Physiological ecology of phototrophs in an iron-depositing hot spring. Appl. Environ. Microbiol. **65:** 5474-5483.

Sabo, E. M. 2006. Characterization of the pelagic plankton assemblage of Lake Matano and determination of factors regulating primary and secondary production dynamics. M.Sc. University of Windsor.

Trouwborst, R. E., A. Johnston, G. Koch, G. W. Luther, and B. K. Pierson. 2007. Biogeochemistry of Fe(II) oxidation in a photosynthetic microbial mat: Implications for Precambrian Fe(II) oxidation. Geochim. Cosmochim. Acta **71:** 4629-4643.

Chapter 4. Anoxygenic phototrophs thrive in an Archean Ocean analogue

Sean A. Crowe[1], CarriAyne Jones[2], Sergei Katsev[3], Cedric Magen[1], Andrew H. O'Neill[4], Arne Sturm[5], Donald E. Canfield[2], G. Douglas Haffner[4], Alfonso Mucci[1], Bjørn Sundby[1,6], and David A. Fowle[5]

1 Earth and Planetary Sciences, McGill University, Montréal, Québec, Canada H3A 2A7

2 Institute of Biology, NordCEE, University of Southern Denmark

3 Large Lakes Observatory and Department of Physics, University of Minnesota Duluth, Duluth, MN 55812

4 Great Lakes Iinstitute for Environmental Research, University of Windsor, Windsor, Ontario, Canada N9B 3P4

5 Department of Geology, University of Kansas, Lawrence, Kansas, USA 66047

6 ISMER, Université du Québec à Rimouski, Rimouski, Québec, Canada G5L 3A1

4.1 Abstract

Considerable discussion surrounds the potential role of anoxygenic phototrophic Fe(II)-oxidizing bacteria in both the genesis of Banded Iron Formations (BIFs) and early marine productivity. However, anoxygenic phototrophs have yet to be identified in modern environments with comparable chemistry and physical structure to the ancient Fe(II)-rich (ferruginous) oceans from which BIFs deposited. Lake Matano, Indonesia, the 8th deepest lake in the world, is such an environment. Here, sulfate is scarce (<20 μmol l^{-1}) and it is completely removed by sulfate reduction within the deep Fe(II)-rich chemocline. The sulfide produced is efficiently scavenged by the formation and precipitation of FeS, thereby maintaining very low sulfide concentrations within the chemocline and the deep ferruginous bottom waters. Low productivity in the surface water allows sunlight to penetrate to the > 100 m deep chemocline. Within this sulfide-poor, Fe(II)-rich, illuminated chemocline, we find a populous assemblage of anoxygenic phototrophic green sulfur bacteria (GSB). These GSB represent a large component of the Lake Matano phototrophic community, and BChl *e*, a pigment produced by low-light adapted GSB, is nearly as abundant as Chl *a* in the lake's euphotic surface waters. The dearth of sulfide in the chemocline requires that the GSB be sustained by phototrophic

oxidation of Fe(II), which is in abundant supply. By analogy, we propose that similar microbial communites, including populations of sulfate reducers and photoferrotrophic GSB, likely populated the chemoclines of ancient ferruginous oceans, driving the genesis of BIFs and fueling early marine productivity.

4.2 Introduction

Early in Earth history, ocean chemistry was very different than today. Sulfate concentrations were exceptionally low, and deep ocean waters were oxygen free and contained abundant ferrous Fe (Fe(II)) (Canfield et al. 2000, Canfield 2005). Oxidation and precipitation of this Fe led to the deposition of Banded Iron Formations (BIFs), conspicuous, ancient, Fe-rich, sedimentary deposits. BIFs are rather common sedimentary rocks formed more than 1.8 billion years ago (Isley and Abbott 1999). Their formation requires long distance transport of dissolved Fe(II) in anoxic, deep-ocean waters and its subsequent oxidation to form ferric Fe (hydr)oxide precipitates (Klein 2005). There has been considerable debate concerning the mechanisms responsible for BIF genesis (Cloud 1973, Braterman et al. 1983, Widdel et al. 1993, Konhauser et al. 2002). Of particular contention are the processes contributing to the production of ferric Fe (Fe(III)), which comprises, on average, 40 % of total BIF Fe (Konhauser et al. 2007). Potential Fe^{3+} production mechanisms include UV-induced Fe(II) oxidation (Braterman et al. 1983), inorganic and biologically-mediated Fe(II) oxidation by oxygen (Holland 1984, Holm 1989, Konhauser et al. 2002), and anoxygenic photrophic Fe(II) oxidation, termed photoferrotrophy (Widdel et al. 1993, Ehrenreich and Widdel 1994, Heising ans Schink 1998, Pierson et al. 1999, Kappler et al. 2005). The UV oxidation of Fe(II) has been demonstrated in the laboratory (e.g. (Braterman et al. 1983)), but not in complex seawater solutions. Furthermore, this mechanism would have been inhibited by the formation of amorphous Fe-silica gels in the ancient silica-saturated ocean waters from which BIFs deposited (Konhauser et al. 2002).

The scarcity of molecular O_2 early in Earth's history would have rendered abiotic Fe(II) oxidation exceptionally slow (Konhauser et al. 2005). However, biological Fe^{2+} oxidation at low oxygen partial pressures is much faster, and this chemoautotrophic metabolism (see review in Canfield 2005) is well known to occur in modern

microaerophilic environments. Provided a sufficient supply of O_2, chemolithoautotrophic Fe(II) oxidation could have been an important source of oxidized Fe to BIFs. Photoferrotrophy, on the other hand, does not require oxygen and could have also contributed substantial oxidized Fe to BIFs. Recent studies have explored the population sizes of phototrophic and non-phototrophic Fe-oxidizing bacteria needed to generate the sedimentary Fe(III) fluxes recorded in ancient BIFs (Konhauser et al. 2002, Kappler et al. 2005). These studies conclude that ancient marine settings likely had sufficient light and nutrients to sustain the necessary bacterial population sizes.

As photoferrotrophic Fe(II) oxidation can operate in the absence of oxygen, it could have generated Fe(III) for BIFs prior to the evolution of cyanobacteria and oxygenic photosynthesis. Indeed, the available evidence shows that anoxygenic photosystems evolved before oxygenic photosystems (Xiong et al. 2000). It has also been proposed that photoferrotrophs could have been the most important primary producers of organic matter on the early Earth before the advent of oxygenic photosynthesis (Canfield et al. 2006).

Previously, anoxygenic phototrophic bacteria were only identified as sulfide oxidizers, and their known occurrence was restricted to the chemocline of environments such as sulfide-containing microbial mats (DesMarais 1995), sulfidic lakes (Overmann 1997) and strongly stratified marine water bodies like the Black Sea (Repeta et al. 1989). The plausibility of photoferrotrophy in ancient ferruginous oceans has been made more tangible by the recent discovery of several different anoxygenic phototrophs, including a variety of purple bacteria (α and γ *Proteobacteria*; see review in Canfield et al. 2005) and a single green sulfur bacterium (*Chlorobium ferrooxidans*) (Heising et al. 1999) that can phototrophically oxidize dissolved Fe(II). To date, however, all known Fe(II)-oxidizing anoxygenic phototrophs have been isolated from iron-rich springs, ditches and other shallow, ephemeral environments (Heising et al. 1999; Heising and Schink 1998; Straub et al. 1999; Widdel et al. 1993). There have been no good modern analogs with which to evaluate the presence and potential activity of anoxygenic phototrophic communities, or microbial ecosystems in general, under conditions comparable to the early ferruginous oceans (Konhauser et al. 2005). In this paper, we highlight the microbial ecology and biogeochemistry of Lake Matano, Indonesia, which exhibits a water column structure and

chemistry resembling the ferruginous conditions construed for the Archean and Early Proterozoic Oceans. In Lake Matano, anoxygenic phototrophs thrive within a ferruginous chemocline, and they are likely sustained by photoferrotrophy.

4.3 Physical, chemical and microbial features of Lake Matano

Lake Matano is situated on Sulawesi Island, Indonesia (Crowe et al. 2008) (Figure 4.1). Its steep bathymetry, great depth (>590 m), and the absence of strong seasonal temperature fluctuations maintain a persistent pycnocline at ~100 m depth, separating an oxic surface mixed-layer from anoxic bottom waters (Figure 4.2a). Sulfate concentrations are low (>20 μmol l^{-1}) in the surface mixed-layer (Figure 4.2b) and sulfate reduction ensues at slow rates in the anoxic waters of the chemocline. Although slow, sulfate reduction rates within the chemocline are sufficient to completely remove sulfate supplied from the surface waters, resulting in deep waters with undetectable sulfate concentrations (Figure 4.2b). This produces very low, but measurable, concentrations of sulfide (Figure 4.2c) which, according to our standard analytical protocol, includes free sulfide as well as sulfide-containing colloids and larger reactive particles, such as NiS and FeS (Luther et al. 2001). Voltammetric measurements of sulfur speciation indicate that free sulfide concentrations are on the order of 0.01 to 0.06 μmol l^{-1}, much less than the total sulfide values reported in Figure 4.2c (see also supporting information). As sulfate is removed in the chemocline, there is no sulfate available to drive sulfate reduction in the anoxic bottom water. This restricts the production of sulfide and allows the accumulation of dissolved ferrous iron to high concentrations (Figure 4.2c). Scavenging of phosphate by allogenic and authigenic iron (hydr)oxides likely limits primary productivity in the surface mixed layer (Crowe et al. 2008), which, together with a low suspended inorganic particulate load, allows light to penetrate well into the anoxic bottom water (Figure 4.3a).

We measured photosynthetic pigment concentrations which track the distribution of the phototrophic communities in Lake Matano. Chlorophyll *a* dominates in the surface mixed layer of the lake (Figure 4.3b). Its low concentration throughout this layer is consistent with low rates of primary production (3.8×10^{-3} mol m^{-2} d^{-1}) by oxygen-producing cyanobacteria and algae. The low rates of photosynthetic C fixation measured

in Lake Matano are similar to those of ultra-oligotrophic high arctic lakes (Markager et al. 1999) and are in line with the suggestion that ferruginous conditions induce nutrient (phosphorus) limitation which restricts primary productivity (Bjerrum and Canfield 2002). Indeed, dissolved inorganic phosphorus (DIP) concentrations in the oxic surface waters of Lake Matano are below our detection limit of 1 nmol l^{-1} (data not shown) and are explained by active scavenging by Fe (hydr)oxide particles.

The transition from the oxic surface waters to the anoxic bottom waters is accompanied by a shift in the dominant photosynthetic pigment from chlorophyll *a* to bacteriochlorophyll *e* (BChl *e*; Figure 4.3b). The latter is a light-harvesting pigment used by brown-colored anoxygenic phototrophic GSB of the family *Chlorobiaceae*, that are especially well adapted to low light conditions (Manske et al. 2005; Overmann et al. 1992). A peak in BChl *e* concentrations between 115 and 125 m delineates a maximum in the population size of anoxygenic phototrophs and coincides with the maximum attenuation of light (Figure 4.3c). The depth-integrated quantity of BChl *e* (10.8 nmoles cm^{-2}) in the anoxic bottom water is nearly as large as that of Chl *a* (14 nmoles cm^{-2}) in the oxic surface water, indicating that GSB are an important component of the phototrophic community in Lake Matano. Furthermore, total carbon fixation rates measured at 118 m depth (0.65 μg l^{-1} h^{-1}) are as high as estimates of photosynthetic carbon fixation in the surface water (0.66 μg l^{-1} h^{-1}). Coincidently, 120 ± 5 m is also the depth at which DIP was previously reported to reach appreciable (> 1 μmol l^{-1}) levels (Crowe et al. 2008) indicating that microorganisms dwelling within the chemocline likely benefit from a supply of P from the underlying anoxic waters.

The specific cell content of BChl *e* in GSB growing under low light conditions can range from 50 to 200 μg BChl *e* mg^{-1} protein (Manske et al. 2005) which yields a protein content of 100 to 400 μg l^{-1} for the GSB community at 118 m depth. A typical range for bacterial cell protein contents of between 0.24 and 3.5 x 10^{-7} μg (Madigan 2006; Zubkov et al. 1999) translates to a relatively high GSB cell density of 0.3-16 x 10^{9} cells l^{-1} (Overmann et al. 1992).

Molecular fingerprinting using the 16S rRNA gene reveals the presence of a mixed bacterial community between 110 and 120 m depth, including several phylogenetically-distinct members of *Chlorobiaceae* (Figure 4.4). Most known

Chlorobiaceae are obligate photolithoautotrophs that utilize the reverse citric acid cycle to fix carbon with sulfide as an electron donor. As mentioned above, *Chlorobium ferrooxidans* is a notable exception that uses ferrous iron as an electron donor (Heising et al. 1999).

4.4 Lake Matano as an ancient ocean analog

Overall, the high ferrous iron concentrations, combined with low sulfate, deep light penetration and other physical and chemical characteristics (Table 1) make Lake Matano an excellent modern analogue for the chemistry and biology of Archean and early Proterozoic Oceans. Our results document measurable water column sulfate reduction at exceptionally low sulfate concentrations and at rates sufficient to completely remove sulfate within the chemocline. Sulfate concentrations in the Archean were < 200 μmol l^{-1} (Habicht et al. 2002) and perhaps even as low as the 20 μmol l^{-1} we find in Lake Matano. By analogy to Lake Matano, it seems likely that sulfate reduction was a significant water column process in early ferruginous oceans leading to substantial or even complete sulfate removal in the water column. This means that pyrite associated with BIFs and other deep water sediments likely formed partially or even wholly within the water column. In contrast, sedimentary sulfate reduction may have been largely restricted to shallower environments within or above the chemocline depth.

Most importantly, our results document that a populous and diverse assemblage of anoxygenic photosynthetic green sulfur bacteria inhabits the chemocline of Lake Matano. Ferrous iron concentrations are up to 30 μmol l^{-1} within the depth interval (100-120 m) in which BChl *e* concentrations are highest (Figure 4.2c and 4.3b, respectively). In this depth interval, the midday light intensity (Figure 4.3a) varies from 1 μmol quanta m^{-2} s^{-1} at the top of the chemocline (100 m) where Fe(II) is undetectable (< 0.5 μmol l^{-1}) to about 0.13 μmol quanta m^{-2} s^{-1} at 120 m, immediately below the depth exhibiting the maximum BChl *e* concentrations. These light intensities exceed those supporting substantial anoxygenic photosynthesis by low-light adapted *Chlorobiaceae* in the Black Sea (Manske et al. 2005). Unlike the Black Sea however, the Lake Matano chemocline has extremely low dissolved sulfide concentrations, suggesting that the populous assemblage of GSB is sustained using the abundant supply of Fe(II) as an electron donor.

Given the small, but measurable, concentrations of free sulfide in the chemocline of Lake Matano (Figure 4.2c), we must consider if the GSB in the lake could be sustained using this sulfide as an electron donor. The lowest known half-saturation constant for sulfide oxidation by green sulfur bacteria is 0.8 μmoles l^{-1} (Van Gemerden 1984), a factor of 13 to 80 greater than the free sulfide concentrations in Lake Matano. Unless the Lake Matano GSB are much more proficient at using sulfide than similar organisms studied to date, sulfide concentrations are too low to support sulfide-driven anoxygenic phototrophy. Thus, we are led to conclude that the Lake Matano GSB population is largely sustained by photoferrotrophy.

We can test the potential contribution of photoferrotrophy to Fe(II) oxidation in Lake Matano by evaluating if the irradiance at 110 m depth is sufficient to phototrophically drive the Fe(II) flux through the chemocline. From Fick's first law (flux = $-KzdC/dx$), we calculate an upward flux of Fe(II) through the chemocline of between 0.034 and 0.27 μmol cm^{-2} d^{-1} (Table 2). The light incident at the top of the chemocline, 1 μmol quanta m^{-2} s^{-1} (Figure 4.3a), translates into a quantum flux of 2.2 μmol quanta cm^{-2} per day for a conservative estimate of 6 daily hours of sunlight. With a typical GSB requirement of 1 to 2 moles quanta per mole of electrons transferred (one electron is transferred to oxidize Fe(II) to Fe(III)) (Overmann and Garcia-Pichel 2006), this light flux is sufficient to phototrophically oxidize the entire flux of Fe(II) through the chemocline (Table 2).

These rates of Fe(II) oxidation are also consistent with the metabolic capacities of known photoferrotrophs. The vertical distribution of BChl *e* in Lake Matano, suggests that most of the phototrophic Fe(II) oxidation occurs within a 10 meter depth interval (110 to 120 meters), yielding average volume-based Fe(II) oxidation rates of 0.034 to 0.27 μmol l^{-1} d^{-1} (Table 2). From laboratory studies, the Fe(II) oxidation rate of photoferrotrophic purple bacteria has been estimated at 14 μmol l^{-1} d^{-1} for a spectral quality of light corresponding to 100-meter water depth in the ocean and a light level of 3 μmol quanta m^{-2} s^{-1}, or 300 % of the light level measured at the top of the Matano chemocline (Kappler et al. 2005). For comparison, if we assume that the rate of phototrophic Fe(II) oxidation varies linearly with light levels at low light intensities, we can scale down the experimental rates (Kappler et al. 2005) by a factor of 3 yielding a

rate of 4.7 μmol l^{-1} d^{-1}. This rate is still more than one order of magnitude higher than our estimates of Fe(II) oxidation rates. Hence, the rates of Fe(II) oxidation observed in the Lake Matano chemocline are well within the physiological capabilities of known photoferrotrophs.

4.5 Conclusions and Extensions

Our results from Lake Matano, Indonesia, provide the first glimpse at the microbial ecosystems that can develop in a stable, ferruginous aquatic environment. We note that ferruginous conditions likely restrict production in oxic waters due to the scavenging of P by Fe (hydr)oxides. We also document the complete removal of the lake's low sulfate concentrations within the chemocline, allowing the accumulation of high iron concentrations at depth. Even where sulfate reduction is most active, free sulfide accumulates to less than 0.1 μmol l^{-1}, likely rendering it unavailable to anoxygenic phototrophs. In contrast, concentrations of Fe(II) are high in the chemocline, and its oxidation likely drives the metabolism of a prominent chemocline GSB population. Therefore, our results demonstrate that anoxygenic phototrophic green sulfur bacteria are not restricted to anoxic sulfidic lakes and euxinic marine basins like the Black Sea, but also flourish under ferruginous conditions which favor photoferrotrophy. As Lake Matano shares so many chemical and physical characteristics (Table 1) with ancient ferruginous oceans, anoxygenic phototrophic communities likely populated those ancient water columns as well and, through their metabolic activities, contributed to water column iron oxidation. Our finding that GSB thrive under conditions similar to those that prevailed during BIF deposition increases the plausibility that photoferrotrophs were involved in the genesis of BIFs. Our results also support the theory of an ancient dynamic global carbon cycle driven by photoferrotrophy before the evolution of oxygenic photosynthesis (Canfield et al. 2006). Indeed, calculations reveal that photoferrotrophy could have driven global primary production rates up to 10 % of present-day values. Based on these calculations, photoferrotrophy would have been, by far, the most active primary producing metabolism before the dawn of oxygenic photosynthesis. Low light adapted GSB would have gained a competitive advantage had microoxic conditions prevailed in the surface waters of the early ferruginous oceans. Such microxic conditions

would have precluded microbial Fe-reduction and the resulting reductive dissolution of Fe (hydr)oxides in the surface waters. Low-light adapted GSB could have gained access to P by dwelling beneath the oxycline where P was liberated from Fe (hydr)oxides in response to microbial Fe-reduction.

There may also be geological evidence that GSB inhabited an ancient marine ferruginous water column. Alkylated 2,3,6-trimethylbenzenes were detected in glacial deposits associated with the ~700 million year old Neoproterozoic Sturtian "Snowball Earth" glaciation (Olcott et al. 2005). This biomarker was interpreted as fossil isorenieratene from green sulfur bacteria and taken to indicate sulfidic water column conditions (Olcott et al. 2005). It is generally argued, however, that the Sturtian deep ocean was ferruginous, giving rise to BIF deposition (Hoffman and Schrag 2002). In light of our work, the putative Neoproterozoic GSB could have thrived within a ferruginous, ice covered, "Snowball Earth" water column.

Still, some important questions remain. While photoferrotrophy is the most likely metabolism for Lake Matano GSB, we have yet to isolate an Fe(II)-oxidizing GSB in pure culture. Such a culture would aid us in better understanding the physiology and overall metabolic capabilities of the GSB in the lake. Also, our work does not rule out the possibility that non-phototrophic Fe(II) oxidation might also be important in driving the Fe(II) flux through the chemocline. Indeed, we have noted the presence of cells with conspicuous morphologies characteristic of the neutrophillic Fe(II) oxidizer *Leptothrix*. Finally, our understanding of the Fe cycle in Lake Matano is still incomplete. In particular, it would be important to constrain the spatial and temporal relationships between Fe(II) oxidation and Fe reduction in supplying Fe(II) and nutrients (e.g. P) to the Fe(II) oxidizing populations. Each of these issues stand as important research opportunities to better understand the microbial ecology and biogeochemistry of element cycling in Lake Matano, and by extension, the dynamics of element cycling in ancient ferruginous oceans.

4.6 Materials and Methods

Water density and ferrous iron concentrations were determined as previously described (Crowe et al. 2008). Sulfide concentrations were measured using the Cline

spectrophotometric method with a 10 cm cell (Cline 1969). Replicate profiles of light transmission were collected *in situ* using a Wet-Labs C-Star transmissometer with a 25 cm path-length operated at a wavelength of 660 nm. Voltammetric analyses and sulfide speciation measurements were conducted on water samples, recovered with Niskin bottles, using Au/Hg amalgam microelectrodes as previously described (Brendel and Luther 1995). Sulfate reduction rates were determined using the ^{35}S radiotracer technique (Fossing and Jorgensen 1989). Sulfate concentrations were determined by measuring total sulfur concentrations using inductively coupled plasma-optical emission spectrometry after 10-fold preconcentration by evaporation and subtracting sulfide from total sulfur (detection limit = 60 nmol l^{-1}). Photosynthetic pigments were extracted in a mixture of methanol, acetone and N,N-dimethylformamide (Hagerthey et al. 2006). The low concentrations of pigments were determined using a 1-m path length capillary cell interfaced to a fiber-optic spectrometer and a UV-Visible light source (Waterbury et al. 1997). The profile of photosynthetically active radiation (PAR) in Figure 4.2 was obtained at mid-day on a representative, cloudless day using a LI-COR 1400-LI light meter.

Rates of C fixation were measured *in situ* at 32 (0.35 μg C l^{-1} hr^{-1}) and 118 m depth (0.65 μg C l^{-1} hr^{-1}) using the $H^{13}CO3$ labeling technique (Slawyk et al. 1977). Total primary production was calculated by normalizing the rate of C fixation at 30 m depth to the chlorophyll *a* concentrations at the same depth. Carbon fixation rates at 10 m intervals were determined by multiplying this factor by the chlorophyll *a* concentrations at the corresponding depth interval. Total primary production was then calculated by summing the C fixation rates for these 10 m intervals within the entire 100 m deep surface oxic layer.

Cellular material was collected on 0.2 μm cellulose acetate or 0.7 μm glass fiber filters. Filters were preserved in ethanol (cellulose acetate filters) or at -80ºC (glass fiber filters). DNA was extracted using a Mo-Bio PowerSoil DNA extraction kit. Small sub-unit (SSU) rDNA was amplified using polymerase chain reaction (PCR) with either the 'universal' bacterial primers 27f and 1492r (cellulose acetate filters) or primers specific for Chlorobiaceae GC341f and GSB822r (glass fiber

filters) (Overmann et al. 1999). The PCR products were cloned into the TOPO cloning vector and transformed into chemically-competent One Shot TOP10 *E. coli*. Plasmid DNA was purified using a PureLink Quick plasmid Miniprep Kit. Forward and reverse sequencing of the purified DNA was performed by Macrogen. Contiguous sequences were assembled using the assembly function in Geneious® and sequence alignments were conducted online using the Greengenes alignment tool (DeSantis et al. 2006a). Chimeric sequences were identified with Bellerophon (v.3) and eliminated from the dataset (DeSantis et al. 2006a). A subset of the 'Hugenholtz' database (DeSantis et al. 2006b) and the Lake Matano clone sequences were exported to PAUP version 4.0b10 for MacIntosh, in which phylogenetic trees were constructed using neighbor-joining, maximum parsimony and maximum likelihood methods (Swofford 1993). Branching topologies were compared for all methods and verified by performing 1000 bootstrap replications using the maximum parsimony method. Lake Matano clone sequences were submitted to GenBank (Accession Nos. EU275404-EU275407).

Fluxes were calculated using Fick's first law. The vertical eddy diffusivity coefficient was calculated from the Thorpe size of overturning eddies (Thorpe and Hall 1977), which was determined from replicate measurements using a free-falling CTD. The values obtained bracket the value of 3900 $cm^2\ d^{-1}$ derived previously using a phenomenological relationship with the Brunt-Väisälä frequency (Crowe et al. 2008), and a value of 2000 $cm^2\ d^{-1}$, which was estimated by comparing sulfate reduction rates with the rate of sulfate diffusion into the chemocline (Zopfi et al. 2001).

Acknowledgements. We acknowledge the help of numerous individuals including: Peter Hehanussa, William Napier, Mike Dutton, Matt Orr, Deky Tetradiono, Lili Lubis, Jennifer Roberts, Peter Søholt, Karla Leslie, Elisabeth Sabo, Sulung Nomosatryo, Gadis Sri Hariyani, Sinyo Rio, Dullah and Sarah Bungin. Mark Mort and Jennifer Archibald helped with the phylogenetic analyses, and Greg Druschel helped with the interpretation of voltammetric scans. Funding was kindly provided by NSERC, INCO Canada Ltd., PT INCO, KU Geology Associates and DNRF. SAC was supported by an NSERC IPGS sponsored by INCO Canada Ltd.

Table 4.1 Physical and Chemical parameters of Lake Matano and the Archean Ocean

	Lake Matano		**Archean Ocean**
	Mixed layer	Anoxic layer	
surface mixed layer	100 m		> 200 m (Kappler et al. 2005)
Fe^{2+}		140 µmol l^{-1}	40-120 µmol l^{-1} (Canfield 2005)
O_2	Saturated	< 1 µmol l^{-1}	< 0.08% PAL* (Canfield 2005)
SO_4^{2-}	< 20 µmol l^{-1}	< 0.1 µmol l^{-1}	< 200 µmol l^{-1} (Canfield 2005)
PO_4^{3-}	< 0.025 µmol l^{-1} (Crowe et al. 2008)	9 µmol l^{-1} (Crowe et al. 2008)	0.03 – 0.29 µmol l^{-1} (Bjerrum and Canfield 2002)
pH	8.6 (Crowe et al. 2008)	7.00 (Crowe et al. 2008)	> 6.5 (Bjerrum and Canfield 2002; Holland 2004)
Euphotic zone	< 130 m		< 150 m (Kappler et al. 2005)
T	25-28°C		~ 40°C (Konhauser et al. 2007)

*Present Atmospheric Levels (PAL)

Table 4.2 Fe(II) fluxes and rates of oxidation in Lake Matano

[a]Kz	Fe(II) gradient	Fe(II) flux	[b]Fe oxidation rate
$cm^2\ d^{-1}$	$\mu mol\ cm^{-4}$	$\mu mol\ cm^{-2}\ d^{-1}$	$\mu mol\ l^{-1}\ d^{-1}$
600-4900	5.6x10-5	0.034-0.27	0.034-0.27

[a]A range of Kz values was estimated from the Thorpe size of overturning eddies (Thorpe and Hall 1977). A previously published value of 3900 $cm^2\ d^{-1}$ (Crowe et al. 2008) and a value (2000 $cm^2\ d^{-1}$) estimated from sulfate reduction rates and sulfate profiles are both within this range (see supporting online material).

[b]calculated assuming a 10 meter interval for Fe(II) oxidation

Figure 4.1 Map showing the location of Lake Matano on Sulawesi Island, Indonesia (inset) and bathymetric map of Lake Matano. The circle marks a central deep water master station, and the area shaded in red is underlain by anoxic water. Modified with permission from Crowe et al., 2008.

Figure 4.2 a) The typical vertical distribution of water density in Lake Matano showing a seasonal pycnocline at 32 m depth and the persistent pycnocline at 110-120 m depth during the month of February 2007; b) The vertical distribution of dissolved sulfate (closed circles) and sulfate reduction rates (open squares); c) The vertical distribution of dissolved oxygen (gray line), iron (open circles) and total diffusible sulfide (ΣH_2S_d) (open diamonds) over the same time period.

Figure 4.3 a) Photosynthetically active radiation profile collected on a sunny day in February 2007; b) The distribution of photosynthetic pigments (open circles = Chl *a*, open diamonds = BChl *e*) collected, respectively, in February and March 2007; c) Light transmission (beam attenuation) profile collected in February 2007.

Figure 4.4 A tree generated using maximum parsimony and displaying the phylogenic relationships between Lake Matano clones and representative members of the Chlorobiaceae family in addition to *Persicobacter diffluens* as an outgroup. Bootstratp support is indicated at the branch points of the tree. Lake Matano clones have up to 95 % sequence similarity to *Chlorobium ferrooxidans*.

4.7 References

Bjerrum, C. J., and D. E. Canfield. 2002. Ocean productivity before about 1.9 Gyr ago limited by phosphorus adsorption onto iron oxides. Nature **417:** 159-162.

Braterman, P. S., A. G. Cairns-Smith, and R. W. Sloper. 1983. Photo-oxidation of hydrated Fe^{2+}- Significance for Banded Iron Formations. Nature **303:** 163-164.

Brendel, P. J., and G. W. Luther. 1995. Development of a gold amalgam voltammetric microelectrode for the determination of dissolved Fe, Mn, O_2, and S(II) in porewaters of marine and fresh-water sediments. Environ. Sci. Technol. **29:** 751-761.

Canfield, D. E. 2005. The early history of atmospheric oxygen: Homage to Robert A. Garrels. Annu. Rev. Earth Planet. Sci. **33:** 1-36.

Canfield, D. E., K. S. Habicht, and B. Thamdrup. 2000. The Archean sulfur cycle and the early history of atmospheric oxygen. Science **288:** 658-661.

Canfield, D. E., E. Kristensen, and B. Thamdrup. 2005. Aquatic Geomicrobiology. Elsevier, San Diego, California, USA.

Canfield, D. E., M. T. Rosing, and C. Bjerrum. 2006. Early anaerobic metabolisms. Philos. Trans. R. Soc. B-Biol. Sci. **361:** 1819-1834.

Cline, J. D. 1969. Spectrophotometric determination of hydrogen sulfide in natural waters. Limnol. Oceanogr. **14:** 454-458.

Cloud, P. 1973. Paleoecological significance of the banded iron-formation. Econ. Geol. **68:** 1135-1143.

Crowe, S. A., A. H. O'neill, S. Katsev, P. Hehanussa, G. D. Haffner, B. Sundby, A. Mucci, and D. A. Fowle. 2008. The biogeochemistry of tropical lakes: A case study from Lake Matano, Indonesia. Limnol. Oceanogr. **53:** 319-331.

DeSantis, T. Z., P. Hugenholtz, K. Keller, E. L. Brodie, N. Larsen, Y. M. Piceno, R. Phan, and G. L. Andersen. 2006a. NAST: a multiple sequence alignment server for comparative analysis of 16S rRNA genes. Nucleic Acids Res. **34:** W394-W399.

DeSantis, T. Z., P. Hugenholtz, N. Larsen, M. Rojas, E. L. Brodie, K. Keller, T. Huber, D. Dalevi, P. Hu, and G. L. Andersen. 2006b. Greengenes, a chimera-checked

16S rRNA gene database and workbench compatible with ARB. Appl. Environ. Microbiol. **72:** 5069-5072.

DesMarais, D. J. 1995. The biogeochemistry of hypersaline microbial mats. Adv. Microb. Ecol. **14:** 251-274.

Ehrenreich, A., and F. Widdel. 1994. Anaerobic oxidation of ferrous iron by purple bacteria, a new type of phototrophic metabolism. Appl. Environ. Microbiol. **60:** 4517-4526.

Habicht, K. S., M. Gade, B. Thamdrup, P. Berg, and D. E. Canfield. 2002. Calibration of sulfate levels in the Archean Ocean. Science **298:** 2372-2374.

Hagerthey, S. E., J. W. Louda, and P. Mongkronsri. 2006. Evaluation of pigment extraction methods and a recommended protocol for periphyton chlorophyll a determination and chemotaxonomic assessment. J. Phycol. **42:** 1125-1136.

Heising, S., L. Richter, W. Ludwig, and B. Schink. 1999. *Chlorobium ferrooxidans* sp nov., a phototrophic green sulfur bacterium that oxidizes ferrous iron in coculture with a "*Geospirillum*" sp strain. Arch. Microbiol. **172:** 116-124.

Heising, S., and B. Schink. 1998. Phototrophic oxidation of ferrous iron by a *Rhodomicrobium vannielii* strain. Microbiol. UK **144:** 2263-2269.

Hoffman, P. F., and D. P. Schrag. 2002. The snowball Earth hypothesis: testing the limits of global change. Terra Nova **14:** 129-155.

Holland, H. D. 1984. Chemical evolution of the atmosphere and oceans. Princeton University Press, Princeton, New Jersey, USA.

Holland, H. D. 2004. The geological history of seawater, p. 583-625. *In* H. D. Holland, Turekian, K.K. [ed.], Treatise on Geochemistry. Elsevier, Amsterdam, The Netherlands.

Holm, N. G. 1989. The $^{13}C/^{12}C$ ratios of siderite and organic matter of a modern metalliferous hydrothermal sediment and their implications for banded iron formations. Chem. Geol. **77:** 41-45.

Isley, A. E., and D. H. Abbott. 1999. Plume-related mafic volcanism and the deposition of banded iron formation. J. Geophys. Res. Solid Earth **104:** 15461-15477.

Kappler, A., C. Pasquero, K. O. Konhauser, and D. K. Newman. 2005. Deposition of banded iron formations by anoxygenic phototrophic Fe(II)-oxidizing bacteria. Geology **33:** 865-868.

Klein, C. 2005. Some Precambrian banded iron-formations (BIFs) from around the world: Their age, geologic setting, mineralogy, metamorphism, geochemistry, and origin. Am. Mineral. **90:** 1473-1499.

Konhauser, K. O., L. Amskold, S. V. Lalonde, N. R. Posth, A. Kappler, and A. Anbar. 2007. Decoupling photochemical Fe(II) oxidation from shallow-water BIF deposition. Earth Planet. Sci. Lett. **258:** 87-100.

Konhauser, K. O., T. Hamade, R. Raiswell, R. C. Morris, F. G. Ferris, G. Southam, and D. E. Canfield. 2002. Could bacteria have formed the Precambrian banded iron formations? Geology **30:** 1079-1082.

Konhauser, K. O., D. K. Newman, and A. Kappler. 2005. The potential significance of microbial Fe(III) reduction during deposition of Precambrian banded iron formations. Geobiology **3:** 167-177.

Luther, G. W., T. F. Rozan, M. Taillefert, D. B. Nuzzio, C. Di Meo, T. M. Shank, R. A. Lutz, and S. C. Cary. 2001. Chemical speciation drives hydrothermal vent ecology. Nature **410:** 813-816.

Madigan, M. T. M., J. M. . 2006. *In* P. P. Hall [ed.], Brock Biology of Microorganisms, Upper Saddle River, New Jersey, USA.

Manske, A. K., J. Glaeser, M. A. M. Kuypers, and J. Overmann. 2005. Physiology and phylogeny of green sulfur bacteria forming a monospecific phototrophic assemblage at a depth of 100 meters in the Black Sea. Appl. Environ. Microbiol. **71:** 8049-8060.

Markager, S., W. F. Vincent, and E. P. Y. Tang. 1999. Carbon fixation by phytoplankton in high Arctic lakes: Implications of low temperature for photosynthesis. Limnol. Oceanogr. **44:** 597-607.

Olcott, A. N., A. L. Sessions, F. A. Corsetti, A. J. Kaufman, and T. F. De Oliviera. 2005. Biomarker evidence for photosynthesis during Neoproterozoic glaciation. Science **310:** 471-474.

Overmann, J. 1997. Mahoney Lake: A case study of the ecological significance of phototrophic sulfur bacteria. Adv. Microb. Ecol. **15:** 251-288.

Overmann, J., M. J. L. Coolen, and C. Tuschak. 1999. Specific detection of different phylogenetic groups of chemocline bacteria based on PCR and denaturing gradient gel electrophoresis of 16S rRNA gene fragments. Arch. Microbiol. **172:** 83-94.

Overmann, J., H. Cypionka, and N. Pfennig. 1992. An extremely low-light-adapted phototrophic sulfur bacterium from the Black-Sea. Limnol. Oceanogr. **37:** 150-155.

Overmann, J., and F. Garcia-Pichel. 2006. The Phototrophic Way of Life, p. 32-85. *In* M. Dworkin, S. Falkow, E. Rosenberg, K.-H. Schleifer and E. Stackebrandt [eds.], The Prokaryotes. Springer, New York, New York, USA.

Pierson, B. K., M. N. Parenteau, and B. M. Griffin. 1999. Phototrophs in high-iron-concentration microbial mats: Physiological ecology of phototrophs in an iron-depositing hot spring. Appl. Environ. Microbiol. **65:** 5474-5483.

Repeta, D. J., D. J. Simpson, B. B. Jorgensen, and H. W. Jannasch. 1989. Evidence for anoxygenic photosynthesis from the distribution of bacteriochlorophylls in the Black-Sea. Nature **342:** 69-72.

Slawyk, G., Y. Collos, and J. C. Auclair. 1977. Use of C^{13} and N^{15} isotopes for simultaneous measurement of carbon and nitrogen turnover rates in marine-phytoplankton. Limnol. Oceanogr. **22:** 925-932.

Straub, K. L., F. A. Rainey, and F. Widdel. 1999. *Rhodovulum iodosum* sp. nov, and *Rhodovulum robiginosum* sp. nov., two new marine phototrophic ferrous-iron-oxidizing purple bacteria. Int. J. Syst. Bacteriol. **49:** 729-735.

Swofford, D. L. 1993. PAUP - a computer-program for phylogenetic inference using maximum parsimony. J. Gen. Physiol. **102:** A9-A9.

Thorpe, S. A., and A. J. Hall. 1977. Mixing in upper ;ayer of a lake during heating cycle. Nature **265:** 719-722.

Van Gemerden, H. 1984. The sulfide affinity of Phototrophic Bacteria in relation to the location of elemental Sulfur. Arch. Microbiol. **139:** 289-294.

Waterbury, R. D., W. S. Yao, and R. H. Byrne. 1997. Long pathlength absorbance spectroscopy: trace analysis of Fe(II) using a 4.5m liquid core waveguide. Anal. Chim. Acta **357:** 99-102.

Widdel, F., S. Schnell, S. Heising, A. Ehrenreich, B. Assmus, and B. Schink. 1993. Ferrous iron oxidation by anoxygenic phototrophic bacteria. Nature **362:** 834-836.

Xiong, J., W. M. Fischer, K. Inoue, M. Nakahara, and C. E. Bauer. 2000. Molecular evidence for the early evolution of photosynthesis. Science **289:** 1724-1730.

Zopfi, J., T. G. Ferdelman, B. B. Jorgensen, A. Teske, and B. Thamdrup. 2001. Influence of water column dynamics on sulfide oxidation and other major biogeochemical processes in the chemocline of Mariager Fjord (Denmark). Mar. Chem. **74:** 29-51.

Zubkov, M. V., B. M. Fuchs, H. Eilers, P. H. Burkill, and R. Amann. 1999. Determination of total protein content of bacterial cells by SYPRO staining and flow cytometry. Appl. Environ. Microbiol. **65:** 3251-3257.

4.8 Supplementary Information (Voltammetric Speciation Analyses)

Examples of voltammograms used to estimate sulfur speciation are shown in SI Figure 4.5. A fast scanning (1000 mV s^{-1}) cyclic voltammogram conducted in water collected from 100 m depth (Figure 4.5a) shows the presence of multiple reduced, diffusible sulfur species. Peaks characteristic of bisulfide, elemental sulfur and colloidal FeS (Luther et al. 2003; Luther et al. 2001) are clearly distinguished and qualitatively demonstrate that the 'free' bisulfide ion constitutes only a fraction of the total dissolved, reduced sulfide pool. Square wave voltammograms (Figure 4.5b) of the same water show peaks characteristic of the same sulfur species identified using cyclic voltammetry. A semi-quantitative analysis (Brendel and Luther 1995) of the bisulfide peak in multiple square wave voltammetric analyses of water collected from between 115 m and 120 m depth indicate bisulfide concentrations between 0.01 and 0.06 μmol l^{-1}; an order of magnitude lower than the concentration of total dissolved sulfide determined using the methylene blue method (Figure 4.2c). The low concentrations of bisulfide compared to total dissolved sulfide indicate that the colloidal FeS species represents a significant fraction of the diffusible sulfide pool in Lake Matano, and by analogy would be expected to be important in sulfur cycling in other Fe-rich environments like the Archean and early Proterozoic Oceans.

Peaks previously attributed to dissolved, reactive and potentially organically-complexed Fe(III) species are also evident in the square wave analyses (Figure 4.5b) (Taillefert et al. 2000). The origin of this voltammetric signal is debated (Crowe et al. 2006). Nevertheless, the signal attributed to reactive soluble Fe(III) is often observed in analyses of Fe-rich sediment porewaters (Taillefert et al. 2000; Taillefert et al. 2002), in anaerobic incubations with Fe-rich sediments (Carey and Taillefert 2005), and in pure cultures of dissimilatory Fe-reducing bacteria (Crowe et al. 2007). The signal has also recently been observed in Fe-oxidizing phototrophic mats (Trouwborst et al. 2007). Taken together, the detection of this putative Fe(III) species in water between 115 m and 120 m depth in Lake Matano suggests the presence of a reactive dissolved Fe(III) species and may be indicative of suboxic, phototrophic Fe oxidation. The observation of this electrochemical signal at 120 m depth in Lake Matano is consistent with the assertion that

photoferrotrophic organisms secrete organic ligands to chelate and stabilize phototrophically generated ferric Fe (Straub et al. 2001).

4.9 Supplementary References

Brendel, P. J., and G. W. Luther. 1995. Development of a gold amalgam voltammetric microelectrode for the determination of dissolved Fe, Mn, O_2, and S(II) in porewaters of marine and fresh-water sediments. Environ. Sci. Technol. **29:** 751-761.

Crowe, S. A., C. Magen, A. Mucci, B. Sundby, and D. A. Fowle. 2006. Electrochemical investigation of bacterial Fe(III) reduction. Geochim. Cosmochim. Acta **70:** A119-A119.

Crowe, S. A., J. A. Roberts, C. G. Weisener, and D. A. Fowle. 2007. Alteration of iron-rich lacustrine sediments by dissimilatory iron-reducing bacteria. Geobiology **5:** 63-73.

Luther, G. W., B. Glazer, S. F. Ma, R. Trouwborst, B. R. Shultz, G. Druschel, and C. Kraiya. 2003. Iron and sulfur chemistry in a stratified lake: Evidence for iron-rich sulfide complexes. Aquatic Geochemistry **9:** 87-110.

Luther, G. W., T. F. Rozan, M. Taillefert, D. B. Nuzzio, C. Di Meo, T. M. Shank, R. A. Lutz, and S. C. Cary. 2001. Chemical speciation drives hydrothermal vent ecology. Nature **410:** 813-816.

Straub, K. L., M. Benz, and B. Schink. 2001. Iron metabolism in anoxic environments at near neutral pH. FEMS Microbiol. Ecol. **34:** 181-186.

Taillefert, M., A. B. Bono, and G. W. Luther. 2000. Reactivity of freshly formed Fe(III) in synthetic solutions and (pore)waters: Voltammetric evidence of an aging process. Environ. Sci. Technol. **34:** 2169-2177.

Taillefert, M., and J. F. Gaillard. 2002. Reactive transport modeling of trace elements in the water column of a stratified lake: iron cycling and metal scavenging. Journal of Hydrology **256:** 16-34.

Trouwborst, R. E., A. Johnston, G. Koch, G. W. Luther, and B. K. Pierson. 2007. Biogeochemistry of Fe(II) oxidation in a photosynthetic microbial mat:

Implications for Precambrian Fe(II) oxidation. Geochim. Cosmochim. Acta **71:** 4629-4643.

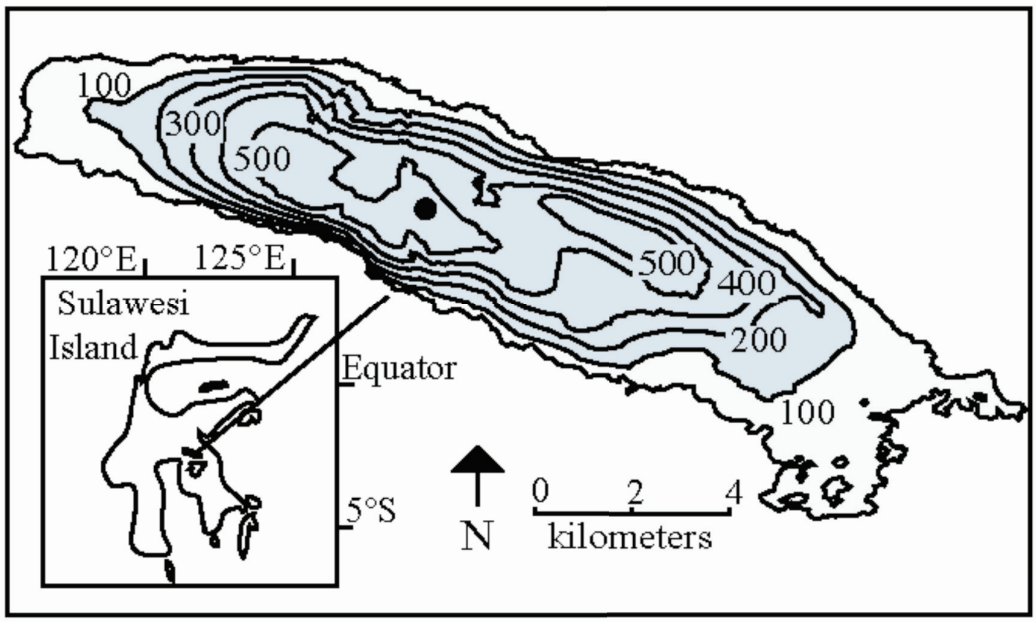
100
300
500
120°E
125°E
Sulawesi
Island
Equator
5°S
500
400
200
100
N
0
2
4
kilometers

Figure 4.1

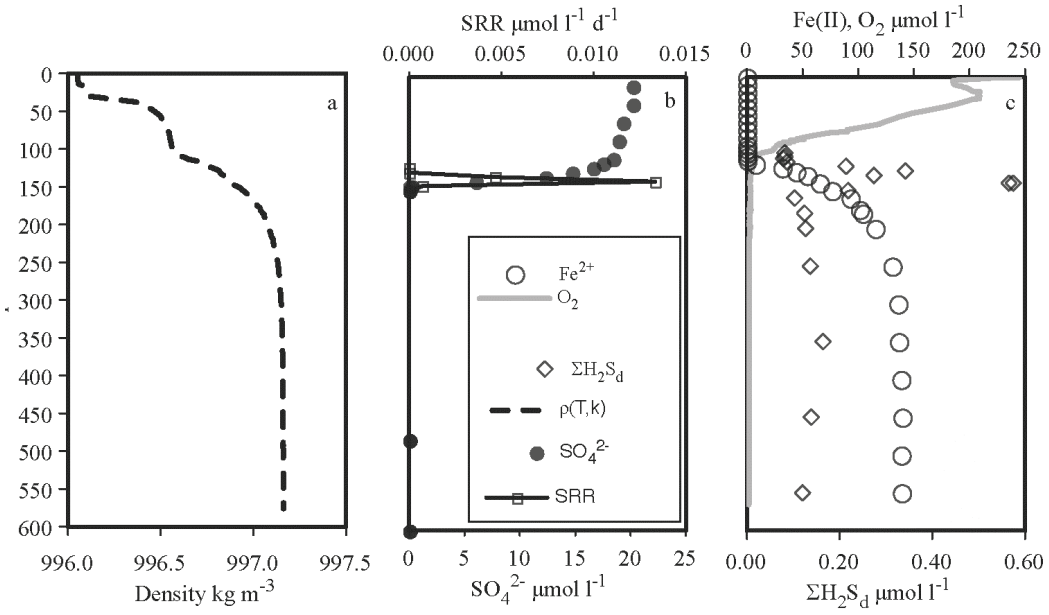
a
b
c
SRR µmol l-1 d-1
Fe(II), O2 µmol l-1
Fe2+
O2
ΣH2Sd
ρ(T,k)
SO42-
SRR
Density kg m-3
SO42- µmol l-1
ΣH2Sd µmol l-1

Figure 4.2

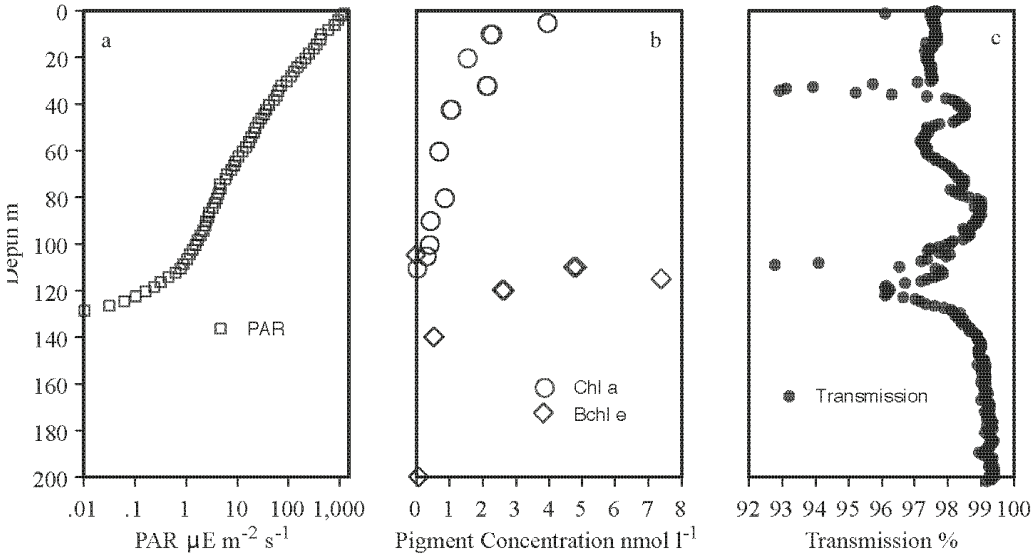
a
b
c
Depth m
0
20
40
60
80
100
120
140
160
180
200
PAR
Chl a
Bchl e
Transmission
.01 .1 1 10 100 1,000
PAR µE m-2 s-1
0 1 2 3 4 5 6 7 8
Pigment Concentration nmol l-1
92 93 94 95 96 97 98 99 100
Transmission %

Figure 4.3

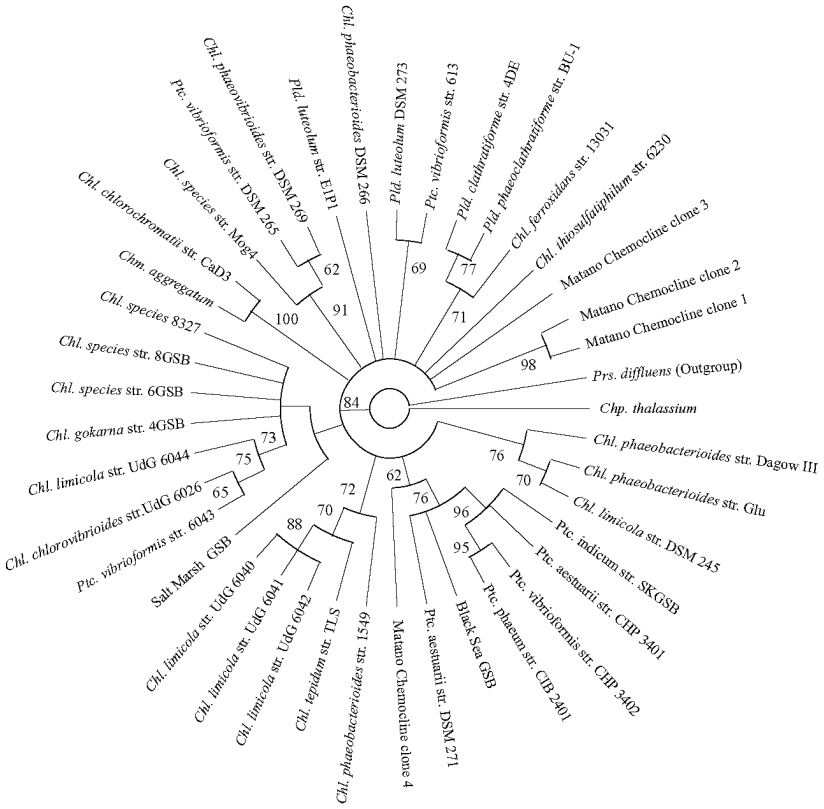
Chl. phaeobacterioides DSM 266
Pld. luteolum DSM 273
Ptc. vibrioformis str. 613
Pld. clathratiforme str. 4DE
Pld. phaeoclathratiforme str. BU-1
Chl. ferroxidans str. 13031
Chl. thiosulfatiphilum str. 6230
Matano Chemocline clone 3
Matano Chemocline clone 2
Matano Chemocline clone 1
Prs. diffluens (Outgroup)
Chp. thalassium
Chl. phaeobacterioides str. Dagow III
Chl. phaeobacterioides str. Glu
Chl. limicola str. DSM 245
Ptc. indicum str. SKGSB
Ptc. aestuarii str. CHP 3401
Ptc. vibrioformis str. CHP 3402
Ptc. phaeum str. CHP 2401
Black Sea GSB
Ptc. aestuarii str. DSM 271
Matano Chemocline clone 4
Chl. phaeobacterioides str. 1549
Chl. tepidum str. TLS
Chl. limicola str. UdG 6042
Chl. limicola str. UdG 6041
Chl. limicola str. UdG 6040
Salt Marsh GSB
Ptc. vibrioformis str. 6043
Chl. chlorovibrioides str.UdG 6026
Chl. limicola str. UdG 6044
Chl. gokarna str. 4GSB
Chl. species str. 6GSB
Chl. species str. 8GSB
Chl. species 8327
Chm. aggregatum
Chl. chlorochromatii str. CaD3
Chl. species str. Mog4
Ptc. vibrioformis str. DSM 265
Chl. phaeovibrioides str. DSM 269
Pld. luteolum str. E1P1
Chl. phaeobacterioides DSM 266
Pld. luteolum DSM 273
Ptc. vibrioformis str. 613
Pld. clathratiforme str. 4DE
Pld. phaeoclathratiforme str. BU-1
Chl. ferroxidans str. 13031
Chl. thiosulfatiphilum str. 6230
Matano Chemocline clone 3
Matano Chemocline clone 2
Matano Chemocline clone 1
Prs. diffluens (Outgroup)
Chp. thalassium
Chl. phaeobacterioides str. Dagow III
Chl. phaeobacterioides str. Glu
Chl. limicola str. DSM 245
Ptc. indicum str. SKGSB
Ptc. aestuarii str. CHP 3401
Ptc. vibrioformis str. CHP 3402
Ptc. phaeum str. CHP 2401
Black Sea GSB
Ptc. aestuarii str. DSM 271
Matano Chemocline clone 4
Chl. phaeobacterioides str. 1549
Chl. tepidum str. TLS
Chl. limicola str. UdG 6042
Chl. limicola str. UdG 6041
Chl. limicola str. UdG 6040
Salt Marsh GSB
Ptc. vibrioformis str. 6043
Chl. chlorovibrioides str.UdG 6026
Chl. limicola str. UdG 6044
Chl. gokarna str. 4GSB
Chl. species str. 6GSB
Chl. species str. 8GSB
Chl. species 8327
Chm. aggregatum
Chl. chlorochromatii str. CaD3
Chl. species str. Mog4
Ptc. vibrioformis str. DSM 265
Chl. phaeovibrioides str. DSM 269
Pld. luteolum str. E1P1
84
62
91
100
69
77
71
98
76
70
62
76
96
95
72
70
88
73
75
65
62
91
100
69
77
71
98
76
70
62
76
96
95
72
70
88
73
75
65

Figure 4.4

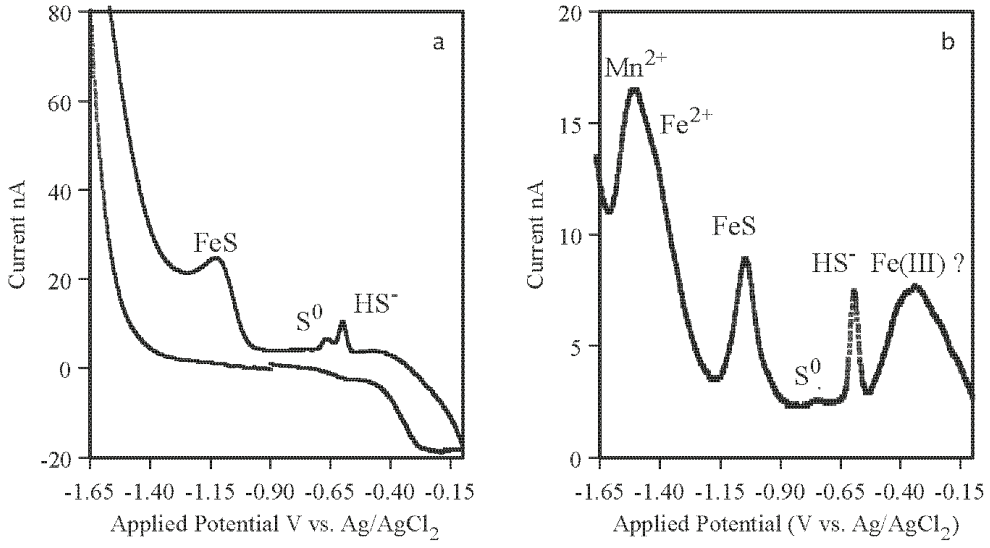
a
80
60
40
20
0
-20
Current nA
FeS
S0
HS-
-1.65 -1.40 -1.15 -0.90 -0.65 -0.40 -0.15
Applied Potential V vs. Ag/AgCl2
b
20
15
10
5
0
Current nA
Mn2+
Fe2+
FeS
HS-
Fe(III) ?
S0
-1.65 -1.40 -1.15 -0.90 -0.65 -0.40 -0.15
Applied Potential (V vs. Ag/AgCl2)

Figure 4.5

Chapter 5. Link between Chapters 4 and 6

5.1 Dissolved gases?

Chapters 2 and 4 documented the accumulation of anaerobic respiration products in Lake Matano's deep waters due persistent stratification. With the exception of rough measurements of alkalinity reported in Chapter 2 (from which CO_2 concentrations can be estimated) and measurements of oxygen and sulfide, dissolved gases in Lake Matano have not be adequately quantified. Indeed, as Lake Matano is persistently stratified there may be risk of gas driven limnic eruption in Lake Matano. Such limnic eruptions have previously occurred in African Lakes (Zhang and Kling 2006). In Chapter 6, I determine the concentrations of dissolved CH_4 and CO_2 in Lake Matano. The isotopic composition of dissolved C is also determined in an attempt to characterize the origins of the different dissolved C species.

5.2 C cycling

Lake Matano receives ample fluxes of ferric hydroxides making Fe(III) by far the most abundant potential terminal electron acceptor for organic matter degradation. The abundance of ferric Fe should suppress methane production as the free energy yield of dissimilatory Fe reduction is greater than that of methanogenesis (Lovley and Phillips 1987; Roden and Wetzel 2003). In Chapter 6, I use flux calculations to estimate the relative importance of Fe reduction and methanogenesis to organic C degradation.

5.3 References

Lovley, D. R., and E. J. P. Phillips. 1987. Competitive mechanisms for inhibition of sulfate reduction and methane production in the zone of ferric iron reduction in sediments. Appl. Environ. Microbiol. **53:** 2636-2641.

Roden, E. E., and R. G. Wetzel. 2003. Competition between Fe(III)-reducing and methanogenic bacteria for acetate in iron-rich freshwater sediments. Microbial Ecology **45:** 252-258.

Zhang, Y. X., and G. W. Kling. 2006. Dynamics of lake eruptions and possible ocean eruptions. Annu. Rev. Earth Planet. Sci. **34:** 293-324.

Chapter 6. The methane cycle in tropical Lake Matano: Methanogenesis, methane accumulation, and anaerobic methane oxidation

Sean A. Crowe[1,7], Sergei Katsev[2], Karla Leslie[3], Arne Sturm[3], Cédric Magen[1], Sulung Nomosatryo[4], Mary Pack[5], John Kessler[6], William Reeburgh[5], Jennifer A. Roberts[3], Luis Gonzalez[3], Alfonso Mucci[1,7], Bjørn Sundby[1,8], and David A. Fowle[3]

1 Earth and Planetary Sciences, McGill University, Montréal, Québec, Canada H3A 2A7

2 Large Lakes Observatory and Department of Physics, University of Minnesota Duluth, Duluth, MN 55812

3 Department of Geology, University of Kansas, Lawrence, Kansas, USA 66047

4 Center for Limnology Research and Development, LIPI, Cibinong, West Java, Indonesia 16911

5 Earth System Sciences, University of California, Irvine, CA 92697-3100

6 Geosciences Department, Princeton University, Princeton, NJ 08544-1003

7 GEOTOP-McGill-UQAM, Montreal, Quebec H3C 3P8, Canada

8 ISMER, Université du Québec à Rimouski, Rimouski, Quebec G5L 3A1, Canada

6.1 Abstract

Organic carbon is oxidized by microorganisms that use a series of terminal electron acceptors defined by free energy yield and availability. Methanogenesis by highly specialized Archea occurs once the availability of these electron acceptors is diminished beyond a thermodynamic threshold which renders the energy yield to low to sustain microbial respiration. In the deep waters of the persistently stratified and Fe-rich Lake Matano, Indonesia, authigenic organic matter is largely degraded through methanogenesis despite the high abundance of Fe (hydr)oxides in the lake's sediments. Dissolved carbon concentration profiles and stable isotope patterns indicate that some of the methane in Lake Matano is consumed by anaerobic oxidation (AOM). The absence of electron acceptors (NO_3^- and SO_4^-), known to oxidize methane anaerobically, in the anoxic layer of Lake Matano and the relatively high abundance of Fe (and Mn) (hydr)oxides suggest that methane oxidation may be coupled to the reduction of Fe (and/or Mn). To our knowledge, this is the first documentation of this pathway in natural environments. Our results demonstrate that methane can be an integral component of the

C cycle, even in Fe-rich environments. By analogy to Lake Matano, methanogens and methanotrophs could have formed an important part of the ferruginous Archean ocean ecosystem.

6.2 Introduction

Unlike their temperate counterparts, deep tropical lakes do not mix seasonally by convective overturn, and persistent stratification tends to develop within the water column (Crowe et al. 2008). The long residence time and the limited ventilation of the bottom water in these lakes promotes anoxia and leads to an accumulation of anaerobic metabolic products. The nearly 600 m deep Lake Matano on Sulawesi Island, Indonesia, is an example of such a lake (Crowe et al. 2008). The lake exhibits weak thermal gradients, yet a persistent pycnocline at around 100 m depth separates a mixed, oxic surface layer from the anoxic bottom water. Exchange of water between the oxic and anoxic layers is slow and on a time-scale similar to temperate meromictic lakes. Owing to the slow exchange, steep concentration gradients in dissolved Fe and Mn species have developed over the 100 m transition zone (metalimnion) between the anoxic bottom water and the oxic surface layer. Given its tectonic origin (Haffner et al. 2001), the sediments and bottom waters of Lake Matano may receive gas inputs from hydrothermal fluids. Therefore, dissolved gases including CO_2 and CH_4 that have been produced biologically or geologically may accumulate in the anoxic bottom water. Concern that methane and CO_2 might reach levels that can cause limnic eruption as observed in Lake Kivu, Lake Nyos, and Lake Lagos in Africa (Zhang and Kling 2006) prompted our study on dissolved gas cycling in Lake Matano.

Several aspects of both methane production and consumption in Lake Matano may be unique. For example, the exceptionally low sulfate concentrations (less than 20 $\mu mol\ l^{-1}$) (Crowe et al. 2008) should minimize competition between methanogens and sulfate reducing bacteria (SRB) for acetate and are therefore conducive to methanogenesis via acetate disproportionation. On the other hand, as microbial ferric Fe reduction yields more free energy than methanogenic acetate disproportionation (Lovley and Phillips 1987; Roden and Wetzel 1996), dissimilatory Fe (and Mn) reducing bacteria would also compete with methanogens for acetate. Indeed, the drainage basin of Lake Matano is dominated by ferruginous lateritic soils (Golightly 1981), and its sediments are very Fe-rich (up to 40 wt %) (Crowe et al. 2008; Crowe et al. 2004). In addition, the lack of sulfate should inhibit anaerobic oxidation of methane (AOM) by limiting the activity

of SRB, an integral partner in the bacterial-archeal consortia responsible for AOM in marine environments (Boetius et al. 2000; Losekann et al. 2007; Orphan et al. 2001). AOM represents a significant sink for methane in sediments and stratified water bodies that are not regularly ventilated (Reeburgh 2007). As Lake Matano is persistently stratified, the absence of AOM could promote methane accumulation and eventually lead to gas ebullition.

The availability of electron acceptors such as sulfate and Fe and Mn (hydr)oxides to non-methanogenic respiratory metabolisms influences both the rate of methane production and the predominance of specific methanogenic pathways. Most methanogenesis proceeds by one or both of two pathways: disproportionation of acetate or reduction of CO_2 with H_2 as the electron donor (Canfield et al. 2005; Reeburgh 2007). Both acetate and H_2 are produced during the fermentative breakdown of organic matter (Canfield et al. 2005; Capone and Kiene 1988; Lovley and Phillips 1987), and the availability of these substrates to methanogens depends on how actively they are consumed by more energetic metabolic pathways. The relative contributions of acetate disproportionation versus CO_2 reduction to total methane production can thus be influenced by acetate and H_2 consumption by the dominant non-methanogenic pathway. If respiratory bacteria outcompete methanogens for acetate, CO_2 reduction may dominate. Conversely, if acetate is not exhausted by respiration then acetate disproportionation should dominate.

Due to its unique physical and chemical attributes, notably the lack of sulfate and the abundance of Fe (hydr)oxides, Lake Matano represents an end-member system in which to evaluate controls on methane production and consumption. As rates and pathways of both methanogenesis and methanotrophy are directly impacted by sulfate availability, the ubiquity of sulfate in most modern environments intrinsically links the methane and S cycles (Capone and Kiene 1988; Reeburgh 2007). In contrast, sulfate was likely scarce during much of the Earth's early history (Habicht et al. 2002), and the marine methane cycle would have operated independently of S. By analogy, the lack of sulfate in Lake Matano may yield insights into the operation of the Earth's earliest marine methane cycle. In this paper, we use geochemical and microbiological techniques to examine methane production and consumption pathways, quantitatively evaluate the

importance of methane to carbon cycling in a sulfate-poor environment, and evaluate the potential risk of methane driven limnic eruption in Lake Matano.

6.3 Methods

Sampling and storage. Sampling was conducted at a central, deep-water location (2°28'00" S and 121°17'00"E) in July 2006 (end of the wet season) and February 2007 (beginning of the wet season) using local fishing boats. All water samples were collected using 5 l Go-Flow (Niskin) bottles attached in series to a stainless steel cable and a hand driven winch. The bottles were placed at depth to an accuracy of ±1 m using a commercial fish finder (Furuno). Water samples for methane determination were drawn directly from the Niskin bottle's spigot using a 60 ml syringe. These samples were transferred from the syringe to pre-evacuated 14 ml crimp-sealed vials that had been flushed with N_2 gas and contained 100 μl of a saturated $HgCl_2$ solution to prevent microbial methane production or oxidation. Water samples, collected for the determination of major cations, were filtered through 0.45 μm nylon membrane syringe filters and acidified immediately to 1 % v/v with trace metal grade HNO_3 (Fisher Scientific). Total alkalinity was determined on water samples transferred to glass bottles and preserved with $HgCl_2$. Samples for total dissolved inorganic carbon (ΣCO_2) determination were drawn from the spigots with a 1 ml syringe and injected directly into a flow-injection analysis system (see below).

Analyses. Water temperature and conductivity profiles were collected *in situ* using a submersible CTD (SeaBird, SBE-19). Methane concentrations in the headspace of the crimp-sealed vials were determined by gas chromatography (Agilent 6890N with a HAYSEP Q 80/100 column) with flame ionization (detection limit was 10^{-7} mmol l^{-1}, relative precision < 1%) (2006) or thermal conductivity (detection limit was 2 x 10^{-5} mmol l^{-1}, relative precision < 1%) (2007) detection. Total alkalinity was determined by potentiometric titration with a dilute HCl solution (Gieskes and Rogers 1973) using an automated Radiometer titrator (Titrilab 865). The ΣCO_2 and dissolved NH_4^+ concentrations were measured by flow injection analysis (Hall and Aller 1992). Isotopic compositions of the CH_4 and CO_2 in headspace samples were determined by gas

chromatography-combustion-isotope ratio mass spectrometry (GC-C-IRMS) using a ThermoFinnigan MAT 253 mass spectrometer interfaced to a ThermoElemental Trace GC Ultra with an Rt-QPLOT column (Restek). $\delta^{13}C_{\Sigma CO2}$ was determined by converting ΣCO_2 to gaseous CO_2 with orthophosphoric acid under a 15-mTorr vacuum. Water vapour was eliminated by double trapping with a liquid N_2-trap followed by a dry-ice isopropyl alcohol trap. $\delta^{13}C$ measurements were made using a VG-Prism™ triple-collector mass spectrometer. All stable C isotopic compositions are reported relative to the V-PDB standard and have a precision of < 0.2 ‰. Samples of particulate organic matter were collected on 0.7 μm glass fiber filers (Whatman). Portions of these filters were analyzed using an elemental analyzer coupled to a ThermoFinnigan MAT 253 mass spectrometer.

Dissolved oxygen measurements were made by linear sweep voltammetry (detection limit = 2.5 μmol l^{-1}) using an Analytical Instrument Systems (AIS) DLK-60 with cell stand. Water samples were transferred directly from the Niskin bottle to a glass voltammetric cell via Tygon tubing. The cell was sealed from the atmosphere using rubber stoppers and o-rings and was flushed with 3 times the cell volume of water before measurement. Measurements were conducted with a three-electrode configuration using a Au-Hg amalgam micro-electrode (50 μm radius), a saturated Ag-AgCl electrode, and a platinum wire as the working, reference and counter electrodes, respectively (Luther et al. 2003).

Samples used to measure the natural radiocarbon content of methane were collected in 15 ml serum vials with an average nitrogen headspace of 5.5 ml from depths of 105, 112, 118, 130, 140, 160, 200, 250, 350, 450, and 550 m. To collect enough methane for radiocarbon measurements, the entire headspace was extracted and combined from depths 105, 112, 118, 130, 140, 160, and 200 m as well as 250, 350, 450, 550 m, respectively. The methane was then prepared for radiocarbon analyses as previously described (Kessler and Reeburgh 2005). The samples were analyzed using ^{14}C-Accelerator Mass Spectrometry at the University of California, Irvine.

The pH of the water column was determined on individual samples using a hand held pH meter (VWR) and an Accumet combination electrode calibrated with 3 NIST-traceable buffers at the ambient surface water temperature (~ 29.5ºC). Major element

(Ca, Mg, Na, K, Si, Mn, and Fe) concentrations in the water column samples were determined by Inductively Coupled Plasma-Optical Emission Spectrometry (ICP-OES; Perkin Elmer Optima 5300 DV). Results of these analyses were used to evaluate the saturation state of water with respect to different mineral phases. Speciation and saturation state calculations were carried out using the JChess geochemical modeling software and the Chess thermodynamic database (Van Der Lee 1993).

Samples of cellular material were collected from 2 l of water on 0.7 μm glass fiber filters and preserved at -80ºC (glass fiber filters). DNA was extracted from these filters using a Mo-Bio PowerSoil extraction kit. 16S rDNA was amplified by polymerase chain reaction (PCR) using the group specific primers listed in Table 6.1. The PCR products were imaged by gel-electrophoresis to check for the positive amplification of the template and to estimate the length of the amplified fragments. The amplified DNA was cloned into the TOPO cloning vector and transformed into chemically-competent One Shot TOP10 *E. coli*. Plasmid DNA was purified using a PureLink Quick plasmid Miniprep Kit. Forward and reverse sequencing of the purified DNA was performed by Macrogen. Contiguous sequences were assembled using the assembly function in Geneious®. Chimeric sequences were identified with Bellerophon (v.3) and eliminated from the dataset (DeSantis et al. 2006b). Nearsest non-chimeric neighbors and isolates were identified using Simrank and sequence alignments were conducted online using the Greengenes alignment tool (DeSantis et al. 2006b). If possible, sequences for tree construction were culled from the greengenes databases and additional sequences were downloaded from the NCBI database. Hypervariable regions of the sequences were eliminated with the Lane Mask (Lane 1991) using the greengenes mask tool. Phylogenetic trees were constructed by maximum likelihood methods using the PHYML (Guindon and Gascuel 2003) plugin in Geneious®. Branching topologies were verified by conducting 100 bootstrap analyses.

6.4 Results

Physical properties of Lake Matano. Lake Matano was density stratified in both July of 2006 and February of 2007. During these months, the water column exhibited pycnoclines between depths of 60 and 90 m and 30 and 60 m, respectively (Figure 6.1).

This shallower pycnocline is consistent with the development of seasonal stratification during the wet season (Crowe et al. 2008). A comparison of the 2006 and 2007 density distributions with those observed in previous years collected at different months of the year (Crowe et al. 2008) shows that the seasonal density gradient is largest during the rainy season (February), and is completely eroded by the middle of the dry season (September). The erosion of the seasonal pycnocline appears to be driven by evaporative cooling of the surface waters during the dry season, resulting in an increase in density. Evaporative cooling during the warmer, dry season may largely drive mixing in the surface water (top 100 m) of Lake Matano.

During 2004, 2005, 2006 and 2007, a deeper pycnocline was present between 100-110 m and 250 m depth in Lake Matano. which persists over at least decadal and likely greater time scales (Crowe et al. 2008). The density gradient between 100 and 250 m appears to be largely unaffected by seasonality and is enhanced by higher concentrations of dissolved solids in the bottom waters (Crowe et al. 2008) (Figures 6.1, 6.2 and 6.3). The absence of a positive thermal gradient in the deep bottom waters reveals that there is no geothermal heat flux from the bottom sediments and dispels the possibility of volcanogenic hydrothermal inputs to the bottom waters. Similarly, a re-examination of older (2004-2005) thermal profiles and profiles collected at various locations throughout the lake provide no evidence for a geothermal heat source in the bottom of Lake Matano.

Distributions of major cations and redox active species. The concentration of major cationic species and Si were greater below 100 m depth than in the surface mixed layer (Figure 6.2). Mg concentrations in both the surface mixed layer and bottom water were relatively high (up to 5 times average stream water, (Faure 1997)) whereas K and Na concentrations are relatively low (less than 15 and 7 times lower, respectively, than average stream water, (Faure 1997)). The concentration profiles of Mg, Ca, Si, Na and K were identical in 2006 and 2007 and similar to those previously reported (Crowe et al. 2008). Ba concentrations (not shown) range from 0.15 $\mu mol\ l^{-1}$ in the surface water to 0.88 $\mu mol\ l^{-1}$ below 500 m. The Ba concentration profile is similar to that of the other major cations. The constancy of these chemical profiles between seasons and years is

consistent with a temporally stable stratification and slow mixing between the surface and bottom water.

This stable stratification is also reflected in the distribution of redox active species (Figure 6.3). Dissolved oxygen concentrations were nearly at saturation in the surface waters and decreased with increasing depth. Hypoxic (< 62.5 μmol l^{-1}) conditions prevailed between 95 and 110 m and sub- to anoxic conditions were reached below 110 m. The profiles of other redox active species (Mn, Fe, SO_4^{2-}, and HS^-) were consistent with the distribution of O_2. There was, however, some overlap between the profiles of dissolved Mn and O_2 within the hypoxic zone; Mn was detected (0.45 μmol l^{-1}) at 105 m depth where O_2 concentrations up to 37 μmol l^{-1} were measured. In contrast, Fe was not detected (0.1 μmol l^{-1}) within the hypoxic zone but was measurable (0.29 μmol l^{-1}) at 110 m, the depth at which O_2 became undetectable (< 2.5 μmol l^{-1}). Sulfate concentrations in the surface mixed layer were low (<20 μmol l^{-1}) and trace sulfide was detected in the anoxic bottom water (Chapter 4). Nitrate and nitrite were undetectable within the water column, with the exception of a small peak (< 200 nmol l^{-1}) of NO_3^- between 90 and 100 m depth (Figure. 6.4a). Particulate Fe and Mn concentrations also peaked near the persistent pycnocline (Figure 6.4b). The vertical distributions of these redox sensitive species were nearly the same as those measured in 2004 and 2005 (Crowe et al. 2008), illustrating the near steady-state nature of redox cycling within the pycnocline of Lake Matano.

Distributions of dissolved CH_4 and $\sum CO_2$. Methane concentrations in Lake Matano ranged from 0.003 mmol l^{-1} in the surface mixed layer to 1.4 mmol l^{-1} in the anoxic bottom water. Vertical profiles of methane concentrations constructed from samples taken in both 2006 and 2007 (Figure 6.5) are nearly identical, which suggests that methane concentrations are close to steady state, like other redox active species (Crowe et al. 2008). At 0.003 mmol l^{-1}, methane is oversaturated with respect to the atmosphere in the surface water and, thus the lake acts as a net source of methane. The methane concentrations in the bottom water are up to 2 % saturation at *in situ* pressures. Below 200 m depth, the concentrations are equivalent to the solubility of methane in water at atmospheric pressure (Henry's Law Constant = 1.3 x 10^{-3} mol l^{-1} atm^{-1}, (Canfield et al.

2005)). Hence, samples collected from below 200 m may have degassed during recovery and actual concentrations may be higher than reported.

Profiles of pH and pCO_2 (computed from carbonate alkalinity and pH measurements using the CO2SYS model and the "freshwater" constants, Lewis and Wallace 1998) are given in Figure 6.5. The $\sum CO_2$ concentrations calculated from the alkalinity measurements are in good agreement with measured $\sum CO_2$ concentrations (not shown) but the former carry smaller uncertainties. Speciation calculations reveal that the dissolved inorganic carbon pool in the surface water (pH 8.60) is dominated by the bicarbonate ion. The concentrations of $CO_{2(aq)}$ in the bottom water of Lake Matano are less than 1 mmol l^{-1} (partial pressures up to 0.023 atm) and well below saturation at *in situ* pressures (~19 atm at 200 m depth).

The water column is supersaturated with respect to a number of mineral species at various depths (Table 6.2). Water is oversaturated with respect to dolomite, $CaMg(CO_3)_2$, and witherite, $BaCO_3$, throughout much of the water column. Ba concentrations are relatively low (< 1 μmol l^{-1}), and witherite is not expected to quantitatively contribute to bulk ΣCO_2 removal from the water column. Although dolomite formation in modern freshwater environments is rare, methanogenic microorganisms are thought to enhance dolomite precipitation by nucleation on their cell walls (Roberts et al. 2004). The presence of methanogens in the Lake Matano chemocline may therefore induce dolomite precipitation in Lake Matano. In the absence of dolomite formation, calcite and siderite precipitation would be expected to be the largest sinks for inorganic C in the surface mixed layer and bottom sediments, respectively.

Isotopic data. The C isotopic composition of CH_4 ($\delta^{13}C_{CH4}$) in the deep bottom water is < -70 ‰ (Figure 6.6a). $\delta^{13}C_{\sum CO2}$ values vary between -7 and -8 ‰ throughout most of the water column except for two negative excursions to nearly -10 ‰ at 104.5 and 122 m depth (Figure 6.6b). The radiocarbon content of CH_4 ($^{14}C_{CH4}$) in the surface water (depths ≤ 200 m) was 77.4 ± 0.2 percent Modern Carbon (pMC) (Stuiver and Polach 1977). The $^{14}C_{CH4}$ content in the deep water (> 250 m depth) was 75.0 ± 0.1 pMC.

Microbial Ecology. Table 6.3 shows the results of PCR amplifications using primers designed to target specific groups of microorganisms. DNA was PCR amplified from depths of 120 m, 118 m, and 102 m using a primer set specific for Type-1 aerobic methanotrophs. PCR products were not obtained from any depths using primers specific for Type-2 aerobic methanotrophs. Primers specific for Archea only amplified DNA from 118 m and 120 m depth. DNA from 118 m depth was also amplified using primers specific for groups of Archea (ANME-1,2, and 3) known to conduct AOM. PCR with primers specific for only ANME-2 failed to yield a PCR product.

DNA amplified using the primers specific for Type-1 aerobic methanotophs was cloned and 5 of these clones sequenced. BLAST queries identified all 5 sequences as >99% similar to *Thiobacillus sp.* which are not aerobic methanotrophs but are known to yield false positive amplifications with the primer-set used (Wise et al. 1999). DNA amplified using the Archeal specific and ANME-1,2,3 specific primer sets was also cloned. A total of 10 clones from the DNA amplified with the Archeal specific primers and 5 clones from the ANME-1,2, and 3 specific primers were sequenced. Phylogenetic analyses were conducted with these sequences as described in the methods section. A maximum likelihood tree is shown in Figure 6.7 which displays the phylogenetic relationships between these clone sequences, other sequences closely related to the Lake Matano clones, sequences from CH_4-rich environments, and organisms isolated in pure culture with known metabolisms. It should be noted that Archea known to conduct AOM have yet to be isolated in pure culture. Clone sequences obtained with primers purportedly specific to ANME-1,2, and 3 (MWC118AM Clones 1,2 and 4) are within the kingdom Euryarchaeota but are not phylogenetically affiliated with other ANME sequences. This is consistent with the results of other studies which have also found that the ANME-F primer can lack specificity for ANME (Schubert et al. 2006). Clone sequences MWC118AM 1, 2 and 4 cluster very tightly with each other and three additional clones obtained with primers specific for Archea (MWC118AR 3,8 and 10). Isolated organisms most closely related to these clone sequences are known methanogens of the family Methanomicrobiaceae which use either lithoautrophic CO_2 reduction or formate disporportionation to generate methane. One other clone, MWC118AR clone 7, also clusters within the Euryarcheaota and is closely related to known methanogens of the

family Methanosaetaceae. The other Archeal clone sequences are widely distributed and fall within the kingdom Crenarchaeota. Many of the isolated organisms closely related to these clones are deeply rooted and thermophyllic.

6.5 Discussion

According to the vertical distribution of CH_4 in the water column of Lake Matano, CH_4 is produced in the sediments and bottom waters and is consumed within the 100 to 200 m depth interval. The sharp methane concentration gradient between 200 and 100 m depth implies the presence of a methane sink, likely methane oxidation in the vicinity of the permanent pycnocline.

Unlike other lakes in which CH_4 accumulates to high concentrations (Schmid et al. 2005), bottom waters in Lake Matano do not have very high dissolved CO_2 concentrations. Based on the measured concentrations, the sum of the partial pressures of the dissolved CO_2 and CH_4 does not exceed 6 % of the *in situ* hydrostatic pressure. Bubble ebullition at depth is therefore unlikely, and the risk of gas-driven limnic eruptions in Lake Matano is low. A catastrophic event (e.g., an earthquake) that would cause isochemical transport of the deep waters to the surface, or a strong cooling of the epilimnetic waters that eliminates the temperature stratification, however, could trigger bubble ebullition.

Methane production pathway. The C isotopic composition of CH_4 ($\delta^{13}C_{CH4}$) (< -70 ‰) clearly indicates a biological origin (Whiticar 1999). A biological origin is also supported by the young age of methane carbon which suggests that the methane is produced by methanogenesis driven by modern organic matter. Metabolic methane accumulates to relatively high concentrations in Lake Matano despite the abundance of Fe and Mn (hydr)oxides which, according to thermodynamic arguments, should inhibit methanogenesis. However, substrate availability is not considered by thermodynamic calculations under standard conditions (Roden 2003). Roden (2003) suggested that the ability of microbial Fe(III) oxide reduction to suppress other terminal electron acceptor pathways in anoxic soils and sediments is controlled by the reactive (i.e., microbially accessible) surface site density rather than the thermodynamic properties of the bulk

(hydr)oxide minerals. The accumulation of sorbed and/or surface-precipitated Fe(II) on Fe(III) (hydr)oxide surfaces renders these surfaces progressively unreactive toward enzymatic reduction and thereby exerts an important control on the long-term reactivity of Fe(III) (hydr)oxides (Roden and Urrutia 2002). Given the high dissolved Fe(II) concentrations (Figure 6.3) in the anoxic bottom waters and sediment porewaters (Fowle et al. 2006) of Lake Matano, surface deactivation of Fe(III) (hydr)oxides that sink through the bottom waters and accumulate in the lake sediments is plausible. Furthermore, the absence of bioturbation in the anoxic bottom sediments would limit recycling of Fe (hydr)oxides and the regeneration of reactive surfaces. Reduced Fe (hydr)oxide cycling, due to lack of bioturbation, is known to enhance rates of methanogenesis relative to rates of Fe reduction (Roden and Wetzel 1996).

In addition to influencing the overall rate of methanogenesis, the abundance of Fe(III) (hydr)oxides may also dictate the predominant methanogenic pathway. In marine systems, methanogenesis occurs largely by CO_2 reduction because SRB outcompete methanogens for acetate (Capone and Kiene 1988; Reeburgh 2007). Oxidation of acetate by sulfate reducers is 1.5 times more energetic than methanogenic acetate disproportionation under standard conditions (Capone and Kiene 1988). In contrast, sulfate reduction by H_2 is only 1.1 times more energetic than CO_2 reduction (Capone and Kiene 1988). Hence, in sulfate-rich environments such as marine sediments, the substrate most accessible to methanogens is H_2, and CO_2 reduction dominates (Capone and Kiene 1988; Reeburgh 2007; Whiticar 1999). In contrast, in freshwaters, the relative dearth of sulfate often allows methanogenic acetate disproportionation to become competitive (Capone and Kiene 1988; Whiticar 1999; Winfrey and Zeikus 1977). Under these conditions, the dominant methanogenic pathway should be determined by the next-most-energetic competitor. In the case of Fe-rich Lake Matano (Crowe et al. 2008), this competitor is likely to be dissimilatory iron-reducing bacteria.

To evaluate the competition for substrates between methanogens and iron reducers, we consider the following reactions:

Methanogenesis:

$$HCO_3^- + 4H_2 + H^+ \rightarrow CH_4 + 3H_2O \ (-159.13 \text{ KJ mol}^{-1}) \quad \textbf{(1)}$$

$CH_3COO^- + H_2O \rightarrow CH_4 + HCO_3^-$ (-753.31 KJ mol $^{-1}$) **(2)**

Fe reduction:

$2Fe(OH)_3 + H_2 + 4H^+ \rightarrow 2Fe^{2+} + 6H_2O$ (-182.82 KJ mol $^{-1}$) **(3)**

$CH_3COO^- + 8Fe(OH)_3 + 14H^+ \rightarrow 2HCO_3^- + 8Fe^{2+} + 20H_2O$ (-1325.46 KJ mol $^{-1}$) **(4)**

Dividing the free energy yield of reaction 3 by the free energy yield of reaction 1 and normalizing to the number of oxidized hydrogen molecules reveals that Fe reduction using H_2 as an electron donor yields 4.6 times more free energy than CO_2 reduction. Fe reduction by acetate oxidation is 3.5 times more energetic than methanogenic acetate disproportionation (calculated by dividing the free energy yield of reaction 4 by that of reaction 2 and normalizing to the number of C atoms oxidized). Accordingly, unlike in sulfate-rich environments, methanogenesis in Fe-rich environments could be expected to proceed predominantly by acetate disproportionation.

An isotope separation factor (ε_C) (Whiticar 1999) of ~65‰ is derived from the difference between the carbon isotopic compositions of methane and $\sum CO_2$ in the deep anoxic bottom waters. In Lake Matano, this value is at the upper end of values observed in systems dominated by acetate disproportionation and is at the lower end of values reported for systems dominated by CO_2 reduction (Whiticar 1999). The computed ε_C values for the Lake Matano bottom waters suggest that methanogenesis in this lake may occur by both pathways.

Archea of both the family Methanomicrobiaceae and the family Methanosaetaceae were detected in the water column at 118 m depth. Methanobacteriacae are known to produce methane through CO_2 reduction, formate disproportionation and many can also disproportionate more complex organic compounds (Canfield et al. 2005). In contrast, all known Methanosaetaceae are obligate acetate disproportionators (Canfield et al. 2005). Thus, organisms capable of both of the principle methanogenic pathways have been detected in the water column and a more detailed microbiological study is needed to elucidate factors governing both the methane production pathways and methanogen ecology.

Methane oxidation pathway. A sharp gradient in the dissolved methane concentration (Figure 6.5) between 100 and 200 m depth implies that methane oxidation occurs at or immediately below the persistent pycnocline. As $^{12}CH_4$ is oxidized more rapidly than $^{13}CH_4$ by methanotrophic bacteria, oxidation of CH_4 results in the production of a ^{13}C-depleted ΣCO_2 pool. Two distinct minima in the $\delta^{13}C_{\Sigma CO2}$ (points I and II in Figure 6.6) at depths of 104 and 120 m delineate the depth range of methane oxidation. Accordingly, enrichment in heavier methane (positive shifts in $\delta^{13}C_{CH4}$) is observed between 110 and 115 m (Figure 6.6a). A simple calculation reveals that the concentrations of methane and $\sum CO_2$ in the deep water are such that a complete oxidation of methane to CO_2 could produce a $\delta^{13}C_{\sum CO2}$ as low as -23 ‰. The higher observed value likely reflects a dilution by heavier epilimnetic $\sum CO_2$. A positive excursion in $\delta^{13}C_{\Sigma CO2}$ between points I and II (Figure 6.6) is likely generated from photosynthesis by a community of green sulphur bacteria at this depth (Chapter 4).

Although methanotrophic bacteria are known to oxidize methane under microaerophilic conditions with O_2 as the electron acceptor, most methane in marine sediments and anoxic basins is oxidized anaerobically (Losekann et al. 2007). Oxygen in Lake Matano becomes undetectable ($\leq$ 2.5 μmol l^{-1}) below 110 m (Figure 6.3), and the peak in $\delta^{13}C_{\Sigma CO2}$ at point II (122 m) indicates that CH_4 oxidation occurs in the presence of little or no oxygen. Although aerobic methane oxidation at such sub-detection oxygen levels may be possible, it could be inhibited by high concentrations of Fe(II). Our calculations (section 6.7) reveal that the kinetics of abiotic Fe oxidation are sufficiently rapid that Fe(II) competes with methanotrophic bacteria for molecular oxygen, potentially favoring anaerobic methane oxidation. Based on the known kinetics of aerobic methanotrophy (Van Bodegom et al. 2004) and abiotic Fe(II) oxidation (Millero et al. 1987), the rate of aerobic methane oxidation could reach a maximum 3.1 x 10^{-11} moles l^{-1} min^{-1} at ~120 m depth. This rate is an order of magnitude lower than the methane oxidation rate (3.5 x 10^{-10} moles l^{-1} min^{-1}) necessary to sustain the $\delta^{13}C_{\Sigma CO2}$ peak at point II (122 m) against the diffusion of heavier ΣCO_2 (see section 6.8). It is also lower than the net methane oxidation rate of 7.3 x 10^{-11} moles l^{-1} min^{-1} estimated from the upward methane flux (see below) assuming that methane oxidation occurs within a 15 m depth interval. Thus, although the uncertainties of the flux calculations are rather large (a factor

of 5), they suggest that CH_4 oxidation around 122 m depth occurs anaerobically. Furthermore, the maximum rate of aerobic methane oxidation calculated in section 6.7 assumes that aerobic methanotrophic bacteria occur at moderately high cell densities of 10^5 cells ml^{-1}. Failure of PCR to amplify DNA of known aerobic methanotrophs from cellular material collected at 118 m (table 6.3) strongly indicates that the densities of aerobic methanotrophs are much lower than 10^5 cells ml^{-1} and renders potential rates of aerobic methane oxidation at point II insignificant. Taken together, the available evidence leads us to conclude that methane oxidation at point II occurs anaerobically.

To date, anaerobic oxidation of methane (AOM) is only known to occur when coupled to the reduction of either sulfate (Boetius et al. 2000) or nitrate (Raghoebarsing et al. 2006). However, both sulfate and nitrate occur at exceedingly low concentrations (Figures. 6.3 and 6.4) within the depth interval of methane oxidation in Lake Matano. Methane oxidation coupled to the reduction of iron or manganese (hydr)oxides has been hypothesized (Konhauser et al. 2005), and is energetically favorable under standard conditions:

$$CH_4 + 8Fe(OH)_3 + 15H^+ \rightarrow HCO_3^- + 8Fe^{2+} + 21H_2O \ (-572.15 \text{ KJ mol}^{-1}) \quad \textbf{(5)}$$

$$CH_4 + 4MnO_2 + 7H^+ \rightarrow HCO_3^- + 4Mn^{2+} + 5H_2O \ (-789.91 \text{ KJ mol}^{-1}) \quad \textbf{(6).}$$

Based on the sharp Mn(II) and Fe(II) gradients, both $Fe(OH)_3$ and MnO_2 should be abundant within the vicinity of the pycnocline. Hence, unless a sparse population of aerobic methanotrophs are highly active at the exceedingly low O_2 concentrations present at 120 m depth, AOM must occur and is likely coupled to reduction of the most abundant electron acceptors, the (hydr)oxides of Fe and Mn. The lack of phylogentic affiliation between our clone sequences and the ANME known to conduct AOM with SO_4^- does not rule out AOM. Indeed, the Archea involved in NO_3^- dependent AOM are not closely related to the ANME. Incubation experiments would be required to conclusively demonstrate this novel methane oxidation pathway and to identify the organisms responsible.

The carbon cycle. The rate of methane oxidation can be estimated from the fluxes of methane between 200 and 100 m depth. Using an average vertical diffusivity coefficient of 0.16 m^2 d^{-1}, estimated using the Brunt-Väisälä stability frequency as described previously (Crowe et al. 2008), and a methane concentration gradient between 200 and 100 m depth of 9.7 x 10^{-3} mol m^{-4} yields a methane oxidation rate of 1.6 x 10^{-3} mol m^{-2} d^{-1}. At steady state, the rate of methane oxidation should be equivalent to the rate of methane production, i.e. methanogenesis. Such rates of methane oxidation and methane production are relatively high and comparable to those observed in the Florida Everglades (King et al. 1990) and freshwater tidal swamps (Megonigal and Schlesinger 1997). At this rate, methane concentrations in the deep waters would reach the present levels within about 1000 years following a mixing event (i.e., overturn). Likewise, these estimates suggest that the lake has not been mixed in the last millennium. Such high rates also suggest that methanogenesis could contribute significantly to organic matter degradation.

The total carbon degradation rate in the bottom waters of Lake Matano was estimated from the ammonium concentration gradient (Figure 6.4), an organic matter C:N ratio of 10, and assuming steady-state. The C:N ratio of the settling organic matter was computed from the ratio of the difference between the $\sum CO_2$ in the surface and bottom water and the NH_4^+ concentrations in the bottom water. The estimated C:N ratio is in good agreement with the measured C:N ratio (12) of POM recovered at 32 m depth. According to the calculation, the total organic matter degradation rate is on the order of 3 x 10^{-3} mol m^{-2} d^{-1} and methanogenesis accounts for roughly 50 % of it. If we assume that acetate disproportionation is the predominant methanogenic pathway, the supply of organic carbon to methanogens must be equivalent to, or greater than, the rate of methanogenesis.

Integrated primary production rates for the surface waters are 3.8 x 10^{-3} mol m^{-2} d^{-1} (Chapter 4), indicating that autochthonous primary production can supply sufficient carbon for the observed rates of methanogenesis. The agreement between the computed and measured C:N ratios and the fact that allochthonous leaf litter has a C:N ratio of 49 further suggests that respiration and methanogenesis in Lake Matano are largely fueled by autochthonous POC. The difference between the total organic carbon degradation and

primary production rates suggest that roughly 78% of the organic matter generated by primary production is degraded whereas the rest is buried in the sediment at a rate of 8.4 x 10^{-4} mol m^{-2} d^{-1}. Lake Matano sediments contain between 5 and 8 wt % organic carbon which, given a deep water sedimentation rate of 0.08 cm yr^{-1} (Crowe et al. 2004), translates to organic carbon burial rates of between 8.5 and 13 x10^{-4} mol m^{-2} d^{-1}, consistent with the rate predicted based on the difference between primary production and respiration rates.

A minimum estimate for the fraction of organic matter degraded through microbial Fe reduction can be made by considering the flux of Fe(II) through the pycnocline. Again, we assume that steady state conditions apply and use the rate of Fe(II) diffusion out of the bottom waters to evaluate Fe-cycling. This diffusive flux is driven by the concentration gradient sustained by Fe(II) oxidation reactions at or near the pycnocline and at steady-state can be used to estimate the rate of Fe(II) production through bacterial Fe(III) reduction in the bottom waters and sediments. However, only a fraction of the total Fe(II) that is produced in the bottom waters and sediments is consumed through oxidation within the pycnocline. The deep waters of Lake Matano are oversaturated with respect to siderite (Table 6.2) and Fe(II) is likely also removed by precipitation and/or adsorbed to sedimentary particles. Thus, Fe(II) production rates calculated from the oxidative Fe(II) flux underestimate the total Fe(II) production rates as they do not include Fe(II) sequestered due to precipitation. Accordingly, a minimum estimate for the carbon degradation rate by Fe reduction, computed from the flux of Fe(II) at the pycnocline, is 2.2 x 10^{-4} mol m^{-2} d^{-1}, less than 10 % of the estimated total C degradation rate (3 x 10^{-3} mol m^{-2} d^{-1}) and only 14 % of the C degraded by methanogenesis (1.6 x 10^{-3} mol m^{-2} d^{-1}).

Methane in an Fe-rich environment. Despite the abundance of Fe in Lake Matano, methanogens effectively compete for substrates and are responsible for significant recycling of C fixed during primary production. Anaerobic oxidation of methane may also occur in Fe-rich environments in the absence of the known AOM electron acceptors, SO_4^- and NO_3^-. In Lake Matano, given the dearth of known AOM electron acceptors, SO_4^- and NO_3^-, Fe and Mn (hydr)oxides appear to be the only available alternate electron

acceptors .Confirmation of this methane oxidation pathway could dramatically alter our view of the global methane cycle as Fe and Mn (hydr)oxides are ubiquitous constituents of soils and sediments and may be mitigating CH_4 release to the atmosphere.

By analogy to the ferruginous Archean oceans, Lake Matano provides a window into the Earth's earliest marine habitats. The active role played by methane in the C cycle of Lake Matano suggests that methogenesis and methanotrophy could have been major metabolic pathways in Archean ocean ecosystems. Methane oxidation coupled to Fe reduction in the Archean Ocean may have modulated methane fluxes to the atmosphere, impacting global climate and O_2 accumulation (Catling et al. 2007a; Catling et al. 2007b).

Acknowledgements. We acknowledge the help of numerous individuals including: Peter Hehanussa, William Napier, Mike Dutton, Matt Orr, Deky Tetradiono, Lili Lubis, CarriAyne Jones, Gadis Sri Hariyani, Sinyo Rio, Dullah and Sarah Bungin. Andrew O'Neill helped with the phylogenetic analyses. Funding was kindly provided by NSERC, INCO Canada Ltd., PT INCO, KU Geology Associates and DNRF. SAC was supported by an NSERC IPGS sponsored by INCO Canada Ltd. We also thank the Québec-Ocean Research Center and their staff for lending us and calibrating the SeaBird SBE-19 CTD, the GEOTOP-McGill-UQAM Research Center, specifically Dr. Jean-François Hélie, for the ΣCO_2 stable isotopic measurements.

Table 6.1. Primers used for PCR amplification of DNA

Primer	Sequence (5'-3')	Target	Ref.
EelMS932r	AGCTCCACCCGTTGTAGT	ANME-2	1
MethT2r	CATCTCTGACCACCATACCGG	Type-2 methanotrophs	2
MethT1df	CCTTCGGGAGCCGACGAGT	Type-1 methanotrophs	2
MethT1br	GATTCCATGCATGTCAAGG	Type-1 methanotrophs	2
ANMEf	GGCTCAGTAACACGTGGA	ANME-1,2,3	3
915r	GTGCTCCCCCGCCAATTCCT	Archaea	1
27f	AGAGTTTGATCCTGGCTCAG	Bacteria	4
1492r	GGTTACCTTGTTACGACTT	universal	4
21fa	TTCCGGTTGATCCYGCCGGA	Archaea	4

[1](Lloyd et al. 2006); [2](Wise et al. 1999); [3](Schubert et al. 2006); [4](Bond et al. 2000)

Table 6.2. Saturation indices (SI = log IAP/$K°_{sp}$) for water at various depths with respect to common carbonate minerals.

Depth (m)	Dolomite $CaMg(CO_3)_2$	Calcite $CaCO_3$	Siderite $FeCO_3$	Rhodochrosite $MnCO_3$	Witherite $BaCO_3$
0	2.2	0.3			1.8
20	2.3	0.4			1.8
44	1.4	-0.1			1.5
60	1.1	-0.2			1.3
90	0.8	-0.4			1.1
104	-0.2	-0.9		-1.7	0.8
110	-0.2	-0.9	-2.1	-0.5	0.9
122	-0.5	-1.0	-0.3	-0.5	0.8
140	-0.7	-1.1	-0.1	-0.7	0.9
160	-0.5	-1.0	0.1	-0.7	1.0
180	-0.4	-0.9	0.1	-0.7	1.1
200	-0.3	-0.9	0.2	-0.7	1.2
250	-0.1	-0.8	0.3	-0.6	1.3
350	-0.3	-0.8	0.3	-0.7	1.2
450	-0.2	-0.8	0.3	-0.7	1.3
550	0	-0.7	0.4	-0.6	1.3

Table 6.3. Results from PCR amplications with group specific primers.

Primer Set	Target organisms	Sample Depth	Amplicon
MethT1df-MethT1br	Type-1 methanotrophs	140	-
		120	-
		118	+
		115	-
		102	+
MethT2r-27f	Type-2 methanotrophs	140	-
		120	-
		118	-
		115	-
		105	-
21fa-915r	Archea	140	-
		120	+
		118	+
		115	-
		105	-
ANMEf-915r	ANME-1,2,3	118	+
21fa-EelMS932r	ANME-2	118	-

Figure 6.1. Representative density profiles from September 2004, June 2005, July 2006 and February 2007 illustrating fluctuations in the seasonal pycnocline within the upper 250m of the water column. The inset presents the entire water column and shows the consistency of the persistent pycnocline between seasons and over several years.

Figure 6.2. Depth distribution of major cations

Figure 6.3. Depth distribution of major redox active species.

Figure 6.4. a) Depth distribution of NO_3^- (February 2007) and NH_4^+ (July 2006 and February 2007); b) Depth distribution of particulate Fe and Mn oxides (February 2007).

Figure 6.5. a) Depth distribution of CH_4 in July 2006 and February 2007; b) Depth distributions of pCO_2 and pH in February 2007.

Figure 6.6. a) C isotopic composition of CH_4 in July 2006 and February 2007; b) C isotopic composition of $\sum CO_2$ in February 2007.

Figure 6.7. Phylogenetic tree displaying the affiliations of 16S rRNA sequences obtained from 118 m depth in Lake Matano using both Archeal specific PCR primers (MWC118AR) and ANME specific PCR primers (MWC118AM). The tree includes reference species from the domain Archea in addition to clones obtained from methane rich environments and the nearest non-chimeric neighbors identified using the greengenes Simrank tool. The tree was constructed using the PHYML Maximum-Likelihood algorithm. Bootstrap analyses of 100 re-samplings were conducted to provide confidence estimates for the tree topologies. These values are given at the nodes as a percentage out of 100.

Figure 6.8. a) Rates of O_2 consumption by methanotrophy (black lines; solid = 10^4 cells ml^{-1}, coarse dashed = 10^5 cells ml^{-1}, fine dashed = 10^6 cells ml^{-1}) and Fe(II) oxidation (gray lines; solid = 3.5 μmol Fe(II) l^{-1}, coarse dashed = 35 μmol Fe(II) l^{-1}, fine dashed = 100 μmol Fe(II) l^{-1}). b) Percentage of oxygen consumed by aerobic methanotrophy versus aerobic methanotrophy plus Fe(II) oxidation (cell density = 10^5 cells ml^{-1}, solid = 3.5 μmol Fe(II) l^{-1}, coarse dashed = 35 μmol Fe(II) l^{-1}, fine dashed = 100 μmol Fe(II) l^{-1}) as a function of dissolved oxygen concentration.

6.6 References

Boetius, A., K. Ravinschlag, C.J. Schubert, D. Rickert, F. Widdel, A. Gleseke, R., Amann, B.B. Jørgensen, U. Witte, and O. Pfannkuche. 2000. A marine microbial consortium apparently mediating anaerobic oxidation of methane. Nature **407:** 623-626.

Bond, P. L., S. P. Smriga, and J. F. Banfield. 2000. Phylogeny of microorganisms populating a thick, subaerial, predominantly lithotrophic biofilm at an extreme acid mine drainage site. Appl. Environ. Microbiol. **66:** 3842-3849.

Canfield, D. E., E. Kristensen, and B. Thamdrup. 2005. Aquatic Geomicrobiology. Elsevier, San Diego.

Capone, D. G., and R. P. Kiene. 1988. Comparison of microbial dynamics in marine and fresh-water sediments - Contrasts in anaerobic carbon catabolism. Limnol. Oceanogr. **33:** 725-749.

Catling, D. C., M. W. Claire, and K. J. Zahnle. 2007a. Anaerobic methanotrophy and the rise of atmospheric oxygen. Philosophical Transactions of the Royal Society a-Mathematical Physical and Engineering Sciences **365:** 1867-1888.

Catling, D.C., M.W. Claire, and K.J. Zahnle. 2007b. Archean methane, oxygen and sulfur. Geochim. Cosmochim. Acta **71:** A151-A151.

Crowe, S. A., A.H. O'Neill, S. Katsev, P. Hehanussa, G.D. Haffner, B. Sundby, A. Mucci, and D.A. Fowle 2008. The biogeochemistry of tropical lakes: A case study from Lake Matano, Indonesia. Limnol. Oceanogr. **53:** 319-331.

Crowe, S.A. S.J. Pannalal, D.A. Fowle, M.T. Cioppa, D.T.A. Symons, G.D. Haffner, B.J. Fryer, R. McNeely, B. Sundby, P.E. Hehanussa. 2004. Biogeochemical cycling in Fe-rich sediments from Lake Matano, Indonesia, p. 1185-1189. 13th International Symposium on Water-Rock Interaction, Saratoga Springs, USA.

Desantis, T. Z., P. Hugenholtz, N. Larsen, M. Rojas, E.L. Brodie, K. Keller, T. Huber, D. Dalevi, P. Hu, and G.L. Anderson. 2006. Greengenes, a chimera-checked 16S rRNA gene database and workbench compatible with ARB. Appl. Environ. Microbiol. **72:** 5069-5072.

Eller, G., L. K. Kanel, and M. Kruger. 2005. Co-occurrence of aerobic and anaerobic methane oxidation in the water column of Lake Plusssee. Appl. Environ. Microbiol. **71:** 8925-8928.

Faure, G. 1997. Principles and Applications of Geochemistry. Prentice Hall, Upper Saddle River, New Jersey, USA.

Fowle, D. A., S. A. Crowe, A. H. O'Neill, G. D. Haffner, B. Sundby, and A. Mucci. 2006. Microbial Ecology and the link between sediment respiration and sediment-water exchange in Lake Matano., p. 7. Symposium on the Malili Lakes Limnology and Ecology.

Gieskes, J. M., and W. C. Rogers. 1973. Alkalinity determination in interstitial waters of Marine Sediments. Journal of Sedimentary Petrology **43:** 272-277.

Golightly, J. P. 1981. Nickeliferous laterite deposits. Economic Geology **75th Anniversary Volume:** 710-735.

Guindon, S., and O. Gascuel. 2003. A simple, fast, and accurate algorithm to estimate large phylogenies by maximum likelihood. Syst. Biol. **52:** 696-704.

Habicht, K. S., M. Gade, B. Thamdrup, P. Berg, and D. E. Canfield. 2002. Calibration of sulfate levels in the Archean Ocean. Science **298:** 2372-2374.

Haffner, G. D., P. E. Hehanussa, and D. Hartoto. 2001. The biology and physical processes of large lakes of Indonesia, p. 183-194. *In* M. Munawar and R. E. Hecky [eds.], The Great Lakes of the World: Food web, health and integrity. Backhuys Publishers.

Hall, P. O., and R. C. Aller. 1992. Rapid, small-volume, flow-injection analysis for ΣCO_2 and NH_4^+ in marine and fresh-waters. Limnol. Oceanogr. **37:** 1113-1119.

Kessler, J. D., and W. S. Reeburgh. 2005. Preparation of natural methane samples for stable isotope and radiocarbon analysis. Limnol. Oceanogr. Methods **3:** 408-418.

King, G. M., P. Roslev, and H. Skovgaard. 1990. Distribution and rate of methane oxidation in sediments of the Florida Everglades. Appl. Environ. Microbiol. **56:** 2902-2911.

Konhauser, K. O., D. K. Newman, and A. Kappler. 2005. The potential significance of microbial Fe(III) reduction during deposition of Precambrian banded iron formations. Geobiology **3:** 167-177.

Lane, D. J. 1991. 16S/23S rRNA sequencing, p. 115-175. *In* E. G. Stackebrandt, M. [ed.], Nucleic Acid Techniques in Bacterial Systematics. Wiley, New York, New York, USA.

Lehours, A. C., C. Bardot, A. Thenot, D. Debroas, and G. Fonty. 2005. Anaerobic microbial communities in Lake Pavin, a unique meromictic lake in France. Appl. Environ. Microbiol. **71:** 7389-7400.

Lewis, E., and D.W.R. Wallace (1998). Program developed for CO_2 system calculations. ORNL/CDIAC-105. Carbon dioxide information analysis center, oak ridge national laboratory, US Department of Energy, Oak Ridge, TN, http://cdiac.esd.ornl.gov/oceans/CO2RPRT.html.

Lloyd, K. G., L. Lapham, and A. Teske. 2006. Anaerobic methane-oxidizing community of ANME-1b archaea in hypersaline Gulf of Mexico sediments. Appl. Environ. Microbiol. **72:** 7218-7230.

Losekann, T., K. Knittel, T. Nadalig, B. Fuchs, H. Niemann, A. Boetius and R. Ammann 2007. Diversity and abundance of aerobic and anaerobic methane oxidizers at the Haakon Mosby mud volcano, Barents Sea. Appl. Environ. Microbiol. **73:** 3348-3362.

Lovley, D. R., and E. J. P. Phillips. 1987. Competitive mechanisms for inhibition of sulfate reduction and methane production in the zone of ferric iron reduction in sediments. Appl. Environ. Microbiol. **53:** 2636-2641.

Luther, G. W., B. Glazer, S.F. Ma, R. Trouwborst, B.R. Schultz, G. Druschel and C. Kraiya 2003. Iron and sulfur chemistry in a stratified lake: Evidence for iron-rich sulfide complexes. Aquat. Geochem. **9:** 87-110.

Martens, C. S., D. B. Albert, and M. J. Alperin. 1999. Stable isotope tracing of anaerobic methane oxidation in the gassy sediments of Eckernforde Bay, German Baltic Sea. American Journal of Science **299:** 589-610.

Megonigal, J. P., and W. H. Schlesinger. 1997. Enhanced CH_4 emissions from a wetland soil exposed to elevated CO_2. Biogeochem. **37:** 77-88.

Millero, F. J., S. Sotolongo, and M. Izaguirre. 1987. The oxidation-kinetics of Fe(II) in seawater. Geochim. Cosmochim. Acta **51:** 793-801.

Orphan, V. J., C. H. House, K. U. Hinrichs, K. D. Mckeegan, and E. F. Delong. 2001. Methane-consuming archaea revealed by directly coupled isotopic and phylogenetic analysis. Science **293:** 484-487.

Raghoebarsing, A. A., A. Pol, K.T. van de Pas-Schoonen, A.J.P. Smolders, K.F. Ettwig, W.I.C. Rijpstra, S. Schouten, J.S.S. Damste, H.J.M. Op den Camp, M.S.M Jetten and M. Strous. 2006. A microbial consortium couples anaerobic methane oxidation to denitrification. Nature **440:** 918-921.

Reeburgh, W. S. 2007. Oceanic methane biogeochemistry. Chem. Rev. **107:** 486-513.

Roberts, J.A., P.C. Bennett, L.A. González, G.L. Macpherson, and K.L. Milliken. (2004). Microbial precipitation of dolomite in methanogenic groundwater. *Geology* **32**: 277-280

Roden, E. E. 2003. Fe(III) oxide reactivity toward biological versus chemical reduction. Environ. Sci. Technol. **37:** 1319-1324.

Roden, E. E., and M. M. Urrutia. 2002. Influence of biogenic Fe(II) on bacterial crystalline Fe(III) oxide reduction. Geomicrobiol. J. **19:** 209-251.

Roden, E. E., and R. G. Wetzel. 1996. Organic carbon oxidation and suppression of methane production by microbial Fe(III) oxide reduction in vegetated and unvegetated freshwater wetland sediments. Limnol. Oceanogr. **41:** 1733-1748.

Schmid, M., M. Halbwachs, B. Wehrli, and A. Wuest. 2005. Weak mixing in Lake Kivu: New insights indicate increasing risk of uncontrolled gas eruption. Geochemistry Geophysics Geosystems **6:** 1-11.

Schubert, C. J., M.J.L. Coolen, L.N. Naritan, A. Schippers, B. Abbas, E. Durisch-Kaiser, B. Wherli, E.C. Hopmans, J.S.S. Damste, S. Wakeham and M.M.M. Kupers. 2006. Aerobic and anaerobic methanotrophs in the Black Sea water column. Environ. Microbiol. **8:** 1844-1856.

Stuiver, M., and H. A. Polach. 1977. Reporting of C-14 data - Discussion. Radiocarbon **19:** 355-363.

Van Bodegom, P., F. Stams, L. Mollema, S. Boeke, and P. Leffelaar. 2001. Methane oxidation and the competition for oxygen in the rice rhizosphere. Appl. Environ. Microbiol. **67:** 3586-3597.

Van Bodegom, P. M., J. C. M. Scholten, and A. J. M. Stams. 2004. Direct inhibition of methanogenesis by ferric iron. FEMS Microbiol. Ecol. **49:** 261-268.

Van Der Lee, J. 1993. CHESS, another speciation and surface complexation computer code. CIG-Ecole des Mines de Paris.

Whiticar, M. J. 1999. Carbon and hydrogen isotope systematics of bacterial formation and oxidation of methane. Chem. Geol. **161:** 291-314.

Winfrey, M. R., and J. G. Zeikus. 1977. Effect of sulfate on carbon and electron flow during microbial methanogenesis in freshwater sediments. Appl. Environ. Microbiol. **33:** 275-281.

Wise, M. G., J. V. Mcarthur, and L. J. Shimkets. 1999. Methanotroph diversity in landfill soil: Isolation of novel type I and type II methanotrophs whose presence was suggested by culture-independent 16S ribosomal DNA analysis. Appl. Environ. Microbiol. **65:** 4887-4897.

Zhang, Y. X., and G. W. Kling. 2006. Dynamics of lake eruptions and possible ocean eruptions. Annu. Rev. Earth Planet. Sci. **34:** 293-324.

6.7 Supplementary Information (Competition between methanotrophs and Fe(II) for O_2)

The rate of oxygen consumption by Fe(II) can be approximated by a second order kinetic law (Millero et al. 1987):

$$\frac{\partial[O_2]}{\partial t} = k[Fe(II)][O_2] \qquad \mathbf{7}$$

where k is the rate constant (mol^{-1} l min^{-1}). The rate of oxygen consumption by methanotrophs follows Monod kinetics (Van Bodegom et al. 2001):

$$\frac{\partial[O_2]}{\partial t} = \frac{\mu_{max}[O_2]B}{(K_{S,O_2} + [O_2])Y} \qquad \mathbf{8}$$

where μ_{max} is the maximum specific growth rate (min^{-1}), $K_{S,O2}$ is the Monod substrate half saturation constant for O_2 (mol l^{-1}), B is the microbial cell density (moles microbial C l^{-1}) and Y is the dimensionless apparent yield (the molar ratio of substrate used to biomass produced).

For typical parameter values (Table 6.4), competition for oxygen between aerobic methanotrophy and Fe(II) is illustrated graphically in figure 6.8a. Irrespective of cell density, methanotrophic oxygen consumption plateaus when the oxygen concentration exceeds 1 μmol l^{-1}, whereas abiotic O_2 consumption by Fe(II) is log-linear at all O_2 concentrations. The percentage of O_2 consumption by methanotrophs vs. total O_2 consumption by methanotrophy and Fe(II) oxidation as a function of ambient O_2 concentration is shown in figure 6.8b for a range of Fe(II) concentrations and a cell density of 10^5 cells ml^{-1}. At low O_2 concentrations, a higher percentage of oxygen is consumed by methanotrophs than by abiotic Fe(II) oxidation. At methanotroph cell densities of 10^5 cells ml^{-1}, typical of microaerophilic zones in methane-rich chemoclines

(Eller et al. 2005; Lehours et al. 2005), and Fe concentrations of 35 μmol l^{-1}, methanotrophy consumes approximately 50 % of the available O_2, at O_2 concentrations less than 1 μmol l^{-1}.

Using the Monod expression for aerobic methanotrophy (equation 2) , cell densities up to 10^5 cells ml^{-1}, and oxygen concentrations up to 5 nmol l^{-1} (the O_2 concentration at 120 m depth was estimated at 4.7 nmol l^{-1} by fitting a logarithmic function ($R^2 = 0.92$) to the O_2 concentration profile between 105 and 110 m and extrapolating to 120 m depth), we estimate that the rate of aerobic methane oxidation is at most 3.1 x 10^{-11} moles l^{-1} min^{-1}. Note that using the measured Fe(II) concentrations and the solubility limit of Fe(III) at pH 7.21 gives an estimated pe of 5.58 which, at equilibrium, translates to O_2 concentrations of 1.4 x 10^{-26} nmol l^{-1}. Thus, unless O_2 is rapidly supplied to 120 m depth, it may be at concentrations much lower than the rough estimates gleaned from the O_2 concentration profile.

6.8 Supplementary Information (Modeling isotope fluxes)

Here, we calculate the methane oxidation rate necessary to sustain the negative excursion in $\delta^{13}C_{\sum CO2}$ in $\sum CO_2$ observed at 122m against the diffusion of isotopically heavier $\sum CO_2$. This rate can be estimated by solving reaction-diffusion equations for both carbon isotopes. Assuming a steady state:

$$\frac{d}{dz}(K_z \frac{d[^{13}C_{\sum CO2}]}{dz}) + R_{13} + \frac{[^{13}C_{\sum CO2}]}{[^{13}C_{\sum CO2}]+[^{12}C_{\sum CO2}]} \sum R = 0$$
$$\frac{d}{dz}(K_z \frac{d[^{12}C_{\sum CO2}]}{dz}) + R_{12} + \frac{[^{12}C_{\sum CO2}]}{[^{13}C_{\sum CO2}]+[^{12}C_{\sum CO2}]} \sum R = 0 \quad \textbf{9}$$

where R_{13} and R_{12} are the required rates of oxidation of the ^{13}C and ^{12}C methane, respectively. The terms 'R' with various subscripts are the rates of all reactions that produce or consume $\sum CO_2$ but do not modify its isotopic composition. The ratio of R_{12} and R_{13} can be expressed in terms of the isotopic composition of the reactant methane: $R_{12}/R_{13} = \alpha[^{12}C_{CH4}]/ [^{13}C_{CH4}]$, where α is an isotope fractionation factor for AOM and is equal to 1.012 (Martens et al. 1999). Expressing the ΣR from equation 9 and substituting it into equation 10, one obtains the required rate of reaction:

$$R = R_{12} + R_{13} \approx R_{12} = \frac{\gamma_{\sum CO2}}{\gamma_{\sum CO2} + \gamma_{CH4}} \left[\frac{1}{\gamma_{\sum CO2}} \frac{d}{dz}(K_z \frac{d[^{13}C_{\sum CO2}]}{dz}) - \frac{d}{dz}(K_z \frac{d[^{12}C_{\sum CO2}]}{dz}) \right] \quad \textbf{10}$$

where $\gamma_{\sum CO2}$ and γ_{CH4} are the ratios of ^{13}C to ^{12}C in $\sum CO_2$ and CH_4, respectively. By calculating the derivatives from discrete measured values, substituting $\gamma_{\sum CO2}$ and γ_{CH4} from their respective $\delta^{13}C$ values, and for a K_z in the range 0.16 $m^2\ d^{-1}$, we obtain R = 5 x 10^{-4} mmol $l^{-1}\ d^{-1}$ (3.5 x 10^{-10} mol $l^{-1}\ min^{-1}$).

Table 6.4. Parameters for kinetic calculations

Parameter	Value	Source
μ_{max}	2.0×10^{-3} min^{-1}	1
$K_{S_{O_2}}$	6.7×10^{-6} mol l^{-1}	1
Y_m	0.296	1
K	mol^{-1} l min^{-1}	2
[Fe(II)]	3.5×10^{-6} to 1.0×10^{-4} mol l^{-1}	
$[O_2]$	10^{-9} to 10^{-4}mol l^{-1}	
Cell density	10^{-4} to 10^{-6} cells ml^{-1}	
C content of methanotroph cell	6.23×10^{-14} mol C $cell^{-1}$	1

[1](Van Bodegom et al. 2001); [2] (Millero et al. 1987)

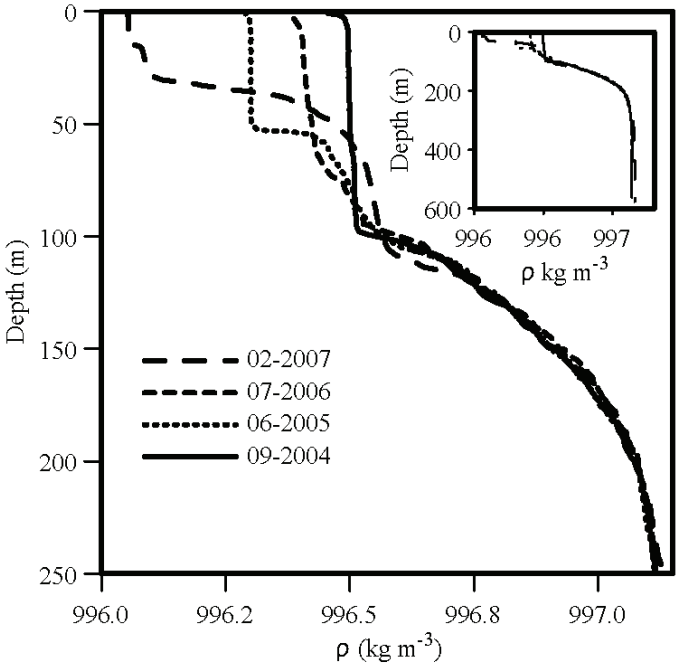
0
50
100
150
200
250
Depth (m)
996.0
996.2
996.5
996.8
997.0
ρ (kg m-3)
02-2007
07-2006
06-2005
09-2004
0
200
400
600
Depth (m)
996
996
997
ρ kg m-3

Figure 6.1

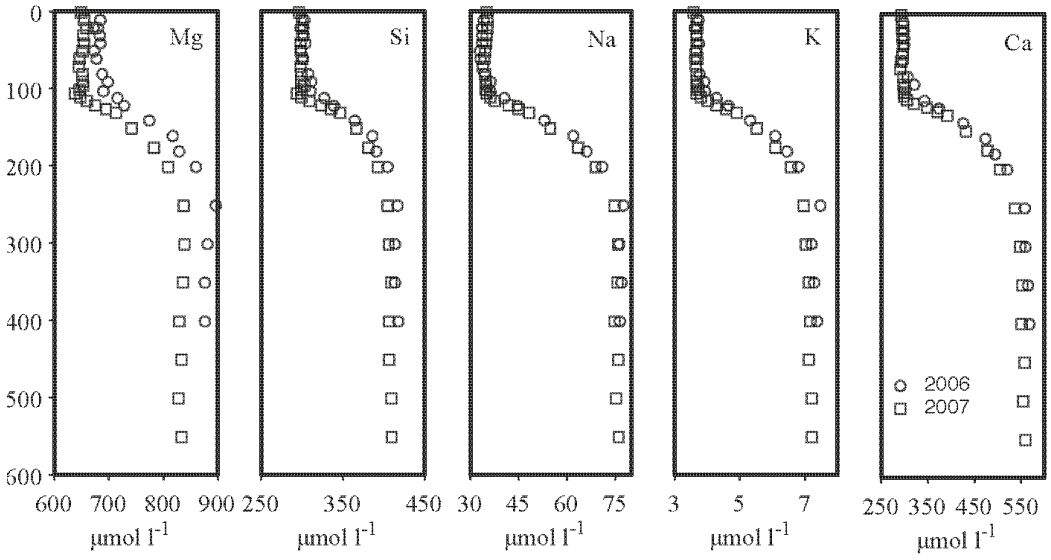
0
100
200
300
400
500
600
Mg
Si
Na
K
Ca
2006
2007
600 700 800 900
250 350 450
30 45 60 75
3 5 7
250 350 450 550
µmol l-1

Figure 6.2

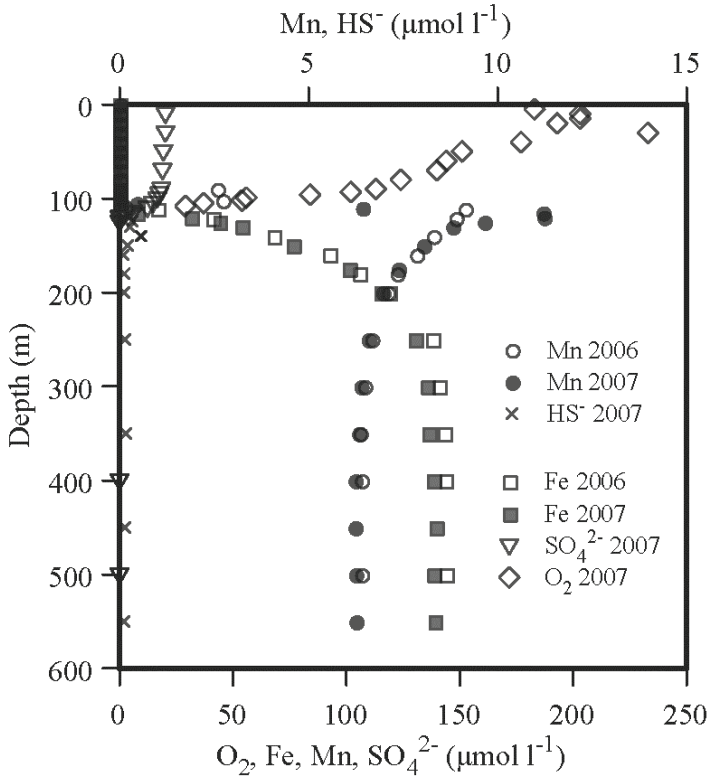
Mn, HS- (µmol l-1)
0
5
10
15
0
100
200
300
400
500
600
Depth (m)
Mn 2006
Mn 2007
HS- 2007
Fe 2006
Fe 2007
SO4 2- 2007
O2 2007
0
50
100
150
200
250
O2, Fe, Mn, SO4 2- (µmol l-1)

Figure 6.3

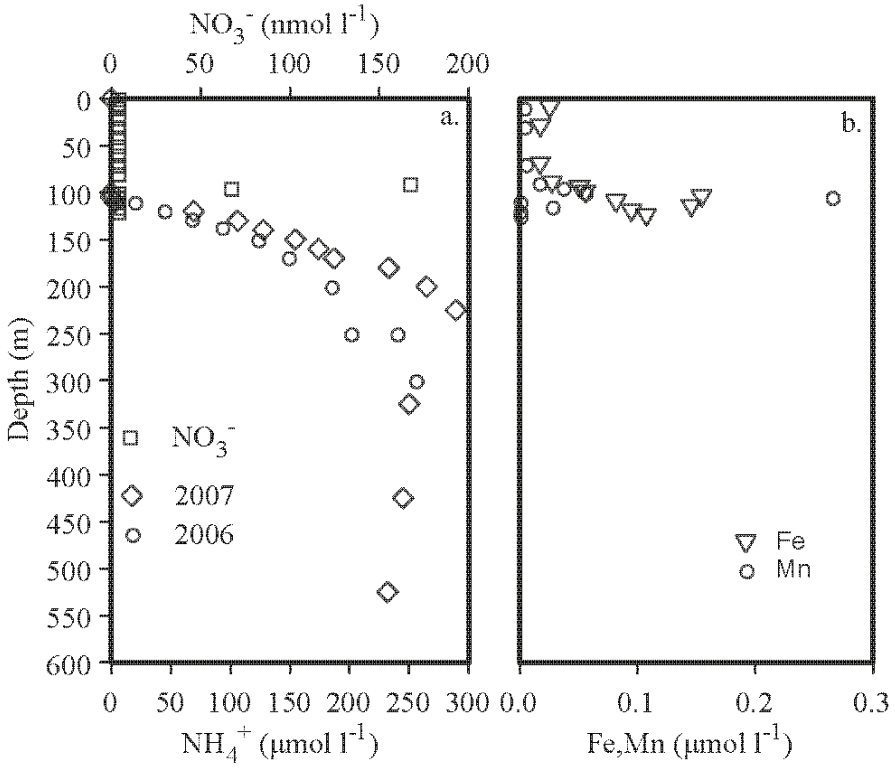
NO_3^- (nmol l^{-1})
0
50
100
150
200
a.
b.
Depth (m)
0
50
100
150
200
250
300
350
400
450
500
550
600
NO_3^-
2007
2006
Fe
Mn
0
50
100
150
200
250
300
NH_4^+ (µmol l^{-1})
0.0
0.1
0.2
0.3
Fe,Mn (µmol l^{-1})

Figure 6.4

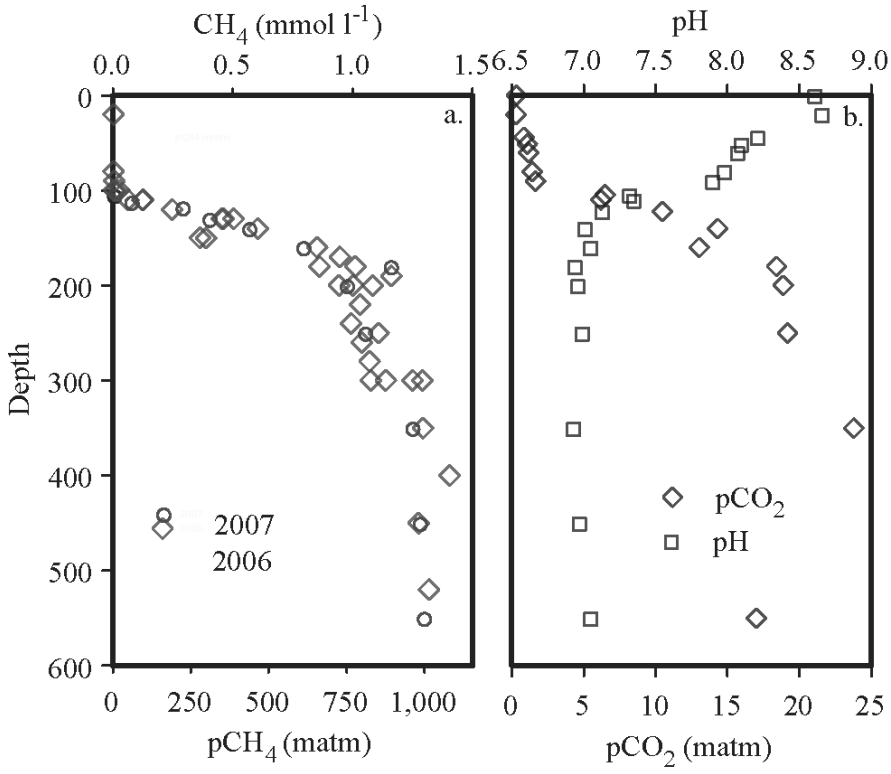
CH4 (mmol l-1)
0.0
0.5
1.0
1.5
pH
6.5
7.0
7.5
8.0
8.5
9.0
a.
b.
Depth
0
100
200
300
400
500
600
2007
2006
pCO2
pH
0
250
500
750
1,000
pCH4 (matm)
0
5
10
15
20
25
pCO2 (matm)

Figure 6.5

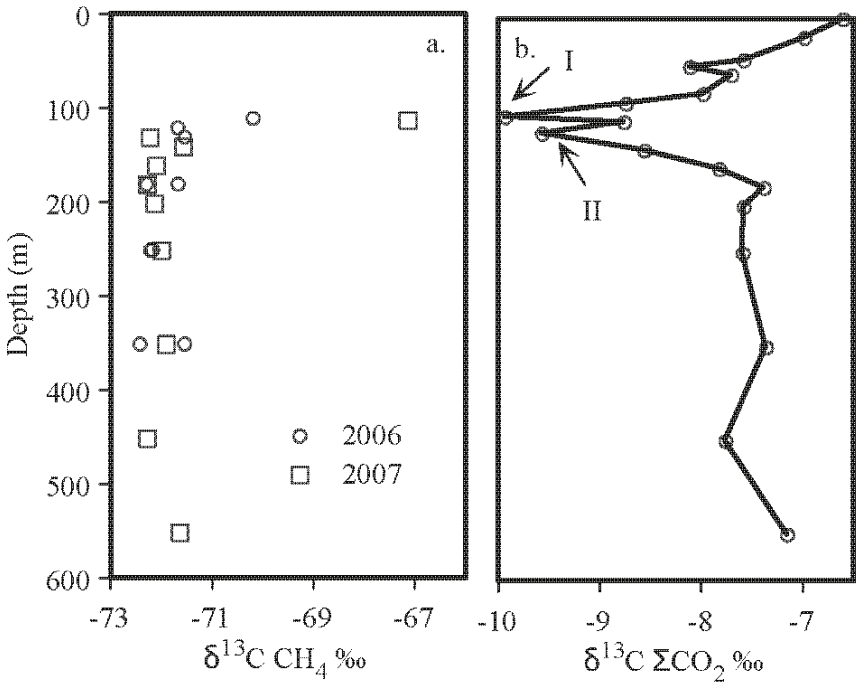
a.
b.
I
II
2006
2007
Depth (m)
0
100
200
300
400
500
600
-73
-71
-69
-67
-10
-9
-8
-7
δ13C CH4 ‰
δ13C ΣCO2 ‰

Figure 6.6

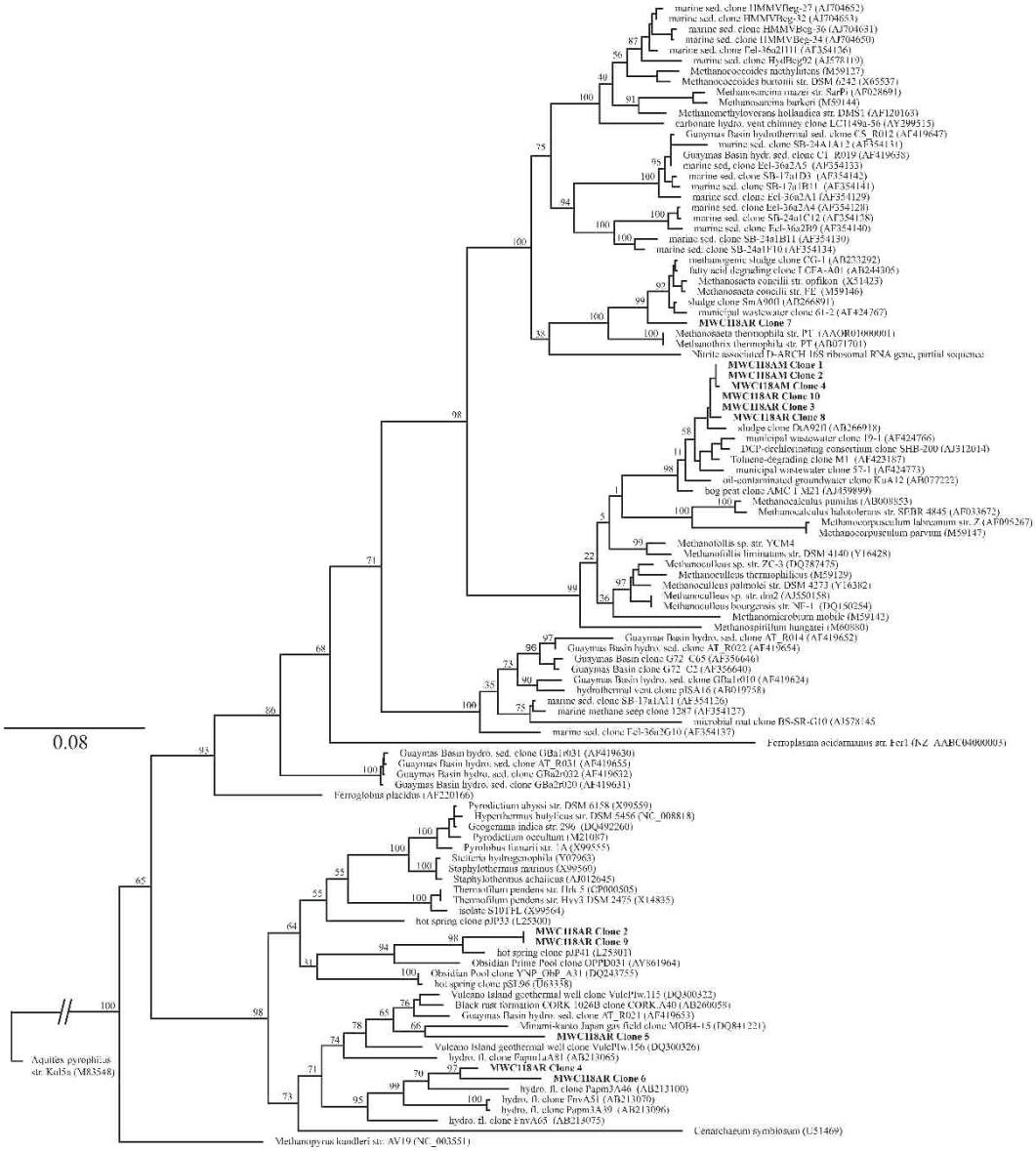
0.08
MWC118AR Clone 7
MWC118AM Clone 1
MWC118AM Clone 2
MWC118AM Clone 4
MWC118AR Clone 10
MWC118AR Clone 3
MWC118AR Clone 8
MWC118AR Clone 2
MWC118AR Clone 9
MWC118AR Clone 5
MWC118AR Clone 4
MWC118AR Clone 6
Aquifex pyrophilus str. Kol5a (M83548)
Methanopyrus kandleri str. AV19 (NC_003551)
Cenarchaeum symbiosum (U51469)

Figure 6.7

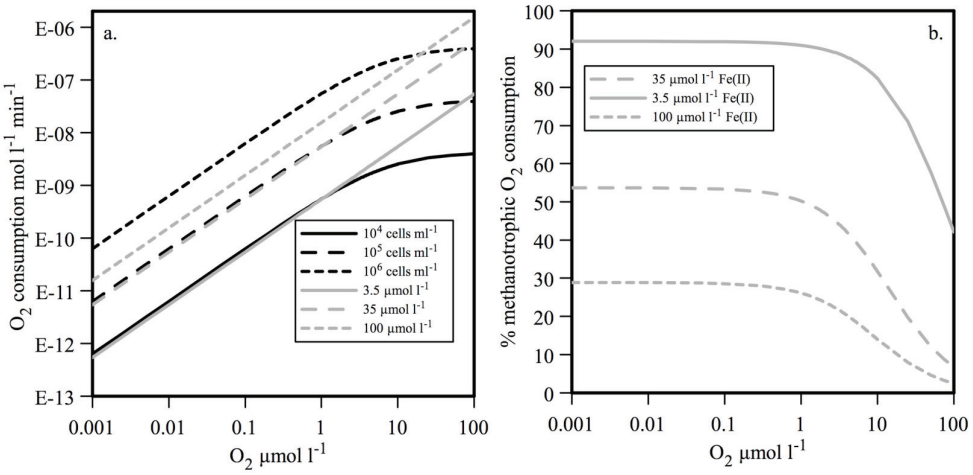
a.
E-06
E-07
E-08
E-09
E-10
E-11
E-12
E-13
O2 consumption mol l-1 min-1
0.001
0.01
0.1
1
10
100
O2 µmol l-1
10^4 cells ml-1
10^5 cells ml-1
10^6 cells ml-1
3.5 µmol l-1
35 µmol l-1
100 µmol l-1
b.
100
90
80
70
60
50
40
30
20
10
0
% methanotrophic O2 consumption
35 µmol l-1 Fe(II)
3.5 µmol l-1 Fe(II)
100 µmol l-1 Fe(II)
0.001
0.01
0.1
1
10
100
O2 µmol l-1

Figure 6.8

Chapter 7. Link between Chapters 6 and 8

7.1 Limiting Primary Production?

After generating a quantitative understanding for the rates of some of the most important biogeochemical reactions in Lake Matano, described in Chapters 2, 4 and 6, I return to the issue of primary production in Chapter 8. In Chapter 2, relatively high concentrations of Cr were detected in Lake Matano's surface waters. These high Cr concentrations were implicated in Chapter 2 and elsewhere (Sabo 2006) in limiting primary production. Thermodynamic equilibrium calculations were used in Chapter 2 to postulate that most of this Cr was in the hexavalent form. The objectives of the research described in Chapter 8 are to determine the speciation and isotopic composition of Cr in Lake Matano and to constrain its origins and rates of water column reduction and removal by sedimentation. The principal aim of Chapter 8 is to gain an appreciation for the potential ecological impacts of Cr in Lake Matano.

7.2 References

Sabo, E. M. 2006. Characterization of the pelagic plankton assemblage of Lake Matano and determination of factors regulating primary and secondary production dynamics. M.Sc. University of Windsor.

Chapter 8. Cr cycling in Wallace's Dreamponds

Sean A. Crowe[1,6], Sulung Nomosatryo[2], Andre Ellis[3], G. Douglas Haffner[4], Bjørn Sundby[1,5], Alfonso Mucci[1,6], and David A. Fowle[7]

1 Earth and Planetary Sciences, McGill University, Montréal, Québec, Canada H3A 2A7
2 Center for Limnology Research and Development, LIPI, Cibinong, West Java, Indonesia 16911
3 Geological Sciences, University of Texas at El Paso, El Paso, TX 79968
4 GLIER, University of Windsor, Windsor, Ontario, Canada N9B 3P4
5 ISMER, Université du Québec à Rimouski, Rimouski, Quebec G5L 3A1, Canada
6 GEOTOP-McGill-UQAM, Montreal, Quebec H3C 3P8, Canada
7 Department of Geology, University of Kansas, Lawrence, Kansas, USA 66047

8.1 Abstract

Lake Matano, Indonesia is among the 10 deepest lakes in the world. It hosts a diverse, endemic ecosystem, is a hotspot for ecological conservation, and is an important regional freshwater resource. High concentrations of Cr(VI) have been detected in its oxic surface waters and reflect the Cr-rich nature of catchment basin geology. Reduction of Cr(VI) by Fe(II) that diffuses upward from anoxic bottom water maintains Cr(VI) concentrations below international guidelines. Rates of Cr(VI) reduction have been calculated using Cr isotope systematics and indicate that Cr reduction rates are limited by slow transport.

8.2 Introduction

Cr is both highly toxic and an essential nutrient depending on its concentration and redox state (Cervantes et al. 2001). The hexavalent Cr (Cr(VI)) species are known carcinogens and cause acute toxicity to aquatic organisms at relatively low concentrations. In contrast, trivalent Cr (Cr(III)) is an essential nutrient. In most rocks, Cr predominantly occurs as Cr(III) and is hosted by poorly soluble minerals such chromite ($(Fe, Mg)Cr_2O_4$) (Oze et al. 2007). Oxidative weathering of these minerals, particularly in the presence of Mn (hydr)oxide surface coatings, causes the release of Cr(VI) to aqueous solutions. As Cr(VI) is more soluble and much less particle reactive than Cr(III), Cr mobility is greatly enhanced in the hexavalent state. Industrial processes such as

electroplating and leather tanning can cause the accumulation of anthropogenic Cr(VI) in water to relatively high concentrations. Water with anomalously high concentrations of Cr may also develop from weathering of Cr-rich ultramafic rocks (Oze et al. 2007). These rocks can be exposed at the earth's surface in tectonically active regions where ultramafic rocks from mid-ocean ridges (ophiolites) have been uplifted (Oze et al. 2007).

Sulawesi Island, Indonesia, situated in one of the most tectonically active regions of the world, is comprised of thick sections of ophiolitic rocks (Monnier et al. 1995) (Villeneuve et al. 2002). The tropical climate has caused intense weathering and the development of extensive lateritic soils (Golightly 1981). The Malili Lakes, termed Wallace's Dreamponds (Herder et al. 2006) because of the potential usage of their endemic sailfin silverside fish populations as a model system for evolutionary research, are the principal freshwater resource to Central and South Sulawesi Island. In addition to their fish populations (Gray and Mckinnon 2006; Roy et al. 2004; Roy et al. 2007), the Malili Lakes are also host to endemic gastropods (Von Rintelen et al. 2004), diatoms (Bramburger et al. 2006), and zooplankton (Sabo 2006), and in general, are characterized by high degrees of species endemism (Haffner et al. 2001). Indeed, the whole of Sulawesi Island has been cited as a hotspot for biological conservation due to its great species endemicity and rapid habitat loss (Myers et al. 2000).

Runoff waters percolating through the lateritic soils and interacting with the underlying ultramafic rocks may deliver significant amounts of Cr to the Malili Lakes (Crowe et al. 2008; Crowe et al. 2004). The lateritic soils within the catchment basins are currently being mined for Ni and development within the region is on the rise. At nearly 600 m depth, Lake Matano is the deepest of the Malili Lakes and one of the ten deepest lakes on Earth (Haffner et al. 2001). Though characterized by high degrees of species endemism, Lake Matano has very low primary productivity (Chapter 4; Sabo 2006). It is persistently stratified and only the surface 100 m of water is oxygenated (Crowe et al. 2008). Below 100 m, oxygen is depleted and products of anaerobic metabolisms (CO_2, CH_4, Fe(II) Mn(II) NH_4^+) accumulate. Previous studies have reported relatively high concentrations of Cr within the surface waters of Lake Matano and have implicated Cr in limiting the productivity of its diverse, endemic aquatic ecosystem (Crowe et al. 2008). In this study we determine Cr speciation in Lake Matano, evaluate its potential sources and

constrain rates of Cr cycling in an effort to better understand its potential to influence the biology of Lake Matano.

8.2 Methodology

Sampling and general limnological parameters. Most parameters were determined as described previously (Crowe et al. 2008). Water samples were collected at various locations and depths within the lake (Figure 8.1) using acid-washed Niskin bottles (30 % acetic acid) attached in series to a nylon rope. A Cr profile through the nearly 600 m deep water column was obtained at a central master station (Figure 8.1). Rainwater was collected directly in acid-washed (14% HNO_3) high density polyethylene (HDPE) bottles during heavy rain periods with low wind. The HDPE bottles were placed on a 1.5 m high pole in a 50 m wide clearing. Rainwater was filtered as described below.

Cr speciation. Cr(VI) concentrations were determined spectrophotometrically using the diphenylcarbazide method and a 1-m long liquid wave capillary cell (LWCC) to achieve Cr(VI) detection limits of 1 nmol l^{-1} (Yao and Byrne 1999). The LWCC was interfaced to a LS1 LL light source (Ocean Optics) and a USB 4000 spectrometer (Ocean Optics) through fiber-optic cables. Samples for Cr(VI) measurements were transferred from the Niskin bottle spigot to nitric acid washed 50 mL syringes (National Scientific) and filtered through 0.45 μm Whatman PVDF syringe filters into Falcon tubes. The diphenylcarbazide reagents were added to the Falcon tubes, and the measurements were made within 15 minutes of sample collection. Samples were introduced to the LWCC using an acid washed 10 mL syringe (National Scientific). The LWCC was rinsed between samples with 10 mL aliquots of Milli-Q water (~18 MΩ) containing the diphenylcarbazide reagents until the baseline returned to zero absorbance. Following the Milli-Q rinse, approximately 5 mL of sample was flushed through the LWCC and a measurement was made at 546 nm after the signal stabilized. Absorbances were corrected by subtracting the signal at a non-absorbing wavelength (700 nm). The analytical precision based on replicate measurements of filtered Lake Matano surface water was 5 % RSD and the detection limit 1 nmol l^{-1}.

Total dissolved Cr was determined on water samples collected as described above and filtered through 0.45 μm Whatman PVDF syringe filters using acid-washed (14 % HNO_3) 50 mL National Scientific all plastic syringes. The filtered water samples were preserved by acidification to 1% v/v with concentrated, trace metal grade HNO_3 (Fisher). Total Cr measurements were conducted by ICP-MS (ELAN 6100 Plus) using a dynamic reaction cell to remove polyatomic interferences. The instrumental detection limit was 0.4 nmol l^{-1}, calculated as 3 times the standard deviation of 10 replicate measurements of an acid blank. The precision (≤ 5% RSD) and accuracy of the method were evaluated using 5 replicate measurements of SLRS-4 (accepted 5.5 ± 0.3 nmol l^{-1}; measured 5.1 ± 0.2 nmol l^{-1}) (Natural Resources Canada) standard reference water.

Cr isotopes. All Cr stable isotope values are reported as δ^{53}Cr in permil. (‰).

$$\delta^{53}Cr\,(‰) = \frac{\left(\frac{^{53}Cr}{^{52}Cr}\right)_{sam} - \left(\frac{^{53}Cr}{^{52}Cr}\right)_{std}}{\left(\frac{^{53}Cr}{^{52}Cr}\right)_{std}} \bullet 1000 \qquad \textbf{1}$$

Where, the chromium standard used is NBS 979, sam = sample and std = standard.
We used the double isotope spike method to correct for any isotopic fractionation that may occur during sample purification and the mass spectrometric measurement. A Cr(VI) double spike was added as early as possible in the sample preparation process (Ellis et al. 2002). After allowing sufficient time for the samples and double spike to equilibrate, the samples were transferred to an anion exchange column (200-400 mesh AG1-X8 resin) with a 2 ml bed volume. The Cr(VI) anion adsorbs to the resin and all cations and weak acid anions elute with 20 ml of 0.1 N HCl. Cr(VI) was eluted from the column using one of two procedures. In the first, Cr(VI) was reduced to Cr(III) using sulfurous acid and eluted with 0.1 mol l^{-1} HCl, and in the second Cr(VI) was reduced to Cr(III) with a mixture of nitric acid and hydrogen peroxide and eluted with the same solution (Schoenberg et al. 2008). Subsequent isotope analyses were performed on a NU-Plasma MC-ICP-MS at the University of Illinois at Urbana-Champaign. Repeated measurements

of $^{50}Cr/^{52}Cr$, $^{53}Cr/Cr^{52}$, and $^{54}Cr/^{52}Cr$ ratios were made and an iterative data reduction routine was used in which the sample's $^{53}Cr/^{52}Cr$ ratio was calculated from measurements made on the spike/sample mixture (Ellis et al. 2002). Fe, V and Ti can cause isobaric interferences on masses 54, 50 and 51 respectively. Fe is monitored by measuring ^{56}Fe and Ti by measuring ^{49}Ti. Along with the samples, the NBS Cr standard 979 or an internal Cr standard was measured on a regular basis. Based on previous standards run as well as duplicates of various samples, our precision was ± 0.2 ‰ at the 95 % level.

Sediment sampling and analyses. Sediments were collected at a 120 m deep site in Lake Matano using a (0.52 m^2 x 0.3 m) Eckman dredge. The core was transferred to a glove bag and sectioned into 0.5 and 1-cm intervals under an inert N_2 atmosphere. Sediment sub-samples were frozen and transported to Canada where they were freeze-dried, fused into beads with lithium tetraborate, and analyzed by X-ray Fluorescence Spectrometry (XRF). The relative accuracy and precision of the Cr determinations were 5 and 0.5 % respectively with a detection limit of 10 ppm.

8.3 Results and Discussion

Cr distribution and speciation in *Lake Matano.* Depth profiles of total dissolved Cr and Cr(VI) are shown in Figure 8.2. Vertical profiles of total dissolved Cr generated in this study (2006 and 2007) are similar and comparable to profiles (2004 and 2005) reported in a previous study (Crowe et al. 2008). The constancy of the profiles over 4 years and different seasons is consistent with steady-state conditions. Total dissolved Cr concentrations reach a maximum of 160 nmol l^{-1} between 40 and 50 m depth within the oxic surface water. The progressive decrease in Cr concentrations below 50 m has been attributed to a downward flux of Cr driven by the reduction of Cr(VI) to Cr(III) by Fe(II) and the subsequent removal of dissolved Cr as a mixed Cr-Fe (hydr)oxide precipitate (Crowe et al. 2008). The original argument was made solely on the basis of the total chromium concentration measurements and thermodynamic estimates of Cr speciation.

The concentrations of total dissolved Cr and Cr(VI) in the surface waters of Lake Matano are identical within the precision (1σ) of the measurements. At depths deeper than 110 m, Cr(VI) concentrations are below our detection limit (1 nmol l^{-1}). This is

consistent with the hypothesis that Cr(VI) is reduced by Fe(II) within the 105 to 110 m depth interval in which both Cr(VI) and Fe(II) exist. The oxic surface waters of Lake Matano are mildly alkaline with a pH of between 8.55 at the surface and 7.29 at 105 m. Speciation calculations suggest that within the oxic surface water, Cr(VI) exists predominantly as the non-protonated and particle unreactive CrO_4^{2-} ion and the mono-protonated $HCrO_4^-$ species only becomes significant at 105 m where it comprises 12% of the dissolved Cr(VI) pool.

Figure 8.2a (inset) shows Cr concentrations below 100 m. Low but detectable (≤ 7 nmol l^{-1}) dissolved Cr concentrations persist in the deep, Fe(II)-rich, anoxic waters but Cr(VI) is undetectable. In other words, all the dissolved Cr in the anoxic water of Lake Matano is trivalent. The Cr(III) concentrations are up to an order of magnitude higher than those observed in the seasonally anoxic Fe-rich hypolimnion of Esthwaite water (Achterberg et al. 1997). Speciation calculations suggest that the predominant dissolved Cr species (>90%) is $Cr(OH)^{2+}$ and that the deep waters of Lake Matano are oversaturated with respect to the minerals chromite (SI = log IAP/K_{sp}; $(Fe, Mg)Cr_2O_4$, SI = 10.96) and eskolaite (Cr_2O_3, SI = 9.53).

The sharp Cr(III) concentration gradient between 180 m and 100 m depth must drive an upward flux of Cr(III) towards the oxic surface water. The gradient is most likely sustained by the oxidation of dissolved Cr(III) by Mn oxides or metal oxidizing bacteria within the pycnocline. The Cr(III) gradient could also be generated by sorption to or coprecipitation with particulate Fe (hydr)oxides that form within the depth interval between 100 and 120 m via Fe(II) oxidation. Conversely, dissolved Cr(III) could be replenished in the bottom waters by sinking particulate or sedimentary Fe (hydr)oxide carrier phases following their reductive dissolution.

Regional distribution of Cr. Total dissolved Cr and Cr(VI) concentrations in streams and lakes of the region are given in Table 8.1, in addition to values for selected pristine and contaminated aquatic environments around the world. Regional Cr concentrations vary from 5 nmol l^{-1} in rainwater to 235 $nmol^{-1}$ in the Patea River. Cr(VI) concentrations are not always consistent with total dissolved Cr concentrations, because the two samples were collected at different times and slightly different locations.

The La Wa and La Molenku streams drain a largely undeveloped area of the Lake Matano catchment basin and are its most significant tributaries (PT INCO personal communication). These streams contain between 72 and 107 nmol l^{-1} dissolved Cr (Table 8.1), almost exclusively in the hexavalent oxidation state. Nevertheless, dissolved Cr and Cr(VI) concentrations in the surface water of Lake Matano are 30 % higher than in the La Wa and La Molenku inflows. The disparity could result from unidentified, Cr-rich streams or groundwaters, dry deposition, or geochemical processes like evaporation that concentrate Cr. The Lemo-Lemo River which drains a largely undeveloped region of the Lake Towuti catchment also contains high concentrations of dissolved Cr (144 nmol l^{-1}, Table 8.1), presumably in the hexavalent oxidation state. Conversely, ground water from Subario Spring, which is situated in a small portion of the Lake Matano catchment underlain by limestone bedrock, has relatively low Cr concentrations (~10 nmol l^{-1}).

The waters of the Malili Lakes region have higher Cr concentrations than global average stream waters (Faure 1997) and oceans (Achterberg and Van den Berg 1997; Rue et al. 1997). Nevertheless, Cr(VI) concentrations in the Malili Lakes are lower than Cr(VI) levels in surface and ground waters interacting with mafic and ultramafic rocks in a variety of locales (Ball and Izbicki 2004; Becquer et al. 2003; Fantoni et al. 2002) and much lower than those at Cr(VI) contaminated sites like the Hanford waste disposal (Levitskaia et al. 2008).

Isotopic composition and fractionation. The isotopic composition of dissolved Cr at various depths in Lake Matano and the La Wa and Patea Rivers are given in Table 8.2. The isotopic composition of Cr in the rivers is lighter (δ^{53}Cr -1.2 to -1.5 ‰) than Lake Matano surface waters (δ^{53}Cr -0.5 to 0.5, mean of -0.25). The δ^{53}Cr in the La Wa and Patea Rivers is, to our knowledge, the lightest Cr measured in a natural system to date (Schoenberg et al. 2008). The global mean δ^{53}Cr of ultramafic rocks, the ultimate source of the Cr in the rivers and Lake Matano, is -0.119 (± 0.113) ‰, a value significantly heavier than the Cr isotopic composition of the rivers and Lake Matano.

Three mechanisms are known to fractionate Cr isotopes: 1) partial reduction of Cr(VI) to Cr(III) (Ellis et al. 2002); 2) non-equilibrium adsorption to hydroxide minerals (Ellis et al. 2004); and 3) the precipitation of chromate bearing minerals (Schoenberg et

al. 2008). Partial reduction of Cr could not explain the isotopically light composition of Cr in the river waters. Reduction of Cr(VI) to Cr(III) leads to an enrichment of the reduced species in the lighter isotope (^{52}Cr) and a concomitant enrichment of the residual Cr(VI) in the heavier isotope (Ellis et al. 2002), the opposite of what would be required to generate the river water $\delta^{53}Cr$ signature. The Cr(VI) bearing mineral crocoite ($PbCrO_4$) preferentially incorporates ^{53}Cr (Schoenberg et al. 2008). Hence, the precipitation of crocoite depletes the remaining, dissolved Cr(VI) in ^{53}Cr. Although the precipitation of crocoite within the catchment soils could account for the heavy $\delta^{53}Cr$ compositions of the La Wa and Patea Rivers, neither the Pb or Cr(VI) concentrations are likely to accumulate to the mmolar levels required to reach crocoite saturation in the catchment soils. This does not preclude that fractionation may result from the precipitation of other Cr(VI) bearing minerals (e.g. the chromate analogue of ettringite, $Ca_6[Al(OH)_6]_2(CrO_4)_3 \cdot 26H_2O$ (Perkins and Palmer 2000); log K_{sp}= -41.46; or the chromate analogue of jarosite, $KFe_3(CrO_4)_2(OH)_6$ (Baron and Palmer 1996); log K_{sp}= -18.4) which would be more likely to be at saturation within the catchment soils. Non-equilibrium adsorption to surfaces of the mineral goethite (α-FeOOH), which is highly abundant in the Lake Matano catchment soils, has been shown to cause isotopic fractionation within Cr(VI) plumes (Ellis et al. 2004). Like partial Cr(VI) reduction, sorption to goethite would also enrich the residual, dissolved Cr(VI) in the heavy isotope. Cr(VI) sorption to goethite is only significant between pH 2 and 6, whereas the weathering of mafic and ultramafic rocks typically yields ground and surface waters with a pH greater than 7. The effect of oxidation on Cr isotopes is yet unknown, but it is possible that oxidative dissolution of Cr(III) minerals may favor release of the light isotope (^{52}Cr) to solution, as is observed for oxidative weathering of ferrous Fe bearing minerals (Rouxel et al. 2003). Thus, based on our current knowledge of Cr isotope systematics, the oxidation of Cr(III)-laden groundwaters and/or the precipitation of a Cr(VI) bearing mineral in the catchment most likely account for the observed composition in the river waters.

The mean isotopic composition of dissolved chromium in the surface water of Lake Matano is more positive than in the inflowing streams. The enrichment in ^{53}Cr likely results from the partial reduction of Cr(VI) across the pycnocline within the lake and is consistent with the concentration and speciation profiles.

Kinetics of Cr(VI) reduction. Previous estimates of Cr(VI) reduction rates in Lake Matano were based on Fick's First Law, applied to the Cr concentration profiles and an estimate of the vertical eddy diffusivity (Crowe et al. 2008). The Cr isotope system provides an independent method of calculating the Cr(VI) reduction rates. The following mass balance equation is used to estimate the flux of Cr(VI) through the redox boundary between 100 and 120 m depth:

$$\Phi_{in} \bullet \left[\frac{^{53}Cr}{^{52}Cr}\right]_{in} = \Phi_{out} \bullet \left[\frac{^{53}Cr}{^{52}Cr}\right]_{red} \qquad \mathbf{2}$$

where Φ_{in} is the flux of Cr into Lake Matano (mol s^{-1}; calculated as the product of the Cr(VI) concentration in the inflowing waters (100.5 nmol l^{-1}) and the inflow rate (24.1 m^3 s^{-1}) (PT INCO, personal communication)), $[^{53}Cr/^{52}Cr]_{in}$ is the absolute isotopic ratio in the inflowing water, and Φ_{out} is the flux of Cr through the pycnocline driven by reduction. The value of $[^{53}Cr/^{52}Cr]_{red}$ for the dissolved Cr(III) in the anoxic bottom waters of the lake was estimated as follows:

$$\left[\frac{^{53}Cr}{^{52}Cr}\right]_{red} = \alpha \bullet \left[\frac{^{53}Cr}{^{52}Cr}\right]_{in} \qquad \mathbf{3}$$

where, α is the instantaneous isotope fractionation factor (0.9966) for the reduction of Cr(VI) to Cr(III) (Ellis et al. 2002). The flux of Cr across the pycnocline, driven by reduction and calculated as described above, is 8.6 x 10^{-4} mol s^{-1}. When integrated over the total surface area of the lake underlain by anoxic Fe(II)-rich water (106.6 km^2, (Crowe et al. 2008)), the corresponding area-specific Cr reduction rate is 7.0 μmol m^{-2} d^{-1}. This rate is within the uncertainty of the rate (6.0 μmol m^{-2} d^{-1}, an uncertainty of a factor of 5 on the estimates of K_z used to calculated the Cr fluxes gives a range of Cr(VI) reduction rates from 1.2 to 30 μmol m^{-2} d^{-1}, [16]) calculated from Fick's First Law. The good agreement between the two estimates suggests that these rates are accurate and gives us confidence in our understanding of Cr cycling within Lake Matano. The flux of

Cr(VI) out of the oxic surface waters is likely driven by the reduction of Cr(VI) to Cr(III) by Fe(II) according to the following reaction (Crowe et al. 2008; Hansel et al. 2003):

$$3Fe^{2+} + CrO_4^{2-} + 8H_2O \rightarrow 4Cr_{0.25}Fe_{0.75}(OH)_3 + 4H^+ \quad \textbf{4}$$

Accordingly, estimates of between 340 and 2700 μmol m^{-2} d^{-1} for the upward Fe(II) flux (Chapter 4) indicate that the supply of Fe(II) at the pynocline is more than sufficient to sustain the Cr(VI) reduction rates. The concentration profiles of dissolved Cr(VI) and Fe(II) (Chapter 4) suggest that Cr reduction occurs within the 5-m depth interval, between 105 and 110 m, where both Cr(VI) and Fe(II) are present. Integrating the area specific rates of Cr(VI) reduction over a 5-m depth interval yields a volume specific rate of between 1.2 and 1.4 μmol m^{-3} d^{-1}. This depth interval contains mean Fe(II) and Cr(VI) concentrations of 190 nmol l^{-1} and 19 nmol l^{-1}, respectively. The reduction of Cr(VI) by Fe(II) has been well studied under laboratory conditions with several studies addressing the kinetics of the reaction under various conditions (Eary and Rai 1991; Fendorf and Li 1996; Millero et al. 1987). In the most comprehensive study (Millero et al. 1987), the reduction of Cr(VI) by Fe(II) was found to be governed by the following rate law:

$$-\frac{d[Cr(VI)]}{dt} = k[Cr(VI][Fe(II)] \quad \textbf{5}$$

which is first order with respect to both the Cr(VI) and Fe(II) concentrations. The rate constant, *k,* under a range of temperature (*T*) and ionic strength (*I*) conditions can be calculated from the following empirical equation:

$$\log k = 11.93 + 0.95\,pH - 4260.1T - 1.06I^{0.5} \quad \textbf{6}$$

For the conditions within the depth interval in which Cr reduction occurs, we calculate a log *k* of 4.62 mol l^{-1} min^{-1}. At the Fe(II) and Cr(VI) concentrations encountered between 105 and 100 m depth, the rate law (Eq. 4) yields a theoretical Cr(VI) reduction rate of 227 μmol m^{-3} d^{-1}. This rate, calculated from purely chemical kinetic considerations, is

much higher than what we observe in Lake Matano. Although Cr reduction can be inhibited by O_2 (Millero et al. 1987), O_2 concentrations are below our detection limit (2.5 μmol l^{-1}) within the depth interval of Cr reduction. Therefore, the reduction of Cr in Lake Matano is likely transport limited.

The reduction of Cr(VI) by Fe(II) and the ensuing sedimentation of a mixed Fe-Cr (hydr)oxide should be reflected in the Cr burial rates. The total Cr concentration in the solids of the upper 10 cm of sediment collected from 120 m depth in Lake Matano is 0.32 wt %. or, assuming a 90% porosity and a sediment density of 2.96 g cm^{-3}, the wet sediment contains 0.30 g Cr cm^{-3} or 5.7 μmol Cr cm^{-3}. Given a deep-water sedimentation rate of 0.08 cm a^{-1} (Crowe et al. 2004), the Cr sediment accumulation rate is 13 μmol m^{-2} d^{-1}. This is in reasonable agreement with the area specific Cr removal rates (6 to 7 μmol m^{-2} d^{-1}) estimated from both the Cr diffusive fluxes and the Cr isotope mass balance. Cr reduction by Fe(II) is an important component of the Cr cycle within Lake Matano and is likely a major pathway in the transport of Cr from the source bedrock of the catchment to its sink in the lake sediment.

Environmental Implications. Dissolved Cr(VI) concentrations in the waters of the Malili Lakes system are well below the World Health Organization's prescribed limit of 960 nmol l^{-1} for drinking water (Oze et al. 2007). The USEPA has established criteria for the highest concentration of Cr in surface water to which an aquatic community can be exposed briefly without causing an unacceptable effect (308 nmol l^{-1} Cr(VI)), and the highest Cr concentration to which an aquatic community can be exposed indefinitely without an unacceptable effect (212 nmol l^{-1} for Cr(VI)) (USEPA 2006). With the exception of the Patea River (assuming the total Cr concentration of 235 nmol l^{-1} is all Cr(VI)), the chromium levels of waters of the Malili Lakes system are well below these limits.

Although these USEPA guidelines were developed based on a rigorous set of criteria, they are largely intended for the aquatic communities of North America. Both the chemistry and biology of the Malili Lakes are dramatically different from those of temperate freshwater systems. For example, Lake Matano is characterized by exceptionally low concentrations of P and very low levels of SO_4^{2-} (Crowe et al. 2008).

Cr(VI) uptake by microorganisms is known to occur through sulfate transport systems and non-specific anion carriers (Cervantes et al. 2001). Consequently, the low sulfate and phosphate concentrations may facilitate CrO_4^{2-} uptake in the Malili Lakes biota rendering its ecosystem more sensitive to Cr(VI). On the other hand, Cr(VI) resistance by several mechanisms is known to develop in a variety of organisms (Cervantes et al. 2001). Given the antiquity of the Lake System (Haffner et al. 2001) and its relative stability (Crowe et al. 2008), the ecosystem may be well adapted to high levels of Cr(VI).

Acknowledgements. The help of numerous individuals is acknowledged including: Peter Hehanussa, William Napier, Mike Dutton, Matt Orr, Deky Tetradiono, Lili Lubis, Jennifer Roberts, Elisabeth Sabo, Gadis Sri Hariyani, Sinyo Rio, Dullah, Sarah Bungin, Cedric Magen, Sergei Katsev, Arne Sturm, Paul Hamilton, Ryan Walter and CarriAyne Jones. PT INCO is acknowledged for providing hydrological data. Funding was kindly provided by NSERC, INCO Canada Ltd., PT INCO, and KU Geology Associates. SAC was partially supported by an NSERC IPGS sponsored by INCO Canada Ltd.

Figure 8.1. Map of the Malili Lakes System (modified from (Herder et al. 2006)) showing the location of the water (circles) and sediment (star) sampling sites.

Figure 8.2. Profiles of total dissolved Cr (a) and hexavalent Cr (b) in Lake Matano to 200 m depth at the central deep-water master station. Inset in (a) shows dissolved Cr concentrations to greater depths.

Table 8.1. Total dissolved Cr and Cr(VI) concentrations (nmol l^{-1}) in the Malili Lakes system and various pristine and contaminated aquatic environments around the world.

Location	Map No.	Dissolved Cr		Cr(VI)
		2006	2007	
La Molenku	1		98	NA
La Wa	2	72	98	107
Subario Spring	4	10	13	13
Matano Master Station (surface)	3	NA	136	130
Sorowako Littoral Zone	5	NA	NA	175
Patea River	6	154	NA	235
Mahalona (surface)	7	NA	206	136
Tominanga	8	188	NA	NA
Lemo-Lemo	10	144	NA	NA
Lake Towuti (surface)	9	NA	72	NA
Rainwater	5	5	NA	NA
		Reference		Cr
Mean Global Stream water		(Faure 1997)		19.2
Western Mediterranean		(Achterberg and Vandenberg 1997)		2-5
Lake Ontario		(Beaubien et al. 1994)		7
Lake Superior		(Beaubien et al. 1994)		1.2
Suboxic North Pacific		(Rue et al. 1997)		1
New Caledonia Ground Water		(Becquer et al. 2003)		1270 (Cr(VI))
Mojave Desert Ground Water		(Ball and Izbicki 2004)		1154 (Cr(VI))
La Spezia (Italy)		(Fantoni et al. 2002)		96-1385 (Cr(VI))
Hanford waste site		(Levitskaia et al. 2008)		$>10^4$

*NA = Not Analyzed

Table 8.2. Chromium isotopic composition of Cr in waters and rocks of the Malili Lakes system

Sample	$\delta^{53}Cr$	$^{53}Cr/^{52}Cr$
LM 10m	-0.5	0.113333305
LM 40m	-0.5	0.113333305
LM 60m	0.5	0.113446695
LM 80m	-0.5	0.113333305
La Wa River	-1.3	0.113242593
Patea River	-1.5	0.113219915
Ultramafic Rocks	-0.119 (Schoenberg et al. 2008)	-

8.4 References

Achterberg, E. P., and C. M. G. Van Den Berg. 1997. Chemical speciation of chromium and nickel in the western Mediterranean. Deep-Sea Research Part II-Topical Studies in Oceanography **44:** 693-720.

Achterberg, E. P., C. M. G. Van Den Berg, M. Boussemart, and W. Davison. 1997. Speciation and cycling of trace metals in Esthwaite Water: A productive English lake with seasonal deep-water anoxia. Geochim. Cosmochim. Acta **61:** 5233-5253.

Ball, J. W., and J. A. Izbicki. 2004. Occurrence of hexavalent chromium in ground water in the western Mojave Desert, California. Appl. Geochem. **19:** 1123-1135.

Baron, D., and C. D. Palmer. 1996. Solubility of $KFe_3(CrO_4)_2(OH)_6$ at 4 to 35 degrees C. Geochim. Cosmochim. Acta **60:** 3815-3824.

Becquer, T., C. Quantin, M. Sicot, and J. P. Boudot. 2003. Chromium availability in ultramafic soils from New Caledonia. Sci. Total Environ. **301:** 251-261.

Bramburger, A. J., G. D. Haffner, P. B. Hamilton, F. Hinz, and P. E. Hehanussa. 2006. An examination of species within the genus Surirella from the Malili Lakes, Sulawesi Island, Indonesia, with descriptions of 11 new taxa. Diatom Research **21:** 1-56.

Cervantes, C., J. Campos-Garcia, S. Devars, F. Gutierrez-Corona, H. Loza-Tavera, J. C. Torres-Guzman, and R. Moreno-Sanchez. 2001. Interactions of chromium with microorganisms and plants. FEMS Microbiol. Rev. **25:** 335-347.

Crowe, S. A., A. H. O'neill, S. Katsev, P. Hehanussa, G. D. Haffner, B. Sundby, A. Mucci, and D. A. Fowle. 2008. The biogeochemistry of tropical lakes: A case study from Lake Matano, Indonesia. Limnol. Oceanogr. **53:** 319-331.

Crowe, S. A., S. J. Pannalal, D. A. Fowle, M. T. Cioppa, D. T. A. Symons, G. D. Haffner, B. J. Fryer, R. Mcneely, B. Sundby, and P. E. Hehanussa. 2004. Biogeochemical cycling in Fe-rich sediments from Lake Matano, Indonesia, p. 1185-1189. 13th International Symposium on Water-Rock Interaction, Saratoga Springs, New York, USA.

Eary, L. E., and D. Rai. 1991. Chromate reduction by subsurface soils under acidic conditions. Soil Sci. Soc. Am. J. **55:** 676-683.

Ellis, A. S., T. M. Johnson, and T. D. Bullen. 2002. Chromium isotopes and the fate of hexavalent chromium in the environment. Science **295:** 2060-2062.

Ellis, A. S. 2004. Using chromium stable isotope ratios to quantify Cr(VI) reduction: Lack of sorption effects. Environ. Sci. Technol. **38:** 3604-3607.

Fantoni, D., G. Brozzo, M. Canepa, F. Cipolli, L. Marini, G. Ottonello, and M. V. Zuccolini. 2002. Natural hexavalent chromium in groundwaters interacting with ophiolitic rocks. Environmental Geology **42:** 871-882.

Fendorf, S. E., and G. C. Li. 1996. Kinetics of chromate reduction by ferrous iron. Environ. Sci. Technol. **30:** 1614-1617.

Golightly, J. P. 1981. Nickeliferous Laterite Deposits. Econ. Geol. **75th Anniversary Volume:** 710-735.

Gray, S. M., and J. S. Mckinnon. 2006. A comparative description of mating behaviour in the endemic telmatherinid fishes of Sulawesi's Malili Lakes. Environ. Biol. Fishes **75:** 471-482.

Haffner, G. D., P. E. Hehanussa, and D. Hartoto. 2001. The biology and physical processes of large lakes of Indonesia, p. 183-194. *In* M. Munawar and R. E. Hecky [eds.], The Great Lakes of the World: Food web, health and integrity. Backhuys Publishers.

Hansel, C. M., B. W. Wielinga, and S. R. Fendorf. 2003. Structural and compositional evolution of Cr/Fe solids after indirect chromate reduction by dissimilatory iron-reducing bacteria. Geochim. Cosmochim. Acta **67:** 401-412.

Herder, F., A. W. Nolte, J. Pfaender, J. Schwarzer, R. K. Hadiaty, and U. K. Schliewen. 2006. Adaptive radiation and hybridization in Wallace's Dreamponds: evidence from sailfin silversides in the Malili Lakes of Sulawesi. Proceedings of the Royal Society B-Biological Sciences **273:** 2209-2217.

Levitskaia, T. G., M. J. O'hara, S. I. Sinkov, and O. B. Egorov. 2008. Direct spectrophotometric analysis of Cr(VI) using a liquid waveguide capillary cell. Applied Spectroscopy **62:** 107-115.

Millero, F. J., S. Sotolongo, and M. Izaguirre. 1987. The oxidation-kinetics of Fe(II) in seawater. Geochim. Cosmochim. Acta **51:** 793-801.

Monnier, C., J. Girardeau, R. C. Maury, and J. Cotten. 1995. Back-arc basin origin for the East Sulawesi Ophiolite (Eastern Indonesia). Geology **23:** 851-854.

Myers, N., R. A. Mittermeier, C. G. Mittermeier, G. A. B. Da Fonseca, and J. Kent. 2000. Biodiversity hotspots for conservation priorities. Nature **403:** 853-858.

Oze, C., D. K. Bird, and S. Fendorf. 2007. Genesis of hexavalent chromium from natural sources in soil and groundwater. P Natl Acad Sci USA **104:** 6544-6549.

Perkins, R. B., and C. D. Palmer. 2000. Solubility of $Ca_6[Al(OH)_6]_2(CrO_4)_3 \cdot 26H_2O$, the chromate analog of ettringite; 5-75 degrees C. Appl. Geochem. **15:** 1203-1218.

Rouxel, O., N. Dobbek, J. Ludden, and Y. Fouquet. 2003. Iron isotope fractionation during oceanic crust alteration. Chem. Geol. **202:** 155-182.

Roy, D., M. F. Docker, G. D. Haffner, and D. D. Heath. 2007. Body shape vs. colour associated initial divergence in the Telmatherina radiation in Lake Matano, Sulawesi, Indonesia. J. Evol. Biol. **20:** 1126-1137.

Roy, D., M. F. Docker, P. Hehanussa, D. D. Heath, and G. D. Haffner. 2004. Genetic and morphological data supporting the hypothesis of adaptive radiation in the endemic fish of Lake Matano. J. Evol. Biol. **17:** 1268-1276.

Rue, E. L., G. J. Smith, G. A. Cutter, and K. W. Bruland. 1997. The response of trace element redox couples to suboxic conditions in the water column. Deep-Sea Research Part I-Oceanographic Research Papers **44:** 113-134.

Sabo, E. M. 2006. Characterization of the pelagic plankton assemblage of Lake Matano and determination of factors regulating primary and secondary production dynamics. M.Sc. University of Windsor.

Schoenberg, R., S. Zink, M. Staubwasser, and F. Von Blanckenburg. 2008. The stable Cr isotope inventory of solid Earth reservoirs determined by double spike MC-ICP-MS. Chem. Geol. **29:** 294-306.

US EPA. 2006. National Recommended Water Quality Criteria (4304T), p. 25. United States Environmental Protection Agency, Office of Science and Technology.

Villeneuve, M., W. Gunawan, J. J. Cornee, and O. Vidal. 2002. Geology of the central Sulawesi belt (eastern Indonesia): constraints for geodynamic models. International Journal of Earth Sciences **91:** 524-537.

Von Rintelen, T., A. B. Wilson, A. Meyer, and M. Glaubrecht. 2004. Escalation and trophic specialization drive adaptive radiation of freshwater gastropods in ancient lakes on Sulawesi, Indonesia. Proceedings of the Royal Society of London Series B-Biological Sciences **271:** 2541-2549.

Yao, W. S., and R. H. Byrne. 1999. Determination of trace chromium(VI) and molybdenum(VI) in natural and bottled mineral waters using long pathlength absorbance spectroscopy (LPAS). Talanta **48:** 277-282.

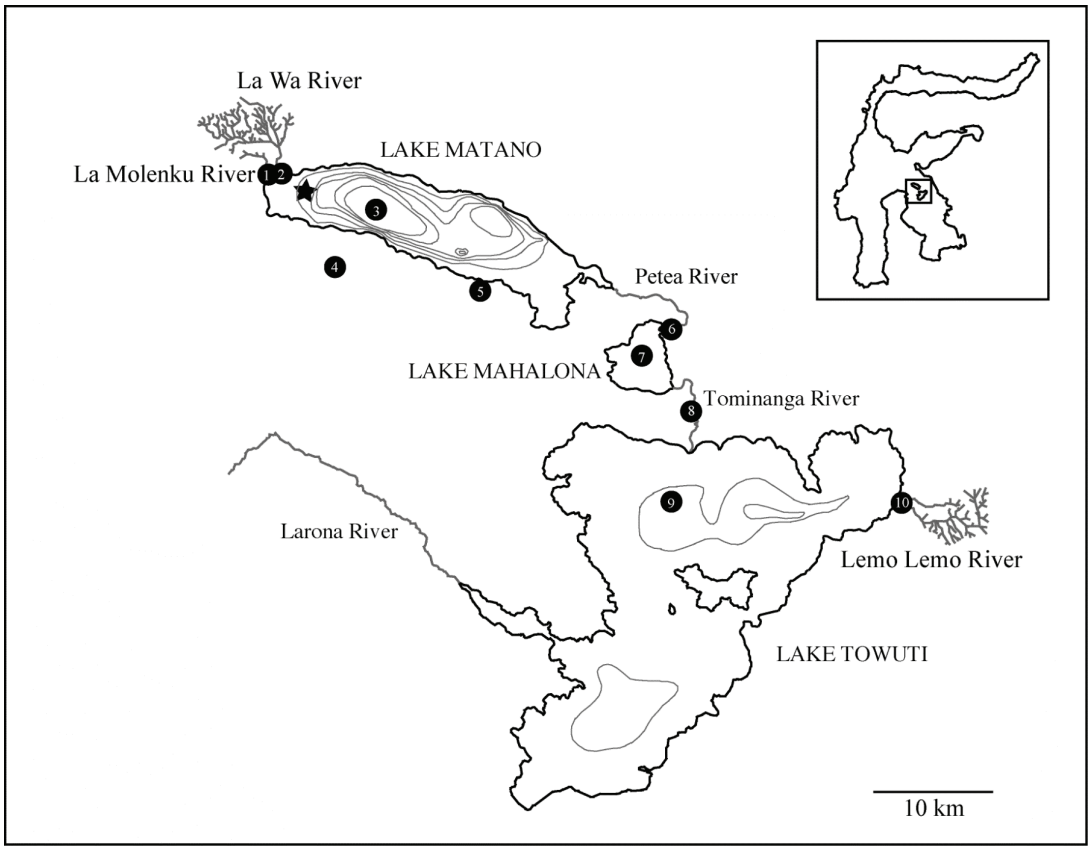
La Wa River
LAKE MATANO
La Molenku River
1
2
3
4
5
Petea River
6
7
LAKE MAHALONA
Tominanga River
8
9
10
Larona River
Lemo Lemo River
LAKE TOWUTI
10 km

Figure 8.1

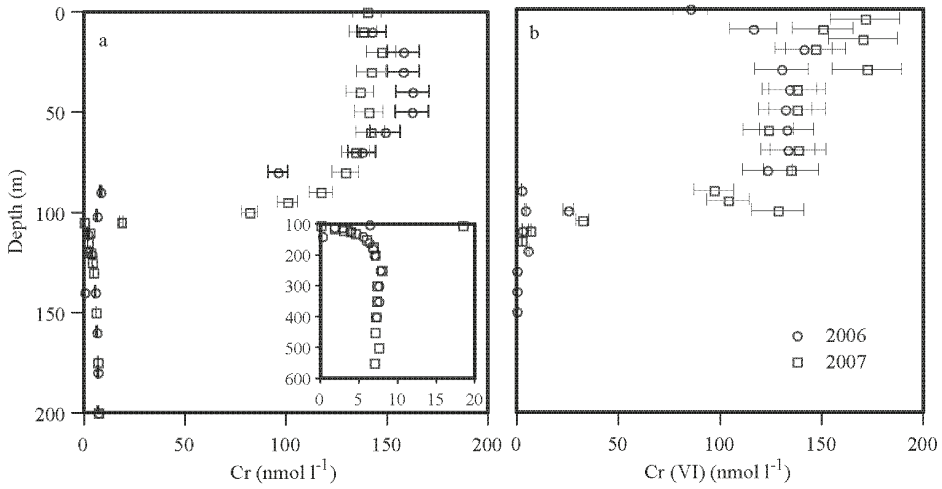

Figure 8.2

Chapter 9. Conclusions

A unique set of geographical, geological, and biological conditions have culminated in the development of an end-member Fe-rich (ferruginous) aquatic ecosystem, Lake Matano. Ferric Fe-rich soils have developed in Lake Matano's catchment basin due to the underlying lithology (ultramafic rocks of ophiolitic origin) and intense tropical weathering (Golightly 1981). These lateritic soils supply an ample flux of Fe-rich particulates to the lake's sediments (Crowe et al. 2004). Lake Matano's steep bathymetry and lack of marked seasonal temperature changes or large inflows impede mixing and cause persistent stratification (Chapter 2). Despite minimal vertical temperature gradients, a stable pycnocline has developed at 100 m depth which separates an oxic surface layer from anoxic bottom water. The available evidence suggests that mixing between these layers occurs on a time-scale of 1000 to 2000 years (Chapter 2).

One remarkable feature of Lake Matano is its very low sulfate concentrations (< 20 $umol^{-1}$) which are exhausted below the pycnocline due to sulfate reduction (Chapter 2 and Chapter 4). In the oceans and many lakes, sulfide produced by sulfate reduction often limits the concentration of Fe(II) in anoxic waters due to the formation and precipitation of iron sulfides. The low rate of sulfide production in Lake Matano allows ferrous Fe to accumulate to high concentrations in its bottom waters (<140 μmol^{-1}) (Chapter 2 and Chapter 4). Authigenic and allogenic Fe (hydr)oxides maintain exceedingly low P concentrations in the oxic surface layer where the lack of P likely restricts rates of primary production which are comparable to ultra-oligotrophic high-arctic lakes (Chapter 2 and Chapter 4). Low primary production in the surface layer allows light to penetrate deep into the Fe-rich (ferruginous) chemocline supporting a novel, deep-water community of *Chlorobiaceae* (Chapter 4). The metabolisms of *Chlorobiaceae* are typically driven by sunlight with sulfide as an electron donor but in Lake Matano, the absence of sulfide indicates they are supported through oxidation of Fe(II).

The high abundance of Fe(III) and its dissimilatory reduction by microorganisms should preclude methanogenesis in Lake Matano based on the greater thermodynamic yield of microbial Fe(III) reduction than methanogenesis (Chapter 6). Yet, methane produced by methanogeneis accumulates to high concentrations in the anoxic bottom water. This methane is partially consumed by anaerobic oxidation of methane (AOM) in

the chemocline despite the lack of known electron acceptors for AOM (NO_3^- and SO_4^{2-}). Thus, AOM in Lake Matano must be coupled to an unknown electron acceptor, the most available alternative being Fe(III). Notwithstanding the Fe-rich nature of Lake Matano, methanogenesis and methanotrophy appear to be important components of the C-cycle. Therefore, ferruginous conditions support substantial communities of methanogens and methanotrophs that are active in Lake Matano's sediments and water column.

Cr(VI) concentrations in the oxic surface layer are relatively high (Chapter 2 and Chapter 8). This reflects the predominance of Cr-rich ultramafic rocks in Lake Matano's catchment basin (Chapter 8). Although high, Cr(VI) concentrations are below international guidelines. Cr(VI) is supplied to the surface layer by inflowing streams and is removed across the pycnocline by reduction with Fe(II). The reduction driven flux of Cr(VI) out of the surface layer is important to maintaining concentrations below guidelines. Cr isotope ratios in Lake Matano's tributaries are the lightest measured to date (compare with data in Schoenberg et al. 2008). Rates of Cr reduction within the chemocline were estimated using both flux calculations (Chapter 2) and Cr isotope systematics (Chapter 8). These rates are in good agreement with each other and are well below rates measured in laboratory experiments suggesting that Cr(VI) reduction in Lake Matano is transport limited.

Ferruginous aquatic conditions are rare in the world today but are similar to what has been construed for the earth's earliest oceans rendering Lake Matano perhaps the best modern analogue for the ecology of ancient ferruginous oceans (Chapter 4). By analogy to Lake Matano, the ancient ferruginous oceans likely supported photoferrotrophic primary producers, Fe-reducing and methanogenic heterotrophs and methanotrophs. Photoferrotrophs may have contributed to BIF deposition whereas Fe reducers and methanogens would have been responsible for C degradation and diagenesis.

Important aspects of the biogeochemistry of Lake Matano remain unresolved. Notably, the N cycle is poorly constrained. For example, there is a strong flux of ammonium from the deep water which is not recorded in the NO_3^- and NO_2^- pools of the surface water. What is the fate of this ammonium? Is it taken up by the microbial community near the pycnocline or, could it be anaerobicaly oxidized either phototrophically or by Fe(III) and Mn(IV)? Although, the concentrations of PO_4^{3-} are low

it Lake Matano's surface waters, it has yet to be determined what specifically limits primary productivity. In nutrient stimulation experiments, the addition of P or N alone did not increase productivity (Sabo 2006) and it took additions of both N and P to stimulate phytoplankton growth. Could N fixation be trace element (i.e. Mo) limited? The specific electron donor driving anoxygenic photosynthesis in the chemocline has not been positively identified. Are these Chlorobiaceae really photoferrotrophs or could they be supported with an alternative electron donor such as NH_4^+ or CH_4? The fraction of CH_4 oxidized aerobically vs. anaerobicly is unknown. Furthermore, the electron acceptor for anaerobic methane oxidation has yet to be positively identified. Cr isotopic compositions of the catchment waters are the lightest recorded to date. No known process is capable of such fractionation. Could it be Cr oxidation by Mn oxides or the precipitation of Cr(VI) bearing minerals? These unresolved issues present significant opportunities for future research.

Crowe, S. A., A. H. O'neill, S. Katsev, P. Hehanussa, G. D. Haffner, B. Sundby, A. Mucci, and D. A. Fowle. 2008. The biogeochemistry of tropical lakes: A case study from Lake Matano, Indonesia. Limnol. Oceanogr. **53:** 319-331.

Golightly, J. P. 1981. Nickeliferous Laterite Deposits. Econ. Geol. **75th Anniversary Volume:** 710-735.

Sabo, E. M. 2006. Characterization of the pelagic plankton assemblage of Lake Matano and determination of factors regulating primary and secondary production dynamics. M.Sc. University of Windsor.

Schoenberg, R., S. Zink, M. Staubwasser, and F. Von Blanckenburg. 2008. The stable Cr isotope inventory of solid Earth reservoirs determined by double spike MC-ICP-MS. Chem. Geol. **29:** 294-306.